Diacylglycerol kinase alpha is a critical signaling node and novel therapeutic target in glioblastoma and other cancers

Charli Dominguez
San Antonio, TX

Bachelor of Science, Baylor University, 2008

A Dissertation (*or Thesis*) presented to the Graduate Faculty
of the University of Virginia in Candidacy for the Degree of
Doctor of Philosophy

Department of Neuroscience

University of Virginia
May, 2013

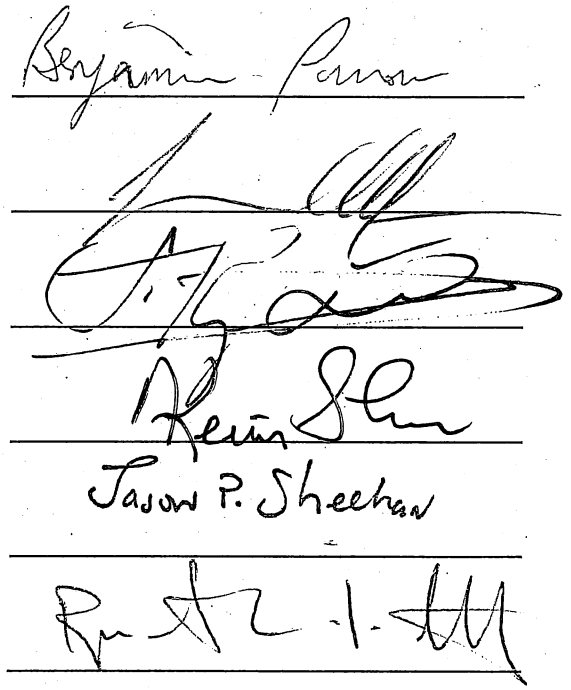

ABSTRACT

While Diacylglycerol kinase alpha (DGKα) has been linked to several signaling pathways related to cancer cell biology, it has been neglected as a target for cancer therapy. The attenuation of DGKα activity via DGKα-targeting siRNA and small-molecule inhibitors, R59022 and R59949, induced caspase-mediated apoptosis in glioblastoma cells and in other cancers, but lacked toxicity in non-cancerous cells. We determined that mTOR and HIF-1α are key targets of DGKα inhibition, in addition to its regulation of other oncogenes. DGKa regulates mTOR transcription via a unique pathway involving cyclic AMP. Lastly, we showed efficacy of DGKα inhibition with shRNA or a small-molecule agent in glioblastoma and melanoma xenograft treatment models, with growth delay and decreased vascularity. Subsequently, the inhibition of the DGKα product PA was investigated as a therapeutic target as well. Combination inhibition of the three PA synthetic pathways was significantly toxic to glioblastoma cells and other cancers, but lacked toxicity in non-cancerous cells. We showed that triple drug combination to inhibit the production of PA has a synergistic effect when compared to either single or double drug combinations. We believe that PA is a promising single target with high impact on cancer biology that can provide a novel approach for treatment-resistant cancers. Lastly, we identified and began to investigate a compound, ritanserin, that is structurally similar to known DGKα small-molecule inhibitors. We have preliminarily shown ritanserin to be toxic to GBM cells, safe in non-cancerous cells, and to have an inhibitory effect on DGKα activity that is comparable to R59022. This study establishes DGKα as a central

signaling hub and a promising therapeutic target in the treatment of cancer, sets the foundation for PA as a potential single target, and begins to investigate ritanserin as a promising compound with potential for quick advancement to clinical trials for cancer therapy.

ACKNOWLEDGEMENTS

All of this work and getting through many years of graduate school would not have been possible without many people that have supported me throughout this time. I would like to thank my mentor, Dr. Benjamin Purow, for being the best mentor anyone could ask for. He has given me endless support, advice, pep talks, and helped me develop into a better scientist over time. My co-worker Dr. Desiree Floyd has been my closest friend in lab and helped me through every aspect of life. She has not only helped me navigate graduate school and experiments, but she has also been a delight to work with, always ready to help and make me laugh when work got overwhelming. I would also like to thank everyone else in lab that has come and gone through the years, especially those that helped contribute to my published work. Dr. Benjamin Kefas for helping to mentor me, Laurey Comeau and Aizhen Xiao for all of their help daily, and lastly the undergraduates I mentored, Melissa Yacur and Alina Khurgel, for assisting me in experiments. Lastly, a special thank you to my committee members, Dr. Roger Abounader, Dr. Jonathan Kipnis, Dr. Kevin Lee, Dr. James Mandell, and Dr. Jason Sheehan, for their help and advice to mold my project and for attending meetings.

On a more personal note, I have had immense support from my parents, my best friend, and community of friends I have found in Charlottesville. I would like to mention a few classmates that helped me stay focused and have fun throughout my graduate school career: Dr. Kimberly Cox, Christine Van Hover, Dr. Mark Fitzgerald, Emily Andre, and Christoph Koch.

TABLE OF CONTENTS

LIST OF DIAGRAMS

LIST OF FIGURES

LIST OF SUPPLEMENTAL FIGURES AND TABLES

INTRODUCTION

I. Glioblastoma Multiforme and Thesis Rationale

According to WHO classifications, CNS tumors can be classified as epdendymomas, oligodendrogliomas, astrocytomas, or glioblastomas. Of CNS tumors, gliomas comprise a group of low- grade and high-grade tumors. High-grade gliomas are the most common brain tumors in adults and are universally fatal. These tumors partially resemble glial cells, but their cell of origin is unclear. The most malignant are those classified as astrocytomas and glioblastomas (1). Glioblastoma refers to grade IV astrocytomas, and tumors with up to 25% of cells that may be oligodendroglioma. GBM encompasses two categories: primary and secondary glioblastomas. Primary glioblastomas are cancers of the CNS that appear *de novo*, without any preexisting sign of tumor growth, while secondary glioblastomas are tumors of the CNS that develop from progression of lower grade gliomas (2). Glioblastoma multiforme (GBM) is the most common primary brain tumor. GBM accounts for >51% of all types of gliomas diagnosed each year (1). Histopathology characteristics of GBM include poor differentiation of neoplastic astrocytes, a reduction in apoptosis, nuclear and cellular atypia, vascular thrombosis, rapid mitotic activity, increased angiogenesis, and pseudopallisading necrosis (3). GBMs are exceedingly treatment-resistant, even with combined surgical resection and radio- and chemotherapy, and always recur (1). These tumors are highly invasive and infiltrate the normal brain parenchyma in a diffuse fashion, which contributes to their resistance (4). The frequency and

lethality of GBM, combined with resistance to treatment, present a critical need for novel therapeutic approaches.

Treatment resistance also arises in GBM and other cancers through their genetic diversity and complexity. It has been shown in cancer, perhaps most elegantly in GBM (5), that multiple signaling pathways are dys-regulated in an individual cell. Thus the inhibition of one or two pathways promotes the up-regulation of other oncogenic pathways—in part through feedback loops—allowing the cancer cell to survive. It is therefore increasingly clear that more effective cancer treatment will require either cocktails of inhibitors or the discovery of critical signaling nodes that can be targeted to block numerous pathways simultaneously. Herein we investigate a possible signaling node as a promising cancer target.

We previously showed Notch to be a potential therapeutic target in glioblastoma (6), and in subsequent efforts to determine its signaling role we have sought to better understand its crosstalk with other pathways. This led us to profile microRNAs regulated by Notch, as we have described previously (7). MiRNA-297 was among the microRNAs found to be up-regulated with Notch inhibition, and upon delivery to glioblastoma cells it was observed to be more toxic than any other miRNA tested in our laboratory. This led us to consider possible targets of miRNA-297. After an extensive search through online databases, we did not find any known oncogenes predicted to be strongly targeted by miRNA-297, but the gene Diacylglycerol kinase alpha was among the top predicted targets.

Treatment resistance also arises in GBM and other cancers through their genetic diversity and complexity. There are numerous signals that converge in each cell and many pathways interact to result in the desired effect on a small number of targets. It has been shown in cancer, perhaps most elegantly in GBM (5), that multiple signaling pathways are dys-regulated in an individual cell. Thus the inhibition of one or two pathways promotes the up-regulation of other oncogenic pathways—in part through feedback loops—allowing the cancer cell to survive. While alterations in the main pathways (AKT, ERK, mTOR, PKC, etc.) are responsible for tumorigenesis and are referred to as oncogenes, there are other non-oncogenes that need to function properly as well (8). According to this idea, targeting important non-oncogenes, proteins may not necessarily be upregulated or malfunctioning like oncogenes, concentrates on a vulnerability of the cancer cells that is context-dependent (9). Attenuation of such additive non-oncogenes could thus prove selectively effective against tumor cells (10).

Related to the idea of the role non-oncogenes play in cancer cell signaling, a new way to approach the search for novel targets in cancer is to look for “funnel factors,” or critical signaling nodes (11). The concept of critical signaling nodes holds that there are single targets through which multiple molecular signals responsible for tumorigenesis and sustainability act (11). The search for every important oncogene altered in various forms of cancer has proven to be a daunting goal. While there is a necessity to isolate oncogenes, focusing on non-oncogene critical signaling nodes will allow identification of additional targets. There has been mounting evidence describing certain oncogenes that are

implicated in several cancers, like AKT, VEGF, HIF1α, EGFR, etc. (12). However, therapies targeting these specific oncogenes have not produced the most optimal outcome (12, 13). It is therefore increasingly clear that more effective cancer treatment will require either cocktails of inhibitors or the discovery of critical signaling nodes that can be targeted to block numerous pathways simultaneously. Herein we investigate a possible signaling node as a promising cancer target.

II. Signaling in Glioblastoma Multiforme and Cancer

The standard treatment of most cancers is a combination of surgery, radiation and cytotoxic chemotherapy, often limited by serious side effects. This established treatment regimen was developed on an oversimplified notion of cancer, but the reality of cancer is far more complex. Recently, the development of molecular targeted therapies has transformed cancer therapy. Targeting molecular signaling pathways that promote tumor formation, growth, and proliferation in cancer has furthered understanding of the mechanisms that drive tumor development and provided novel therapeutic approaches (14).

i. Mammaiian Target of Rapamycin (mTOR)

One pathway that is dysregulated in cancer and has been the focus of multiple targeted therapies is the phosphatidylinositol 3-kinase (PI3K)/AKT/mTOR pathway (1, 15). This signaling pathway is involved with cell survival, proliferation, and angiogenesis. To briefly summarize, PI3K phosphorylates inositol phospholipids to produce phosphatidylinositol-3,4,5-

triphosphate (PIP3). PIP3 activates the serine/theronine kinase AKT through promoting translocation to the inner membrane, where it is phosphorylated by phophoinositide-dependent kinases (PDKs) (16). AKT is regulated by phosphatase and tensin homolog (PTEN) and interacts with many critical substrates, particularly mTOR (17). mTOR is a serine-theonine kinase that modulates a range of cellular processes such as cell growth, metabolism, autophagy, and proliferation (18). mTOR is found in two distinct complexes, mTORC1 and mTORC2, that differ in their subunit formation and response to rapamycin. mTORC1 is made of a complex that includes mTOR and regulatory associated protein of mTOR (Raptor) and is highly sensitive to rapamycin. AKT indirectly activates mTORC1 though TSC2, and downstream targets are S6 Kinase and 4EBP1 (19). mTORC2 is a complex of mTOR and rapamycin-insensitive companion of mTOR (Rictor) (20). Increased mTORC2 activity, along with increased Rictor expression, has been associated with poor survival in glioma patients (21). Importantly, mTORC2 phosphorylates AKT (19). Because of its central role in regulating various cellular pathways, mTOR has become the focus of a myriad of cancer studies. Some inhibitors, such as rapamycin and everolimus, have advanced to clinical trials yet have proved disappointing in the patient setting (22). As with other single molecule targeted therapies, resistance can occur with mTOR inhibitors, and the discovery of multiple mTOR complexes is fairly recent. The disappointing results seen with mTOR inhibitors in the past may be due to other complexes, so a method to decrease total mTOR expression could prove to be advantageous. New strategies to approach mTOR

attentuation will allow for a better understanding of mTOR signaling and the potential for combination inhibition of mTOR signaling.

ii. HIF-1α

It is very common for solid tumors to have regions of hypoxia, which is a result of outrowing the vascular supply. The low oxygen tension in these areas triggers the adaptation of cancer cells to survive in a hypoxic environment. Tumor cell adaptation leads to an aggressive and metastatic cancer phenotype that is associated with the resistant to treatment and poor patient outcome (23). Key to the cellular hypoxic response is the transcription factor, hypoxia-inducible factor-1 (HIF-1). HIF-1 is a heterodimer that consists of HIF-1α and HIF-1β subunits (24). In normoxic conditions, von Hippel-Lindau (VHL) tumor suppressor protein negatively regulates HIF-1α by degradation via ubiquitination, which is dependent on prolyl hydroxylation of HIF-1α. When hypoxia occurs, HIF-1α becomes stabilized and translocates to the nucleus, where it can bind HIF-1β to form the HIF1 complex (25). This complex is then allowed to bind to hypoxia response element (HRE) sequences on target genes, and recruits co-activator cAMP-dependent element binding protein (CREB)-binding protein and other proteins to activate transcription (26). The dysregulation of HIF-1 results in the resistance to treatment and an aggressive phenotype. Combined with evidence that HIF-1 is over-expressed in most cancers (27) and that radiation itself activates HIF-1 (28), this presents a pressing need to target HIF-1 activity in tumors.

iii. Cyclic Adenosine Monophosphate signaling

Recently, cyclic adenosine monophosphate (cAMP), which is involved in a broad range of cellular signaling, has been implicated in cancer biology. cAMP is a second messenger that is produced via the GPCR-mediated activation of adenylyl cyclases at the plasma membrane (29), and is degraded by cAMP phosphodiesterases (PDEs). cAMP activates PKA, which then phosphorylates and activates various transcription factors, including CREB (30). Elevation of cAMP levels has been shown to inhibit cell proliferation (31), induce apoptosis (32), and regulate mTOR signaling (33) in various established tumor cell lines. Given numerous cancer signaling pathways effected by cAMP and the mounting evidence that cancer cells favor low levels of cAMP for survival, there may be a role for modulating cAMP activity as a means to treat cancer.

Diagram 1: PI3K/AKT/mTOR signaling

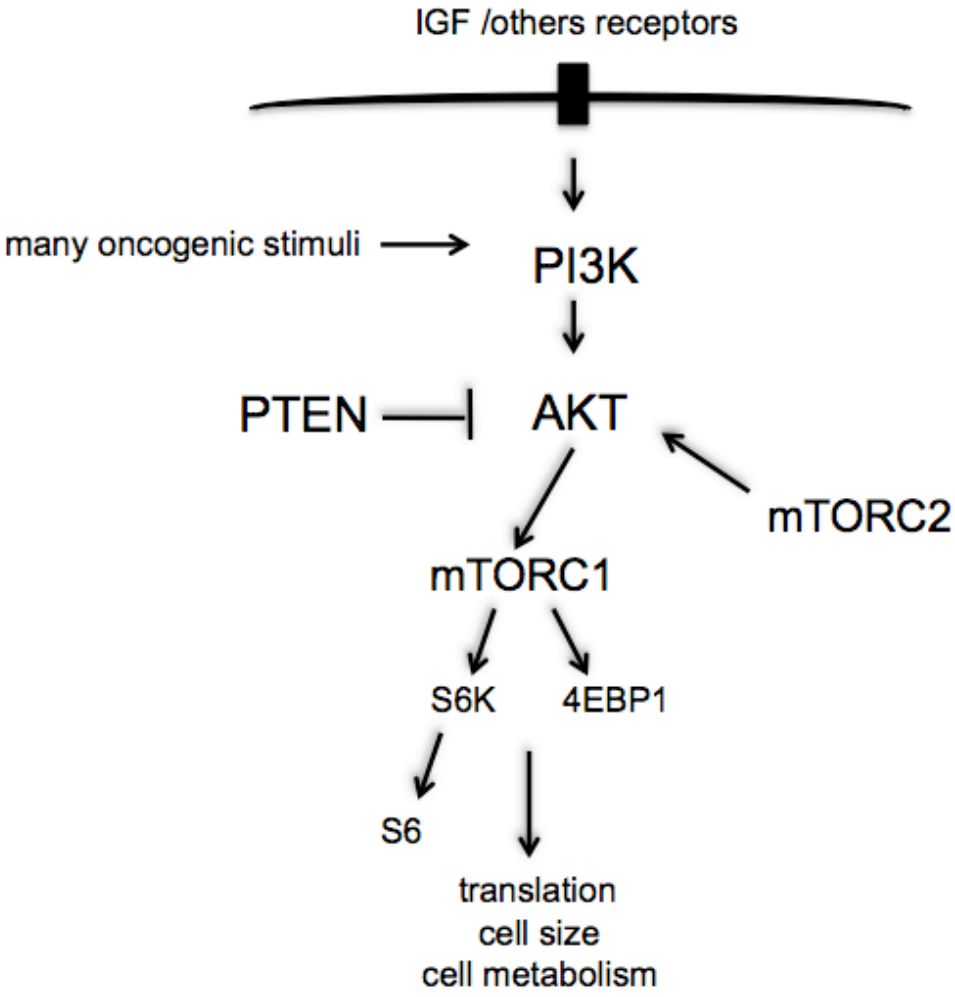

Diagram 1: HIF-1 signaling

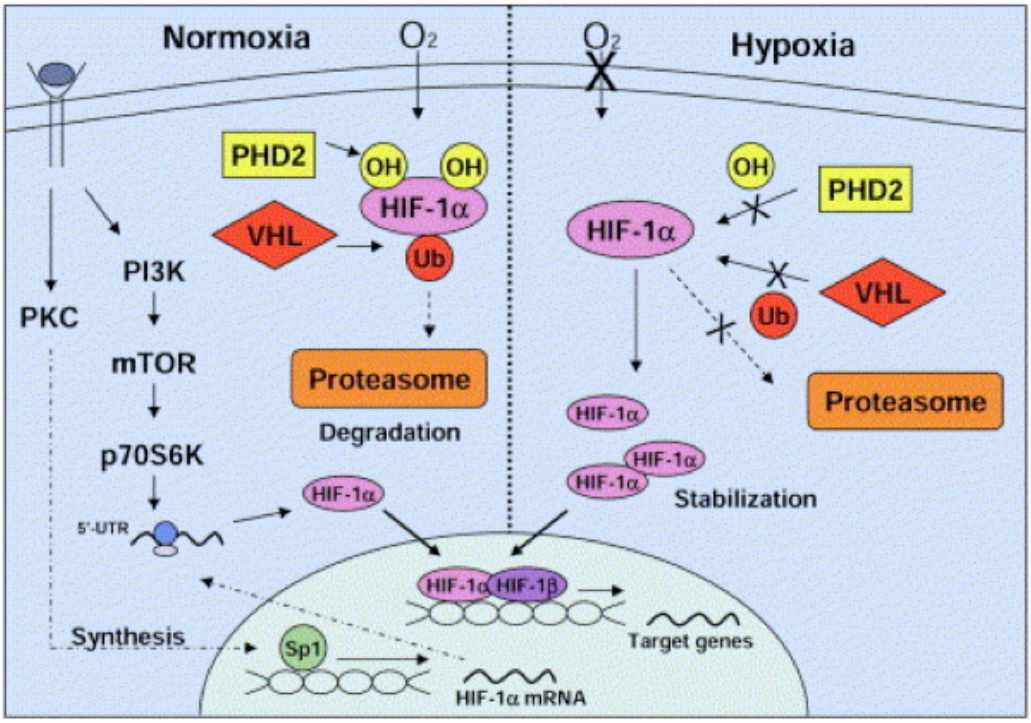

Diagram from (34)

III. Diacylglycerol Kinase Alpha

We previously showed Notch to be a potential therapeutic target in glioblastoma (6), and in subsequent efforts to determine its signaling role we have sought to better understand its crosstalk with other pathways. This led us to profile microRNAs regulated by Notch, as we have described previously (7). MiRNA-297 was among the microRNAs found to be up-regulated with Notch inhibition, and upon delivery to glioblastoma cells it was observed to be more toxic than any other miRNA tested in our laboratory. This led us to consider possible targets of miRNA-297. After an extensive search through online databases, we did not find any known oncogenes predicted to be strongly targeted by miRNA-297, but the gene Diacylglycerol kinase alpha was among the top predicted targets.

Diacylglycerol (35) is a membrane lipid that is an established second messenger activating several signaling proteins, most of which have been implicated in cancer (36). DAG is typically metabolized through diacylglycerol kinases (DGKs), resulting in the creation of phosphatidic acid (37). Phosphatidic acid (PA) is a phospholipid that is found at relatively low levels compared to other lipids, yet it has been implicated in regulating a number of signaling pathways and proteins (38). Given their broad significance, proper balance and regulation of DAG and PA levels is necessary. DGKs phosphorylate DAG to produce PA, and therefore it is hypothesized that this kinase can act as a crucial regulator of these two lipids by supressing DAG and generating PA (39). Diacylglycerol kinases comprise a family of proteins that is well conserved, and found in such

diverse species and groups as Drosophila melanogaster, C. elegans, mammals, and plants (37). This enzyme activity was first recognized by Hokin and Hokin, who discovered the phosphorylation of DAG to PA by a kinase they referred to as diglyceride kinase (40). DGKα activity gained attention for its role in the PI (phosphatidylinositol) cycle. It was purified from pig brain and found to be 80kDa (41). Upon purification of this kinase, further studies suggested that this enzyme may be regulated by phosphorylation and translocates to the plasma membrane when active (42). Research in this area has progressed; there are now 10 mammalian DGK isoenzymes identified, classified into 5 different subtypes (38). While all mammalian DGKs have 2 or 3 cysteine-rich domains and a conserved catalytic region, they differ from one another by substrate specificity, primary structure, and tissue distribution (43).

There are 5 different subtypes. The DGK type 1 group (α, β, and γ) has calcium-binding EF hand motifs, a recoverin- like homology domain in the N-terminus, and two cysteine-rich regions in the regulatory domain (44). While all type 1 DGKs are structurally similar, they do vary in tissue distribution, functionality, and cellular localization. DGKα is abundantly expressed in T cells, lymphocyte-rich tissues, bone marrow (45), and brain tissue (43). DGKα has been implicated in a variety of cellular functions apart from other type 1 DGKs. Through the administration of siRNA specifically targeting DGKα, this enzyme was shown to play a positive role in the proliferation and migration of endothelial cells (46). DGKα also has a positive regulatory role in T cells as well. This kinase is highly expressed in T cells, in which IL-2 driven proliferation is dependent upon

phosphatidic acid produced by the phosphorylation of diacylglycerol by DGKα. This interaction is made evident by the enhanced IL-2 induced G1 to S phase transition with upregulated DGKα activity (47). DGKα plays a role in the regulation of apoptosis in melanomas. While DGKα is expressed in several melanoma lines, it is not expressed in noncancerous melanocytes. Overexpression of DGKα suppressed TNF-α-induced apoptosis, while siRNA silencing of this kinase did the opposite (48). Other type 1 DGKs did not reproduce these effects. This study also found that DGKα negatively regulates TNF-α-induced apoptosis through activation of NF-kB. There is a mounting case for DGKα regulating cell survival, proliferation, migration, and apoptosis signaling in a variety of cellular environments. The need for further investigation of DGKα as a possible therapeutic target in cancer is evident, given its numerous connections to oncogenic pathways.

i. Diacylglycerol Kinase Inhibitors

Since the purification of the 80kDa DGK by Kanoh et al., several inhibitors have been explored. The first DGK inhibitor investigated was R59022 (6-{2-{4-[(4-fluorophenyl)phenyl-methylene]-1-piperidinyl}ethyl}-7-methyl-5H-thiazolo-(3,2-a)pyrimidin-5-one), in a study on its effect on diacylglycerol in the inositol lipid cycle in red blood cell membranes (49). According to initial reports, R59022 successfully inhibited DGK activity. This was made evident by selective decrease in [^{32}P] PA membrane loading, while other lipids assayed remained unaffected. Two important claims on R59022 were made from this study: R59022 selectively inhibits DGK activity and the rate-limiting factor of R59022 inhibition appears to

be diacylglycerol levels in the membranes used. R59949 (3-{2-4-[bis(4-fluorophenyl)methylene]-1-piperidinyl)ethyl}-2,3-dihydro-2-thioxo-4(1H)quinazolinone), a second inhibitor, was first investigated in platelets. Administration of this compound inhibited DGK activity in platelet membranes and intact platelets in a concentration-dependent manner (50). This was made evident by the marked decrease in [^{32}P] PA incorporation into the membrane and [^{32}P] PA formation upon R59949 administration.

Following these studies, the search for more DGK attenuators expanded with the use of diacylglycerol analogs. In a wide scale study, DAG analogs that varied in the head group but maintained a conserved acyl length chain (C_8) were utilized to explore the specificity of DGK inhibition and the kinase itself (51). Results from this study show that two analogs stood out as inhibitors, diC_8-ethylene glycol and 1-monooleylglycerol. While this study attempted a novel method to attenuate DGK activity, there were flaws to the experimental design used. One confounding variable observed in early studies of DGK inhibition was the use of anionic lipids as substrates, which is one of the major experimental conditions in the study by Bishop et al. Anionic lipids may react with the cationic functional groups of R59949 and R59022, which would simply reverse the initial anionic lipid activation (Reviewed in (52)). While these drugs were not used in the study mentioned above, this confounding variable renders the results incapable of being compared to specific DGK inhibitor drugs and complicates replication. Lastly, the concentrations of DAG analogs used in the aforementioned study were in the 100-500μM range, which are significantly

higher concentrations than published inhibition concentrations of both R59949 and R59022. Given these issues, R59949 and R59022 are the widely accepted DGK inhibitors and will be focused on here.

Although R59949 and R59022 are both functional inhibitors of DGKα, the inconsistent published results pose the need for further investigation on the selectivity of these drugs. Both inhibitor drugs were found to inhibit Ca^{2+}-dependent DGKs, while more weakly affecting those independent of calcium. To figure out how R59949 interacts with DGKα, full length and truncated mutants were expressed (52). Successful inhibition of DGKα was observed in both the full-length DGKα enzyme and the truncated mutant lacking the Ca^{2+}-binding EF hand. The mutant with the catalytic domain absent did not show inhibition by R59949. Based on this study, it can be concluded that both R59022 and R59949 are selective for type I DGKs, particularly DGKα. Lastly, while R59949 is more selective, both interact with the catalytic domain to inhibit DGKα activity (52).

IV. Oncogenic Cellular Networks Associated with DGKα inhibition

While the consequences of DGKα inhibition have been largely unexplored in direct relation to tumor maintenance, inhibiting this kinase has been utilized in several published works regarding tangential subjects. Noteworthy studies that investigate the inhibition of DGKα and subsequent decrease of phosphatidic acid production demonstrate effects on hypoxia-inducible factor expression, VEGF, HGF, and IL-2. It is becoming increasingly evident from such studies that DGKα

is a kinase that has far-reaching effects on mediating oncogenic cellular networks.

i. DGKα and Hypoxia

Hypoxia is one hallmark of the tumor microenvironment that tumor cells must adjust to in order to survive and grow. In the absence of oxygen, the activity of hypoxia-inducible factors (HIFs) is induced (23). HIF-1α and HIF-2α are normally recognized by mammalian proline hydroxylases (PHDs) and von Hippel-Lindau (VHL) tumor suppressor protein for subsequent ubiquitinization and degradation. In a recent publication, administration of DGKα inhibitor R59949 decreased HIF-1α levels (53). To verify whether or not this reduction was a direct consequence of R59949 inhibition of DGKα, [^{32}P] PA was measured. Decreased levels of PA synthesis verified that the specific inhibition of DGKα was the direct source of the observed changes in expression levels. DGKα inhibition induced these changes in HIF-1α levels through increasing endogenous PHD activity, resulting in increased VHL-HIF-1α binding. This link between DGKα activity and HIF expression levels indicates another branch of cancer cell biology that DGKα may target, since HIF induction has been implicated in supporting cell survival in hypoxic conditions by enhancing the expression levels of proteins involved with angiogenesis, invasion, metabolic adaptation, and apoptosis protection (23).

ii. DGKα and Angiogenesis

For some time now, angiogenesis has been explored as a target for cancer treatment, given its role in tumor growth and metastasis. GBMs utilize angiogenesis to satisfy the demand for nutrients in order to maintain a

microenvironment to thrive. Angiogenesis is promoted by angiogenic factors secreted by hypoxic tissues such as vascular endothelial growth factor (VEGF). VEGF-A initiates angiogenesis through the activation of signaling pathways such as PI3-kinase and PLC-γ. This cellular cascade causes endothelial cells to migrate, proliferate, and organize into new blood vessels (54). Given that DGKα is involved in the aforementioned pathways, inhibition of this kinase has been used to investigate its role in angiogenesis. Specifically, DGKα interaction with VEGF-A signaling has been studied by the use of R59949, a DGKα dominant-negative mutant, and specific RNA interference (46). When VEGF-A angiogenic response was stimulated, DGKα activity levels were seen to increase in PAE-KDR aortic cells and HUVEC endothelial cells. This report also showed that R59949 inhibited VEGF-induced chemotaxis and DNA synthesis. The conclusion drawn from this study is that DGKα activity is required for VEGF-induced angiogenesis.

iii. DGKα product phosphatidic acid and mTOR

Mammalian target of rapamycin (mTOR) is one common oncogene by which tumor progression occurs through suppression of apoptotic signals (20). mTOR has a major role in the regulation of cell growth, proliferation, metabolism, and survival through the regulation of protein synthesis (55). Recently phosphatidic acid (PA) has been shown to play a role in the regulation of mTOR complexes. Although expressed at low levels when compared to other lipids, PA has been shown to mediate growth factors and hormones in mammalian cells, more specifically those with mitogenic properties. When PA production is

suppressed, the phosphorylation of S6K and pAKT^{ser473} is attenuated in kidney carcinoma and breast cancer cell lines, which are downstream of mTORC1 and mTORC2, respectively. In concurrence with this observation, the effect of PA absence on phosphorylation can be reversed with the addition of 100uM exogenous PA. Interestingly, mTORC1 and mTORC2 were broken down when PA production was suppressed and were incapable of being restored with the addition of a cross-linking reagent, which contrasts with rapamycin breakdown of the complexes (20). From this work it can be surmised that PA works to stabilize the complexes formed with mTOR. Another link in this association is through ERK signaling. With the addition of PA, increased activity is seen in mTORC1, p-ERK, and S6K when compared to non-treated cells. This effect is ablated with the administration of a MEK inhibitor, which localizes this effect upstream of mTOR and ERK1/2 (18). With this evidence it has become apparent that mTOR may be another pathway that is affected by the proper functioning of DGKα. If DGKα is inhibited and production of PA is attenuated, the downstream effect can negatively regulate the activity of mTOR by destabilizing and breaking down the complexes formed. The ability of this kinase to interact with multiple cancer dependent pathways, suggests DGKα as a promising signaling node for treatment of GBM.

All of this taken together poses a mounting case for DGKα regulating cell survival, proliferation, migration, and angiogenesis signaling in a variety of cellular environments. The need for further investigation of DGKα as a possible therapeutic target in cancer is evident, given its numerous connections to

oncogenic pathways. Herein we show in GBM and other cancers that DGKα is a critical signaling node essential for several oncogenic pathways and is a promising therapeutic target.

METHODS

Cell lines and patient samples

U87, U251, MDA-MB-231, Hela, A-375, and human fibroblast cell lines were obtained from ATCC (Manassas, VA). Astrocytes were purchased from Lonza (Walkersville, MD). Tumor stem cell lines 0308, 0206, and 0822 were derived and validated as described previously (56). All cell lines were maintained in a 37°C incubator with 5% CO_2. Patient samples were obtained from the Tumor Bank at the University of Virginia under an approved IRB protocol.

Cell transfection

The effects of DGKα knockdown by siRNA were examined in U251MG (GBM), U87MG (GBM), 0308 (GBM stem cell), A-375 (melanoma), MDA-MB-231 (breast cancer), and HeLa (cervical cancer) cell lines. Cells were plated in six-well tissue culture plates at a density of between 4.0×10^4 – 6.0×10^4 per well and transfected 24 hours later. Cells were transfected with Oligofectamine (Invitrogen) according to the manufacturer's protocol, with a concentration of 10nmol/L siRNA.

Immunoblots

Immunoblots were performed as previously described (6) Primary antibodies included DGKα (ProteinTech), phospho-AKT, HIF-1α, phos-mTOR, c-Myc, and PARP. All antibodies were obtained from Cell Signaling unless otherwise noted. Horseradish peroxidase-conjugated secondary antibodies to

rabbit or mouse immunoglobulin G were used (1:7500, Jackson Immunology Labs, Bar Harbor, ME).

Annexin V Staining

Cells were harvested 4 days post-transfection and Annexin V staining was performed according to the manufacturer's description (BD Biosciences, San Jose, CA).

Caspase 3/7 assay

Cells were harvested with trypsin (Fisher MediaTech, Pittsburgh, PA). Caspase 3/7 assay was performed according to the manufacturer's description (Promega Madison, WI). After one-hour incubation at 25°C, each sample was measured in a Promega Glomax 20/20 Luminometer.

Real-time quantitative PCR

Cells were lysed using Qiazol (Qiagen) and then transferred to QIAshredder columns (Qiagen) and centrifuged at 10,000 g for 3 minutes, then RNA isolated using the RNeasy kit according to the manufacturer's instructions (Qiagen). RT-PCR on 500 ng of RNA using the miScript reverse transcription kit (Qiagen) was used to generate cDNA. From 100 ng of cDNA template, quantitative real-time PCR analyses for FDPS1, FDPS2, HMGCR, SCD, DGKα, and 18S were performed using their specific forward primers and reverse primers according to the manufacturer's protocol (Qiagen). 18S was used as a control.

Applied Biosystems (StepOnePlus) real-time PCR system was used to carry out the quantitative PCR, using hot start 95°C (15m), then denaturation 95°C (15s) with annealing at 58°C (30s), extension 72°C (30s) for 40 cycles, followed by a melt curve analysis. Data analysis for differences in gene expression between control and treated cells, or normal and GBM tissue, was carried out using Microsoft Excel: housekeeping gene primer Ct values were subtracted from test primer values to find the $\Delta\Delta$Ct, then $\Delta\Delta$Ct was found by subtracting the average ΔCt of the vehicle-treated sample from itself and the drug-treated samples. Fold change was calculated using the formula Fold Change = $2^{-\Delta\Delta Ct}$.

Phosphatidic acid rescue experiments

U251MG and U87MG were transfected or treated with small-molecule inhibitors as above. Simultaneously, exogenous phosphatidic acid (Avanti Polar Lipids, Alabaster, AL) at either 33 mM or 50 mM and vehicle (v:v) of a 1:2 methanol and chloroform solution were administered. Treatment was repeated every 24 hours.

Cellular lipid extraction and LPA, PA, and DAG profile assays

Total lipid was extracted from GBM cells by methods described previously (57-60). The cellular content of DAG, LPA and PA profiles was analyzed by LC/MS on a Shimadzu Prominence UFLC (Ultra Fast Liquid Chromatography) system equipped with a C8 column (Nucleodur 5 μm, 2 × 125 mm, Machery-Nagel) and detection was carried out using an Applied Biosystems 4000 Q Trap

triple quadrupole LC/MS/MS system equipped with an electrospray ionization system. For PA and LPA, multiple reaction monitoring protocols in negative mode were developed for each phosphatidic acid using commercial pure phosphatidic acids and the most intense product ions were selected for the analysis of biological samples. For DAG, analyses were carried out by monitoring product ions generated by neutral loss (60) of ammoniated acyl groups [RCOOH + NH_3] from DAG's ammonium adducts $[M + NH_4]^+$ as previously described (61). Quantitative methods for the measurement of glycerolipids were performed using the chromatographic and spectrometric methods described above in conjunction with the use of 0.1 nmol C17 LPA and C17 ceramide as an internal standard, for LPA/PA and DAG respectively, to correct for recovery and the protein concentration of the cellular lysates. The amount of each species of glycerolipid in biological samples was calculated from the peak areas obtained using the software that controls the LC/MS system (Analyst 1.5, Applied Biosystems). Raw peak areas were corrected for recovery and sample loading as described above and then transformed into amounts of analyte using standard curves made with commercial glycerolipids.

cAMP assay

The cells were treated with DGK-α inhibitor R59022 (Sigma-Aldrich) at 10μM for 5 days or transfected with DGK-α siRNA. cAMP concentration were determined in cell lysates from cell culture of $3.5X10^5$ cells using commercially available assay (cAMP competitive Elisa kit; Thermo Scientific, Rockford, IL)

following the manufacturer's instructions. The assay is based on the competition between cAMP in the standard or sample and Alkaline Phosphatase conjugate cAMP (cAMP-AP) for a limited amount of cAMP monoclonal antibody bound to an Anti-Rabbit IgG pre-coated 96 well plate. The assay is colorimetric, and absorbance is read at 405 nm.

Luciferase assay

The cells were transfected with DGKα siRNAs for 4 hours using oligofectamine or treated with DGKα inhibitor R59022 10 μM, PDE4 inhibitor rolipram 40 μM, exogenous cAMP 20 or 80 pmol for 3 days and subsequently transfected with β-galactosidase (2 ng/ul), mTOR promoter luciferase reporter or empty promoter vector (Switchgear Genomics Inc., Menlo Park, CA) following the manufacturer's instructions for 48 hours. Luciferase assays for mTOR activity were performed using the LightSwitch Assay System (Switchgear Genomics Inc.) and for β-galactosidase activity using Galacto-Light Plus™ beta-Galactosidase Reporter Gene Assay System (Applied Biosystems, Carlsbad, CA). Luminescence was measured on a Promega GloMax 20/20 luminometer and normalized as described previously (7). mTOR luciferase activities were double-normalized by dividing each well by both β-galactosidase activity and the average luciferase/β-galactosidase value in a parallel set done with constitutively-expressed luciferase expression vector.

Pharmacological reagents

The small molecule inhibitors R59022 {6-[2-[4-[(4-Fluorophenyl)phenylmethylene]-1-piperidinyl]ethyl]-7-methyl-5H-thiazolo-[3,2-a]-pyrimidin-5-one} and R59949 {3-[2-[4-[Bis(4-fluorophenyl)methylene]-piperidin-1-yl]ethyl]-sulfanylidene-1H-quinazolin-4-one} were obtained from Sigma-Aldrich (St. Louis, MO).

Small interfering RNA (siRNA) duplexes were synthesized by Sigma-Aldrich (St. Louis, MO). Oligofectamine (Invitrogen) was used for transfection of siRNA into cells per manufacturer's instructions and as previously described (6). siRNA sequence was as follows: DGKα: 5' GGAUUGACCCUGUUCCUAA

Estimates of blood-brain barrier penetration of small-molecule inhibitors

R59022 and R59949 were evaluated for their predicted ability to cross the blood-brain barrier (BBB) using the ACD/ADME software (ACD Labs, Toronto, Canada) (62). The module used for predictions is Pharma Algorithms (63), which provides a comprehensive evaluation of blood-brain barrier penetration potential of compounds in rodents. Each compound of interest is given an estimate whether it would be permeable enough to exhibit CNS activity. Qualitative classification is based on reliable and theoretically reasonable predictions of the rate and extent of BBB permeation (expressed as LogPS and LogBB constants respectively) governed by passive diffusion.

LogBB predictive model is based on a data-set containing >500 brain to plasma partitioning ratios (expressed as LogBB constants) measured in mice and rats. Under the assumption of passive transport across the BBB, LogBB is

viewed as a cumulative effect of drug binding to plasma and brain constituents. Calculations therefore use octanol/water logP (main determinant of brain tissue binding) and unbound fraction in plasma (fu, plasma) as input parameters.

LogPS module provides more detailed output of the ionization-specific predictive model of BBB permeability in rats. The model was developed using in-vivo experimental data of rates of passive diffusion across BBB for >200 compounds, expressed as LogPS constants. Calculations are performed using essential physicochemical properties such as lipophilicity, ionization constants, hydrogen bonding parameters, and molecular size (calculated or experimental if available) as inputs (63).

LogPS module provides more detailed output of the ionization-specific predictive model of BBB permeability in rats. The model was developed using *in vivo* experimental data of rates of passive diffusion across the BBB for over 200 compounds, expressed as LogPS constants. Calculations are performed using essential physicochemical properties such as lipophilicity, ionization constants, hydrogen bonding parameters, and molecular size (calculated, or experimental if available) as inputs (63).

In vivo **treatment models**

Mouse protocols were approved by the IACUC committee at the University of Virginia. Eight-week-old male SCID/NCr Balb/C mice (from NCI) were stereotactically implanted with 25,000 0308 GBM stem cells in 10 mL of Neurobasal media. The surgical procedure was done as described previously (7).

Convection-enhanced delivery of lentiviral particles (Sigma-Aldrich) containing shRNA was done at 7 days post-implantation. Animals were randomly divided into 2 groups: control group (7 mice) receiving control shRNA and treatment group (6 mice) receiving DGKα shRNA. Convection-enhanced delivery (CED) was done using the same coordinates as for the tumor implantation. The CED volume was 10 mL as well, at a speed of 300nL/min. The solution also contained 1:2000 polybrene and 7.5% mannitol to promote spread of infusate. General appearance, neurologic status, and body weight were monitored daily, and mice were euthanized when they demonstrated signs of illness, pain, or 20% weight loss.

Alternatively, following the same protocol mentioned above, 100,000 U87 GBM cells were implanted in 10 mL of DMEM media. Beginning at 7 days post-implantation of tumor cells, mice were given daily intraperitoneal injections with either DMSO (v:v), 2 mg/kg, or 10 mg/kg of R59022 dissolved in DMSO in 50 mL volume.

Immunohistochemistry

Immunohistochemical staining with anti-CD34 antibody (EMD Millipore, Billerica, MA) and anti-cleaved caspase-3 antibody (EMD Millipore), with horseradish peroxidase-conjugated secondary antibody, was done on frozen mounted slices by the University of Virginia Biorepository and Tissue Research Facility using standard techniques.

Plasma R59022 extraction and quantitation

R59022 was extracted from mouse plasma using a modified Bligh-Dyer extraction method. To a 5 mL polypropylene tube containing 100 µl of sample, 500 µl methanol (MeOH), 250 µl chloroform ($CHCl_3$), and 100 µl dH_2O were added, mixed, and incubated on ice for 30 min. To extract, 250 µl $CHCl_3$ and 200 µl 0.2 M sodium chloride (NaCl) were added. The organic phase was dried and suspended in 100 µl of a mixture of $CHCl_3$:MeOH (1:1), and 50 µl was injected into a Shimadzu LC-20AD LC system equipped with a Discovery (Supelco) C18 column (50mm × 2.1 mm, 5 µm bead size). The LC was coupled to a triple quadrupole mass spectrometer (Applied Biosystems 4000 Q-Trap). R59022 was measured in positive mode using the following transition: 460.3 →193.1. Mass spectrometer settings, obtained by direct infusion of a 1 µM solution in Solvent B, were as follows: DP: 66, EP: 10, CE:43, CXP: 14; Ion spray voltage: 5500; Temperature: 500; Curtain gas; 40. Chromatography was carried out using a mobile phase A consisting of 79% H_2O, 20% MeOH, 1% formic acid; and a mobile phase B consisting of 99% MeOH, 1% formic acid. The solvent gradient was as follows: 0.5 min 100% solvent A, a linear gradient to reach 100% solvent B at 5.6 min, 4.3 min 100% solvent B, 1 min 100% solvent A. Total flow was 1 ml/min. Retention time was 3.9 min. Quantification was carried out by measuring peak areas using commercial software (Analyst 1.5.1).

Statistics

In vitro experimental results were analyzed by two-tailed Student's t-test and plotted with Microsoft Excel (Microsoft Corp, Redmond, CA). The *in vivo* experimental results were analyzed using the Kaplan-Meier function utilizing both

the Log-rank (Mantel-Cox) test and the Gehan-Breslow-Wilcoxon test in GraphPad Prism 5 (GraphPad Software, Inc., San Diego, CA). Refutation of the null hypothesis was accepted for p-values of less than 0.05. Error bars indicate standard deviation from the mean in all figures.

DIACYLGYLCEROL KINASE ALPHA AS A CRITICAL SIGNALING NODE IN CANCER

I. Introduction

High-grade gliomas are the most common brain tumors in adults and are universally fatal. These tumors partially resemble glial cells, but their cell of origin is unclear. Glioblastoma multiforme (GBM), grade IV glioma, is the most common and aggressive variant. GBMs are primary cancers of the CNS that appear *de novo* or arise from low-grade gliomas (1) and account for >51% of all gliomas diagnosed each year. GBMs are exceedingly treatment-resistant, even with combined surgical resection and radio- and chemotherapy, and always recur (1). These tumors are highly invasive and infiltrate the normal brain parenchyma in a diffuse fashion, which contributes to their resistance (4). The frequency and lethality of GBM, combined with resistance to treatment, present a critical need for novel therapeutic approaches.

Treatment resistance also arises in GBM and other cancers through their genetic diversity and complexity. It has been shown in cancer, perhaps most elegantly in GBM (5), that multiple signaling pathways are dys-regulated in an individual cell. Thus the inhibition of one or two pathways promotes the up-regulation of other oncogenic pathways—in part through feedback loops—allowing the cancer cell to survive. It is therefore increasingly clear that more effective cancer treatment will require either cocktails of inhibitors or the discovery of critical signaling nodes that can be targeted to block numerous

pathways simultaneously. Herein we investigate a possible signaling node as a promising cancer target.

We previously showed Notch to be a potential therapeutic target in glioblastoma (6), and in subsequent efforts to determine its signaling role we have sought to better understand its crosstalk with other pathways. This led us to profile microRNAs regulated by Notch, as we have described previously (7). MiRNA-297 was among the microRNAs found to be up-regulated with Notch inhibition, and upon delivery to glioblastoma cells it was observed to be more toxic than any other miRNA tested in our laboratory. This led us to consider possible targets of miRNA-297. After an extensive search through online databases, we did not find any known oncogenes predicted to be strongly targeted by miRNA-297, but the gene Diacylglycerol kinase alpha was among the top predicted targets.

Diacylglycerol is a membrane lipid that is an established second messenger activating several signaling proteins, most of which have been implicated in cancer (36). DAG is typically metabolized through diacylglycerol kinases (DGKs), resulting in the creation of phosphatidic acid (37). Phosphatidic acid (PA) is a phospholipid that is found at relatively low levels compared to other lipids, yet it has been implicated in regulating a number of signaling pathways and proteins (38). Though there are ten known DGK enzymes, Diacylglycerol kinase alpha (DGKα) has been implicated in a variety of cellular functions apart from other DGKs. Through siRNA knockdown of DGKα, it was shown to play a positive role in the proliferation and migration of endothelial cells (46). DGKα also plays a role

in the regulation of NF-κB in melanomas. While DGKα is expressed in several melanoma lines, it is not expressed in noncancerous melanocytes (48). Of note, DGKα synthesis of PA can be attenuated by two established small molecule inhibitors: R59022 {6-[2-[4-[(4-Fluorophenyl)phenylmethylene]-1-piperidinyl]ethyl]-7-methyl-5H-thiazolo-[3,2-a]-pyrimidin-5-one} and R59949 {3-[2-[4-[Bis(4-fluorophenyl)methylene]-piperidin-1-yl]ethyl]-sulfanylidene-1H-quinazolin-4-one}. Both R59022 and R59949 are selective for DGKα and the relative specificity of these inhibitors has been previously demonstrated (52). A recent report showed that the inhibition of DGKα by the small-molecule drug R59949 regulated the build-up of hypoxia-inducible factor-1α (HIF-1α) levels, a response to hypoxia and a hallmark of the tumor microenvironment (53). Another report showed that R59949, a DGKα dominant-negative mutant, and specific RNA interference each inhibited VEGF-induced chemotaxis and DNA synthesis in HUVEC endothelial cells (46). The same study also showed a correlation between VEGF-A stimulation and increasing DGKα levels. All of this taken together poses a mounting case for DGKα regulating cell survival, proliferation, migration, and angiogenesis signaling in a variety of cellular environments. The need for further investigation of DGKα as a possible therapeutic target in cancer is evident, given its numerous connections to oncogenic pathways. Herein we show in GBM and other cancers that DGKα is a critical signaling node essential for several oncogenic pathways and is a promising therapeutic target.

All of this taken together poses a mounting case for DGKα regulating cell survival, proliferation, migration, and angiogenesis signaling in a variety of cellular environments. The need for further investigation of DGKα as a possible therapeutic target in cancer is evident, given its numerous connections to oncogenic pathways. Herein we show in GBM and other cancers that DGKα is a critical signaling node essential for several oncogenic pathways and is a promising therapeutic target.

II. RESULTS

Attenuation of DGKα causes toxicity in glioblastoma cells

To assess the effect of this inhibition in established GBM cell lines, DGKα was silenced with siRNA and inhibited via small-molecule inhibitor, R59022. Percent cell death by trypan blue was significantly increased in both U87 and U251 cell lines when compared to controls (Fig. 1). In conjunction with the observed cell toxicity, cell viability by alamarBlue assay was significantly reduced with DGKα silencing in both GBM cell lines (Supplemental Fig. S1). To visualize cell toxicity changes after DGKα knockdown, U251 GBM cells were stained with Hoechst and propidium iodide, revealing a decrease in total cell number with an increase in membrane-compromised cells after DGKα knockdown (Fig. 2). An immunoblot for DGKα was also done to verify transfection efficiency in both GBM cell lines as well (Fig. 3). The toxicity seen in GBM cells was consistently observed with relative rapidity after treatment with either siRNA or small-molecule inhibitors targeting DGKα. We sought to confirm that cell death was being induced and by what mechanism. Typically, cell count assays were performed between 72-96 hours post treatment, showing a rapid effect on cell numbers given the typical time course for siRNA knockdown. A slowing in cell proliferation was considered unlikely, given no change in BrdU incorporation measured by ELISA assay (data not shown). Autophagy was also explored, but there was no difference in LC3-II levels by immunoblot (data not shown). To assess the possibility of cell death, Annexin V assay via FACS analysis was performed on the U87 and U251 GBM lines and the A-375 melanoma line (Fig.

4), with the results indicating an increase in Annexin V-positive cells with DGKα knockdown. Next, caspase-mediated apoptosis was investigated at both 24- and 36-hour time points. After transfection, there was a significant increase in caspase-3/7 activity in cells upon silencing DGKα in U87 and U251 GBM cells, as well as in melanoma cells (Fig. 5). In addition, we observed an increase in cleaved PARP expression in cell lysates in which DGKα expression was silenced (Fig. 6). These results suggest that DGKα inhibition causes cell toxicity in cancer cells through caspase-mediated apoptosis.

DGKα is up-regulated and increases cell numbers in human glioblastoma

Next, we sought to determine if DGKα might have oncogenic properties, given the substantial effect that silencing has on GBM cell proliferation. In U87, U251, and A-375 cells, forced over-expression of DGKα by transient transfection resulted in a significant increase in cell proliferation (Fig. 7). Next, in order to establish long-term over-expression of DGKα, we infected U87, U251, and A-375 cells with a lentiviral DGKα vector. DGKα over-expression significantly increased tumor cell proliferation (Fig. 7) *in vitro*. Upon quantification of DGKα protein by immunoblot in both normal brain and GBM human tissue samples, we found there to be modest but significant increases in levels of DGKα protein in GBMs (Fig. 8). Also, both normal and GBM tissue samples were analyzed to determine mRNA levels of DGKα (Fig. 8). While the difference in mean DGKα mRNA levels was not significant, some GBM samples had markedly increased DGKα mRNA,

and more samples need to be analyzed to determine significance. Lastly, other data available online from the Cancer Genome Atlas (64) indicate amplification of DGKα in 1-4% of GBM and several other cancers (Supplemental Table 1). Nonetheless, the moderate over-expression of DGKα in GBM cells seems inconsistent with the apparent addiction to its expression, suggesting this may be an example of "non-oncogene addiction"—in which cancer cells have a disproportionate dependency on a gene that is not over-expressed (9).

Glioblastoma toxicity is a specific effect of decreased DGKα activity

DGKα produces phosphatidic acid (PA) through the phosphorylation of diacylglycerol. In order to verify that the cellular toxicity observed in GBM cells is a specific consequence of the attenuation of DGKα activity, we investigated the role of PA. Knockdown of DGKα was performed in GBM cells as above and exogenous PA added. Notably, the substantial cytotoxicity in GBM and melanoma (Fig. 9) cells upon DGKα knockdown was rescued with exogenous PA. Similarly, PA administration also rescued the phenotype observed upon treatment with small-molecule inhibitor R59022 (Fig. 10) in GBM cells. Lastly, to confirm that PA levels were decreased with DGKα knockdown, PA levels were measured through mass spectrometry. Total PA levels were significantly decreased in U251 GBM cells after transfection with DGKα siRNA (Fig. 11). These results establish a role for DGKα production of PA in cancer cell viability.

Attenuation of DGKα causes toxicity through regulating key oncogenic pathways

DGKα and its product phosphatidic acid have been linked to several established oncogenic pathways, including mTOR (65), HIF-1α (53), and Akt (66). To evaluate the effects that silencing DGKα has on these possible mediators, immunoblots were done in GBM cells with DGKα knockdown. There was a significant decrease in total mTOR and phos-mTOR $_{ser2448}$ in GBM cells (Fig. 12) and melanoma cells with attenuation of DGKα activity (Fig. 12). HIF-1α and phos-mTOR$_{ser2448}$ were decreased by DGKα knockdown in GBM cells (Fig. 12) as well. In addition, we found that DGKα knockdown decreases c-Myc levels and phosphorylation of Akt$_{ser473}$ (Supplemental Fig. S2). We were also prompted to assess whether DGKα inhibition influences the SREBP (sterol regulatory element binding protein) cholesterol synthetic pathway by two recent reports, the first linking mTOR and the phosphatidic acid modulator lipin to SREBP activity (67), and the second establishing SREBP as oncogenic and a therapeutic target in GBM (68). Following DGKα knockdown in glioblastoma cells, we determined mRNA levels of the SREBP targets farnesyl diphosphate synthase (FDPS), HMG-CoA reductase (HMGCR), and stearoyl CoA-desaturase (SCD) (67). After normalization, each of the genes tested had significantly reduced mRNA levels when compared to control (Supplemental Fig. S3A). To assess whether any of these DGKα mediators might be central for the cytotoxicity of DGKα knockdown/inhibition in GBM cells, we performed “rescue” experiments with over-expression of wild-type mTOR and constitutively active HIF-1α. Over-

expression of mTOR and HIF-1α alone each partially rescued the toxicity from DGKα knockdown and inhibition, and when combined the phenotypic rescue was slightly stronger in both GBM and melanoma cells (Fig. 13). However, a similar over-expression of c-Myc failed to rescue the toxicity (Supplemental Fig. S3B). Taken together, these data suggest that decreased expression of mTOR and HIF-1α play substantial roles in the cytotoxicity observed with DGKα knockdown and inhibition in cancer.

DGKa regulates mTOR transcription through modulation of cyclic AMP levels

A similar degree of phenotypic rescue from DGKα knockdown occurred with a wild-type mTOR expression vector as with a constitutively-active mTOR vector (data not shown). This, combined with a strong correlation of DGKA and mTOR mRNA expression in the TCGA GBM data (Fig. 14) (Supplemental Table 2), suggested that DGKα might regulate mTOR expression. Given prior reports that PA promotes activity of phosphodiesterases decreasing cyclic AMP and that a cAMP-modulated transcription factor could drive mTOR transcription (69) (70), we hypothesized that DGKα was diminishing cAMP levels to prompt a rise in mTOR transcription. To initially evaluate this, we first assessed the effects on mTOR expression of DGKα knockdown with a lentiviral shRNA. We observed a significant decrease in mTOR mRNA levels with prolonged DGKα knockdown versus control (Fig. 15). Given this result, we used an mTOR promoter reporter luciferase assay to determine if DGKα transcriptionally regulates mTOR. With

attenuation of DGKα activity via siRNA and small-molecule inhibitor, there was a significant decrease in mTOR promoter activity in GBM and melanoma cells (Fig. 16 and 17). To evaluate whether DGKα was significantly affecting cAMP levels in GBM cells, ELISA was performed after DGKα activity was attenuated via siRNA and small molecule inhibitor. This revealed significant increases in cAMP levels with DGKα knockdown and inhibition in GBM and melanoma cells (Fig. 18 and 19). To determine if cAMP regulates mTOR transcription in GBM, cells were treated with exogenous cAMP and mTOR promoter activity assessed by luciferase assay; we observed a significant decrease in mTOR transcription (Fig. 20). In addition, cells treated with the phosphodiesterase-4D inhibitor rolipram also demonstrated a significant decrease in mTOR transcription (Fig. 21). Next, we assessed the role DGKα plays on predicted downstream targets in these non-cancerous cells to determine if the regulation seen above is particular to cancer cell signaling. With attenuation of DGKα activity in astrocytes, we did not observe the increase in cAMP levels seen in GBM cells (Fig. 22). Furthermore, in astrocytes exogenous cAMP (Fig. 23) and rolipram (Fig. 24) did not affect mTOR promoter activity. These data further supporting the role of cAMP in cancer cells in the hypothesized pathway (Fig. 25). These data indicate for the first time that DGKα regulates mTOR transcription, likely via modulating cAMP levels. This novel pathway regulating mTOR expression may have implications not only for the role of DGKα in GBM, but also for studies of the role of cAMP and of mTOR regulation in cancer.

Relative lack of cytotoxicity of targeting DGKa in non-cancerous cells

Classically, one of the disadvantages of therapeutic treatments for cancer is the negative side effects due to nonspecific effects on non-cancerous cells. To assess the effect of DGKα inhibition on non-cancerous cells, we utilized normal human astrocytes and fibroblasts. First, we silenced DGKα expression in astrocytes with siRNA and confirmed transfection efficiency with an immunoblot (Fig. 26), with no significant effect on cell numbers. We then attempted to assess toxicity of the small-molecule inhibitors on these non-cancerous cells, and similarly did not observe any significant decrease in cell viability at concentrations toxic in GBM lines (Fig. 27 and 28). These data suggest that DGKα knockdown and inhibition are preferentially toxic to cancer cells, possibly in part because a major downstream mechanism in cancer cells is unaffected in normal cells.

DGKα inhibition is cytotoxic in multiple cancer lines

Given the toxicity observed in GBM cell lines, its impact on major oncogenic pathways, the previous report on DGKα over-expression in melanoma cells (48), and its amplification in subsets of several cancers (described above), we sought to determine if DGKα is a potential therapeutic target in other types of cancer as well. First, lysates from various cancer cell lines and normal human astrocytes and fibroblasts were evaluated by immunoblot to assess the basal DGKα levels in each cell line used in this work (Fig. 29). Also, in melanoma,

cervical, and breast (Fig. 30) cancer cell lines the percent cell death after knockdown of DGKα or inhibition via small-molecule inhibitor R59022 (10 μM) was assessed by trypan blue cell counts. Second, to evaluate the potential therapeutic window of the small-molecule inhibitor R59022, we conducted a dose response assay in each cancer and normal cell line used above. Each cell line was treated with doses ranging from 5 μM to 100 μM, with DMSO (volume:volume) controls at each dose. Percent cell survival was evaluated at 4 days for each dose and dose-response curves plotted (Fig. 31). Cancer cell lines were substantially more sensitive to R59022 than normal cells.

DGKα knockdown and inhibition affect tumor growth, angiogenesis, and survival of mice with intracranial and subcutaneous tumors

To test DGKα knockdown as a potential therapy, we first utilized a GBM stem cell (GSC) xenograft treatment model in mice. DGKα knockdown via lentiviral vector was tested against a GSC line *in vitro* (Supplemental Fig. S4) and *in vivo*. First, 0308 GSCs were stereotactically injected into the brain of immunodeficient SCID mice and given a week to become established. Lentiviral particles containing control or DGKα shRNA were delivered via convection-enhanced delivery, to increase delivery volume and to promote diffusion of the virus. The treatment group had significantly increased survival ($p = .0073$), and MRI images also showed significantly smaller tumor size in this group as well (Fig. 32).

To predict whether one of the small-molecule DGKα inhibitors would penetrate the blood-brain barrier (BBB) sufficiently, we utilized an in silico algorithm based on the BBB penetration of hundreds of diverse compounds in rodents. This algorithm predicted that R59022 (Fig. 33) would have adequate BBB penetration while R59949 (Fig. 34) would not, despite their very similar structures (Supplemental Table 3) (63).

Next, the DGKα small-molecule inhibitor R59022 was utilized *in vivo* to initially evaluate the therapeutic potential of systemic DGKα inhibition. SCID mice were implanted with U87 GBM cells by the techniques above. After tumor establishment, mice were given daily intraperitoneal injections of either DMSO or 2mg/kg of R59022 for 12 consecutive days. The treatment group had significantly increased survival ($p=.01$) (Fig. 35). It is important to note that there was no decrease in mouse weights with R59022 treatment at doses of 2 or 10 mg/kg (data not shown).

To further evaluate the effects of R59022 administration, U87 GBM cells were injected into the flank of nude mice to establish subcutaneous tumors. Daily injections were given as above, and we noted that mean tumor volumes were significantly smaller after treatment with the DGKα inhibitor (Fig. 36) (Supplemental Table 4A). When we allowed some tumors from mice treated with R59022 time to catch up in size with tumors from DMSO-treated mice, the resected tumors displayed an obvious difference in vascularity (Fig. 37). Given this change in vascularity, immunohistochemistry for CD34 was performed to visualize blood vessels at the microscopic level. There was a sharp decrease in

blood vessel density in the treated tumors (representative image in Fig. 38). To assess for apoptosis in these resected tumors, immunohistochemistry for cleaved Caspase-3 (Fig. 39) was performed, indicating clear signs of apoptosis in tumors after DGKα inhibition.

To determine if systemic DGKα inhibition might have therapeutic potential against other cancers, we also tested it with subcutaneous implantation of A-375 melanoma cells. After daily intraperitoneal injections with the inhibitor R59022, mean tumor volume of treated mice was significantly smaller in comparison to control mice (Fig. 40) (Supplemental Table 4B).

Lastly, as the DGKα small-molecule inhibitors have not previously been evaluated *in vivo,* we performed an initial pharmacokinetic study. Blood plasma levels of R59022 were evaluated via mass spectrometry at several time points after a single intraperitoneal dose of 10 mg/kg. These studies revealed a short-half life and peak concentration at 2 hours (Fig. 41). Ongoing studies are being conducted to further evaluate the pharmacokinetics and explore the pharmacodynamics of this drug. These results underscore the potential of DGKα as a therapeutic target, since significant benefit was observed with just a single local infusion of lentiviral shRNA or short course of a small-molecule inhibitor. Optimized delivery of DGKα inhibitors *in vivo* could greatly enhance their efficacy against GBM and other cancers.

Figure 1

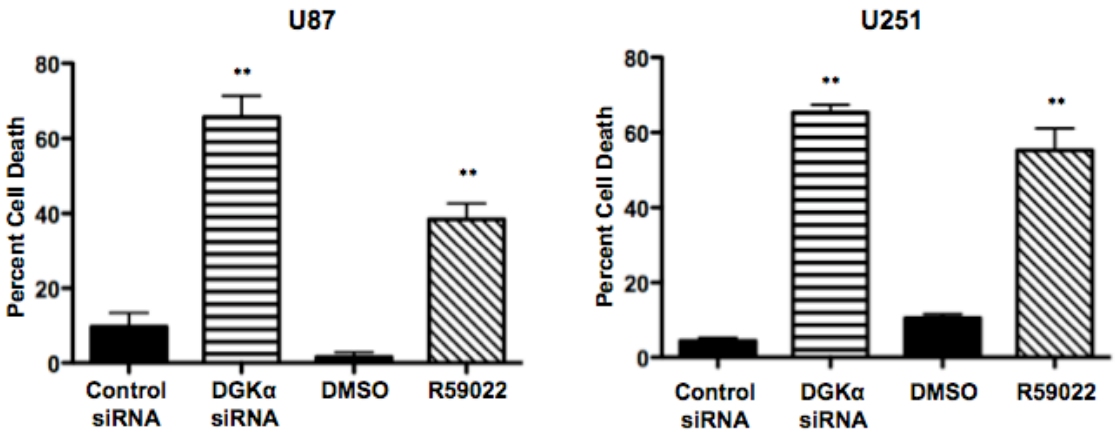

Figure 1. DGKα knockdown was assessed in GBM cells U87 and U251 via transfection with either control or DGKα siRNA and inhibition via treatment with DMSO (v:v) or R59022 at 10 μM. Percent cell death was evaluated after 4 days. (*, P<0.05 and **, P<0.01, Student t test).

Figure 2

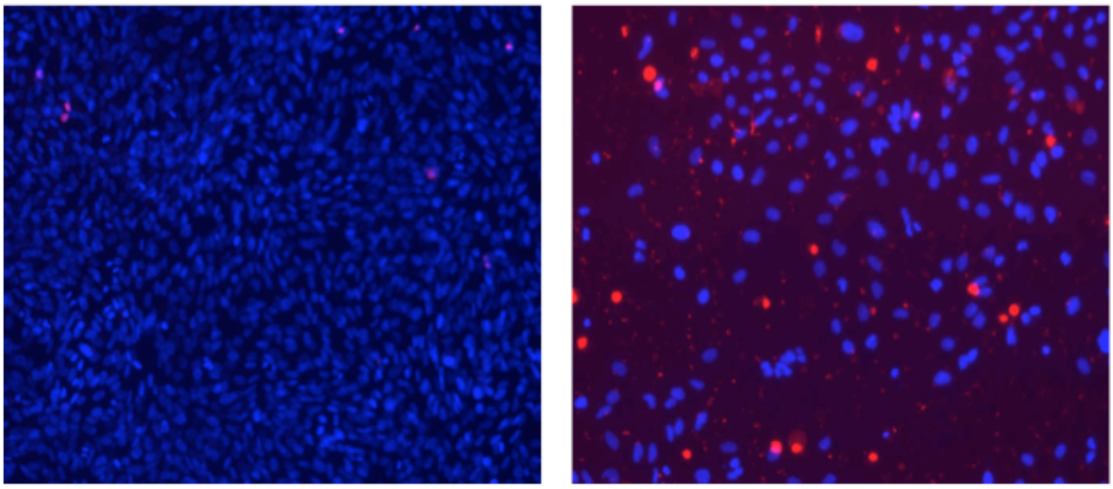

Figure 2. To visualize cell death changes after DGKα knockdown, U251 GBM cells were stained with Hoechst and propidium iodide.

Figure 3

Figure 3. An immunoblot was used to verify transfection efficiency with siRNA in U87 and U251 cell lysates at 72 hours with α-tubulin as control.

Figure 4

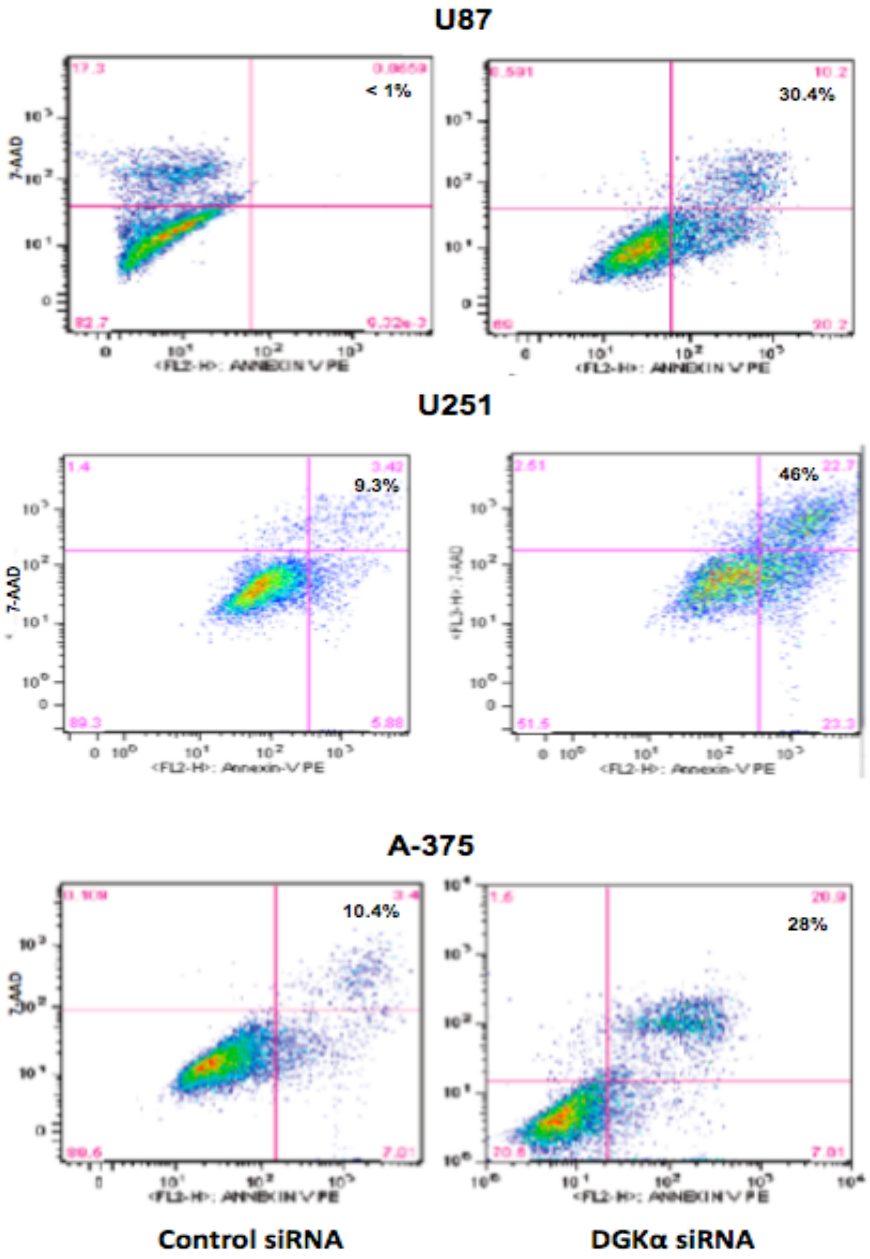

Figure 4. FACS analysis was performed on U87, U251, and A-375 cell lines showing an increase in Annexin V-stained cells after DGKα knockdown.

Figure 5

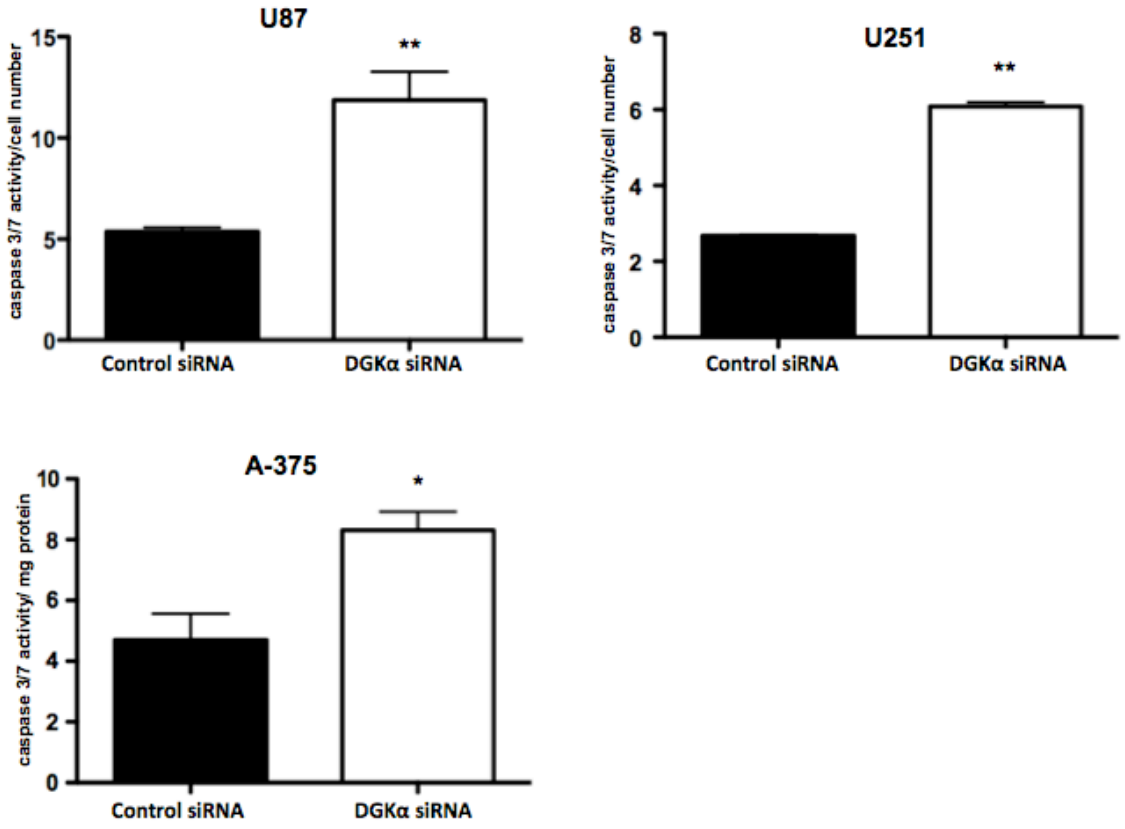

Figure 5. Caspase 3/7 activity was measured 36-72 hours after DGKα knockdown in U87**,** U251, and A-375 melanoma cells. (*, P<0.05 and **, P<0.01, Student t test).

Figure 6

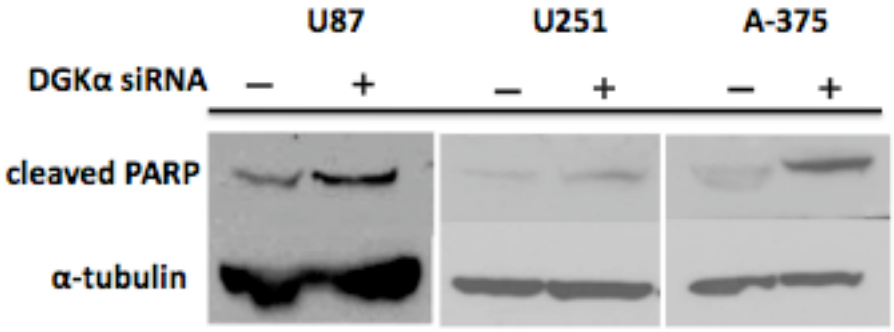

Figure 6. Protein levels of cleaved PARP were also increased in U251, A-375, and U87 cells after DGKα silencing.

Figure 7

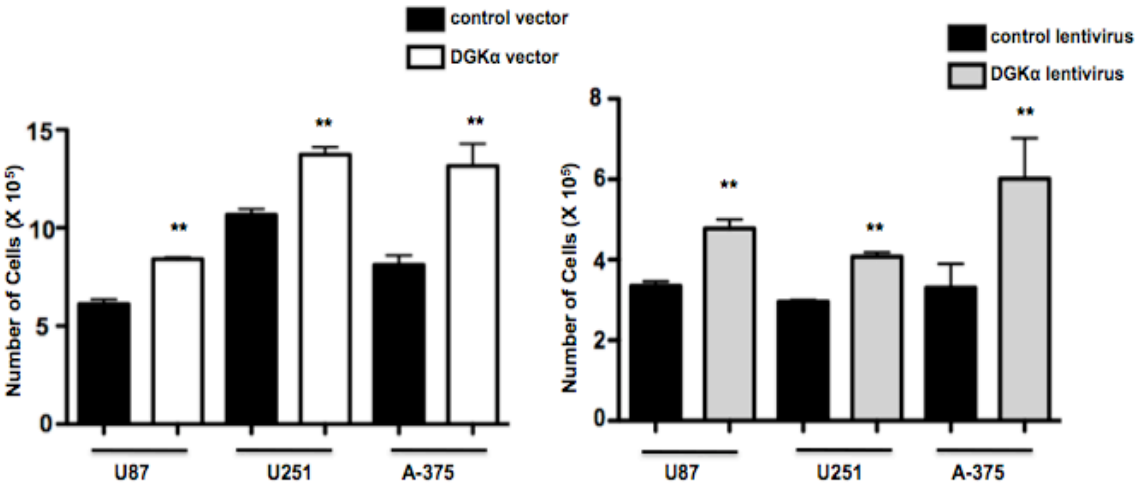

Figure 7. Cell numbers for U87 and U251 glioblastoma and A-375 melanoma cells were assessed 72 hours after over-expression of DGKα by plasmid transfection versus control plasmid (TOPO-TA plasmid, Invitrogen). DGKα was also over-expressed via lentiviral infection in U87, U251 and A-375 cells to assess the effect on cell proliferation when compared to control cells. (*, $P<0.05$ and **, $P<0.01$, Student t test).

Figure 8

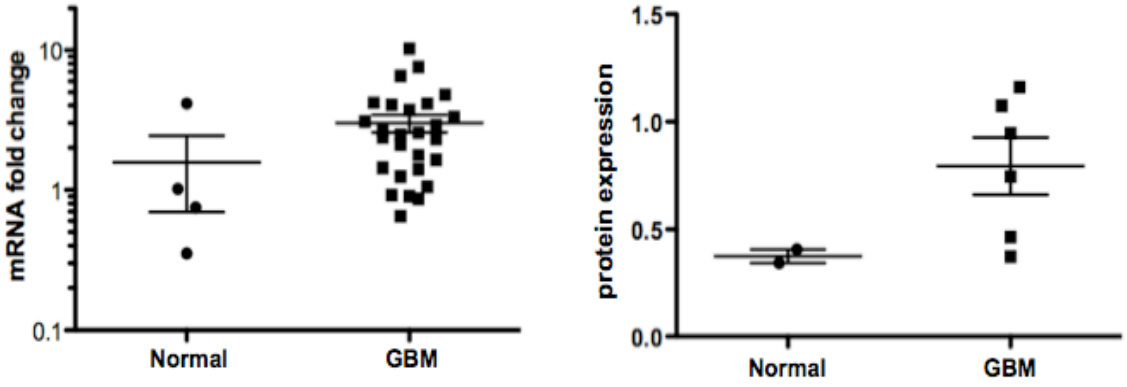

Figure 8. DGKα mRNA levels were quantified by qRT-PCR and normalized by 18S RNA in normal versus GBM human tissue samples. DGKα levels in human tissue samples were also evaluated by measured intensity of immunoblot in GBM samples and compared to normal brain after normalizing by the ratio of DGKα intensity to α-tubulin intensity.

Figure 9

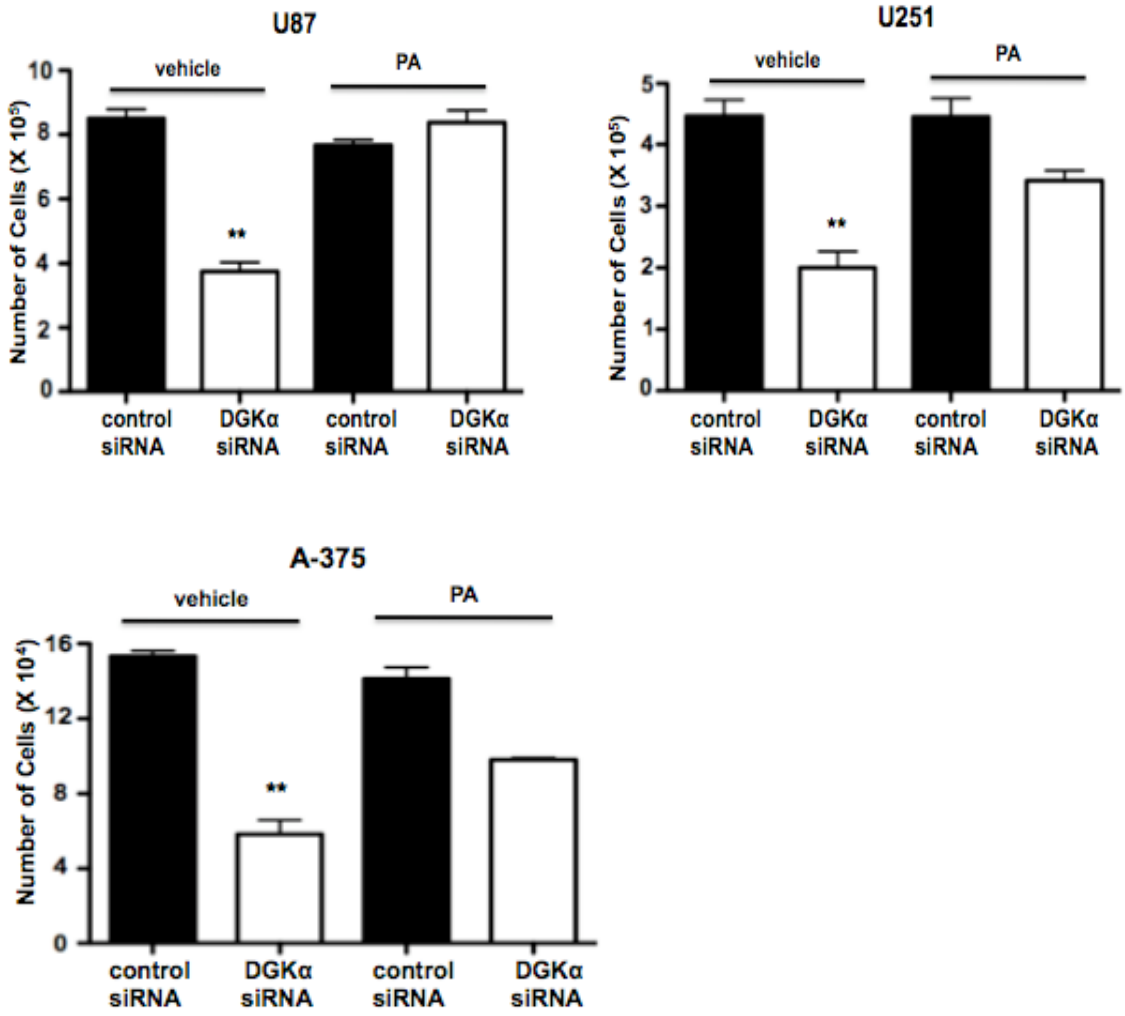

Figure 9. U87 and U251 GBM cells, and A-375 melanoma cells were transfected with control or DGKα siRNA with simultaneous administration of exogenous PA at 33 uM or vehicle (1 MeOH : 2 Chloroform, v:v). Full phenotypic rescue of decreased cell viability was observed upon delivery of PA to DGKα siRNA transfected cells. (*, $P<0.05$ and **, $P<0.01$, Student t test).

Figure 10

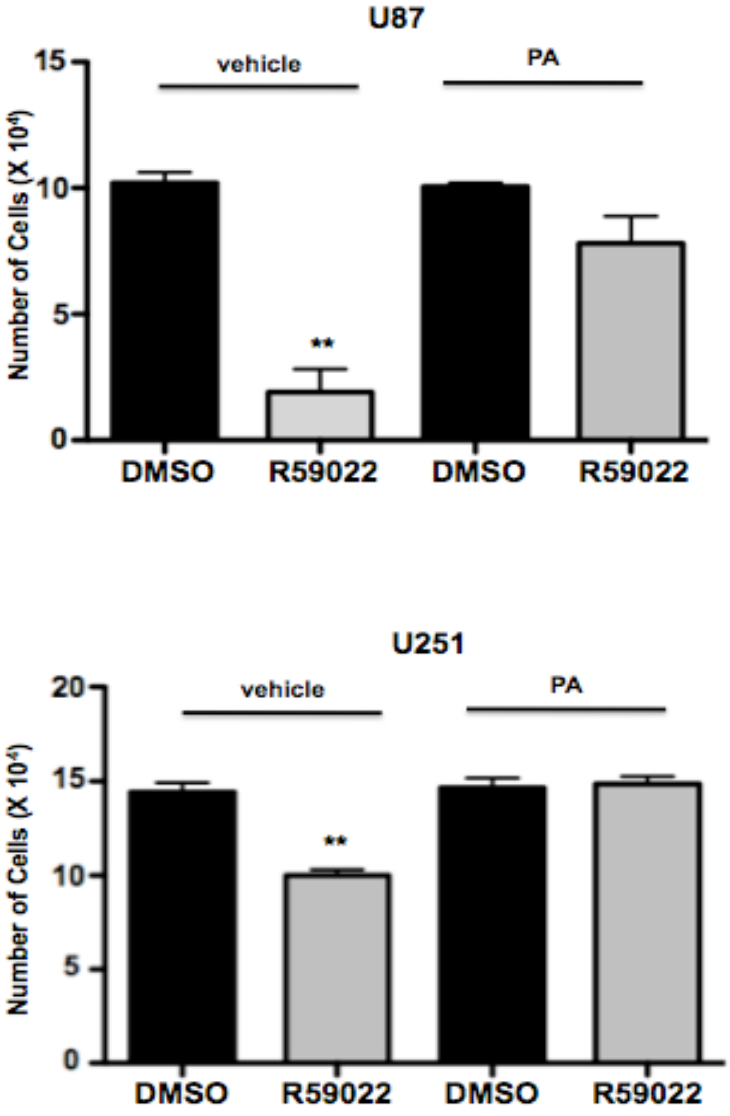

Figure 10. U251 GBM cells treated with DMSO or R59022 at 5 uM with simultaneous administration of exogenous PA at 33 uM or vehicle (1 MeOH : 2 Chloroform, v:v). Full phenotypic rescue of decreased cell viability was observed upon delivery of PA to DGKα siRNA transfected cells. (*, $P<0.05$ and **, $P<0.01$, Student t test).

Figure 11

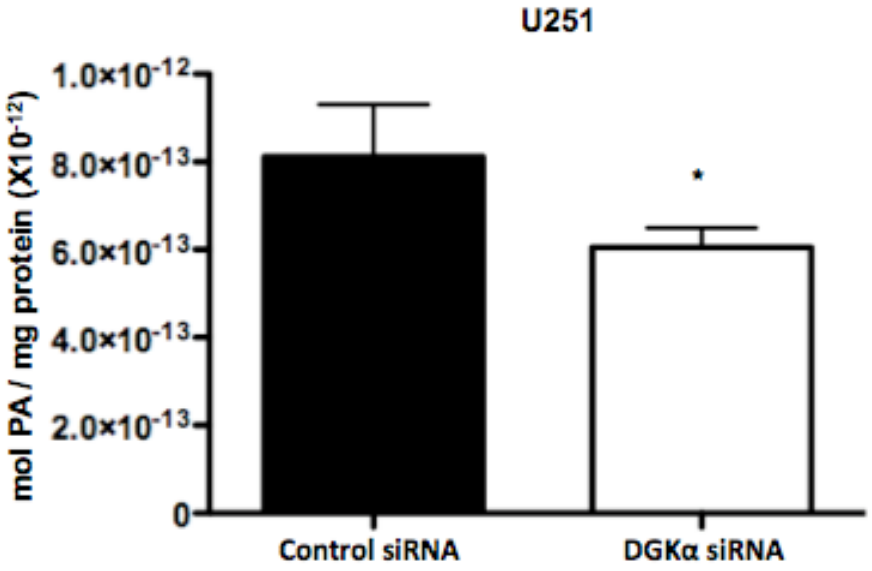

Figure 11. After transfection with siRNA, mass spectrometry was utilized to show a decrease in total PA levels in lipid lysates from U251 cells. (*, $P<0.05$ and **, $P<0.01$ Student t test).

Figure 12

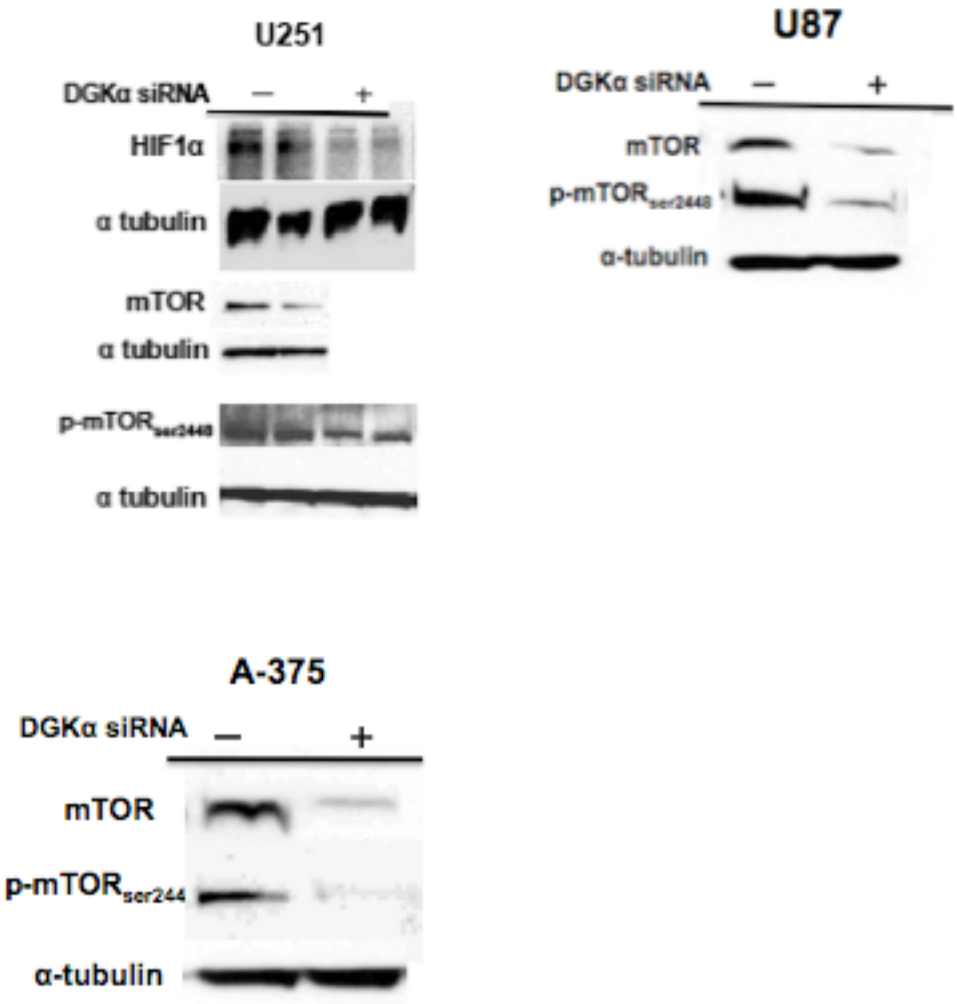

Figure 12. Immunoblot analysis of HIF-1α, total mTOR, and phos-mTOR$_{ser2448}$ in U251 cells transfected with DGKα or control siRNA. Total mTOR and phos-mTOR$_{ser2448}$ were decreased in U87 cell lysates, as well as in A-375 cell lysates.

Figure 13

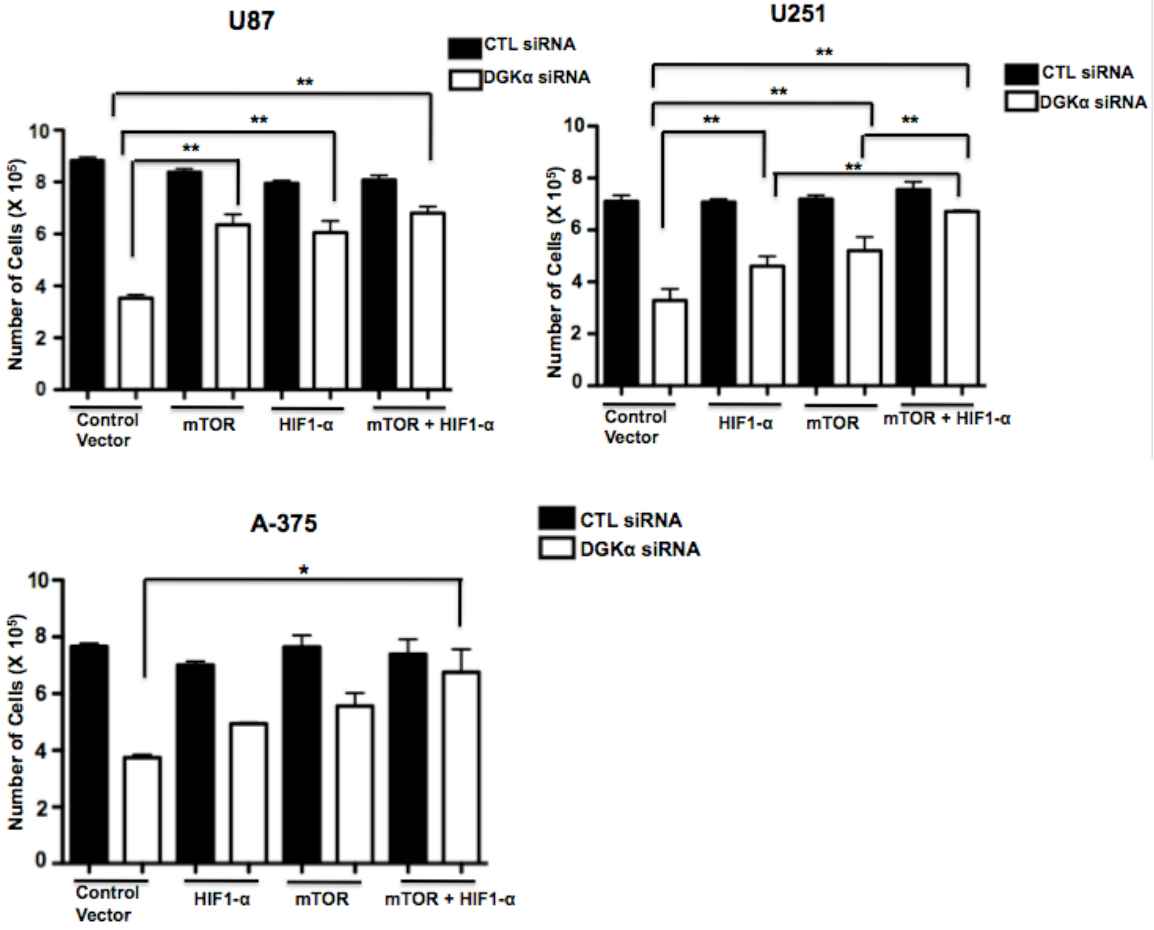

Figure 13. To verify the role HIF-1α and mTOR play in the observed cell toxicity, each was over-expressed through plasmid transfection and cell proliferation was assayed in U87 cells, U251 cells, and A-375 cells transfected with siRNA. (*, $P<0.05$ and **, $P<0.01$ One-way ANOVA, Bonferroni's post-test).

Figure 14

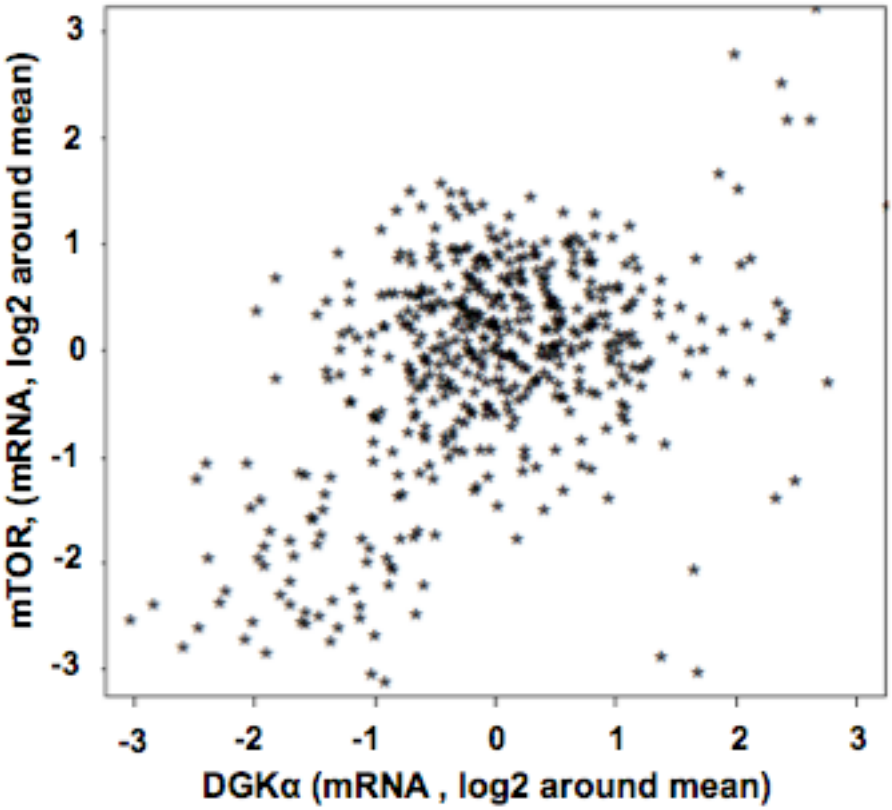

Figure 14. Plot of *DGKA* versus *mTOR* mRNA expression levels in 576 human GBM samples (from TCGA via cBio website). Spearman's correlation test performed with a p-value of $6.159e^{-16}$ and a Pearson's correlation test p-value of $< 2.2e^{-16}$.

Figure 15

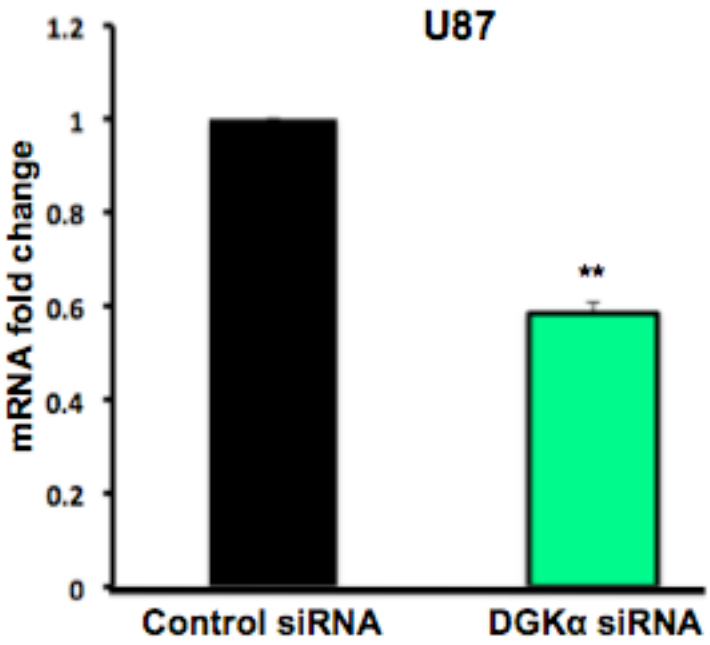

Figure 15. In U87, mRNA levels of mTOR were quantified by qRT-PCR in response to DGKα knockdown via shRNA and fold expression changes in comparison to control shRNA are shown. (*, $P<0.05$ and **, $P<0.01$ Student t test).

Figure 16

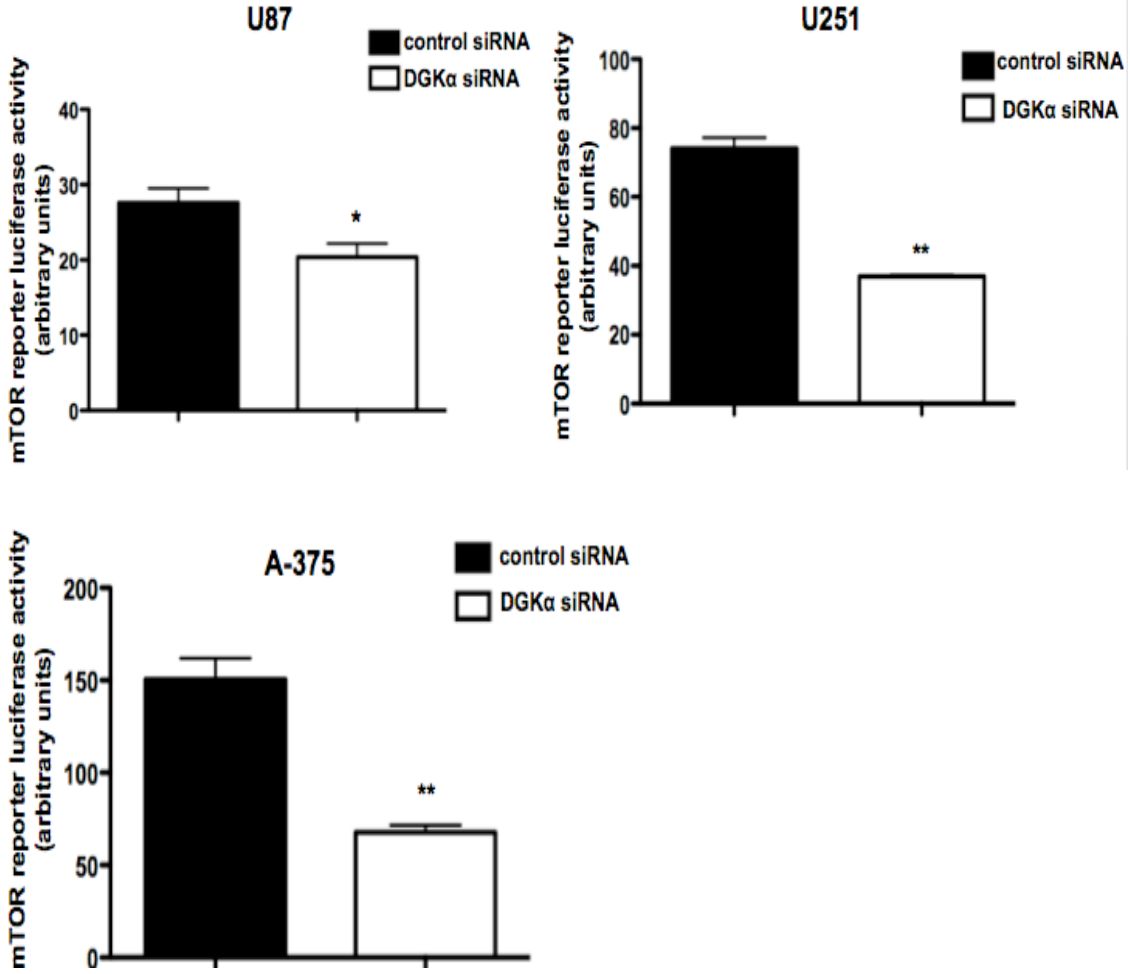

Figure 16. In U87, U251, and A-375 cells the effects of DGKα knockdown via siRNA on mTOR transcription were evaluated through mTOR promoter luciferase activity assay. (*, P<0.05 and **, P<0.01 Student t test).

Figure 17

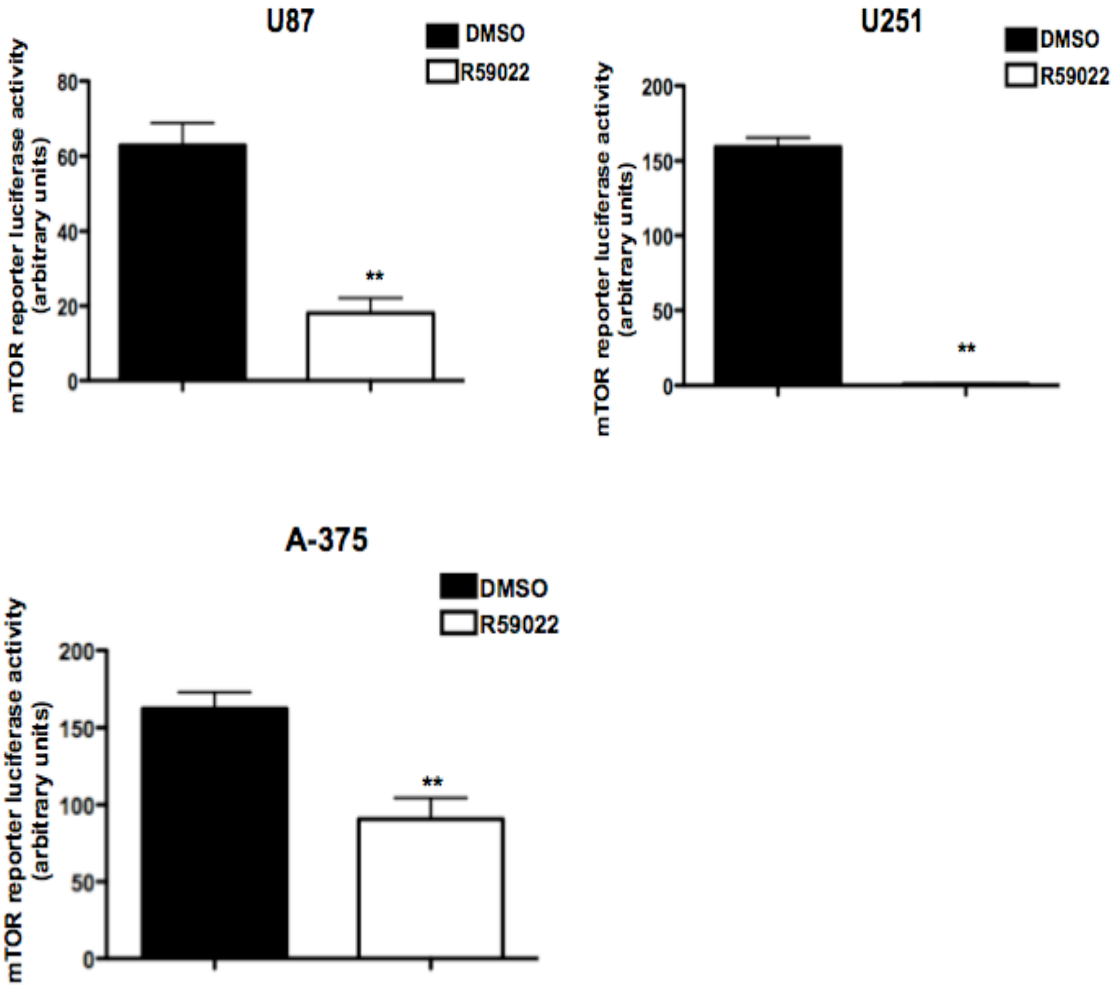

Figure 17. In U87, U251, and A-375 cells the effects of DGKα inhibition via small-molecule inhibitor on mTOR transcription were evaluated through mTOR promoter luciferase activity assay. (*, P<0.05 and **, P<0.01 Student t test).

Figure 18

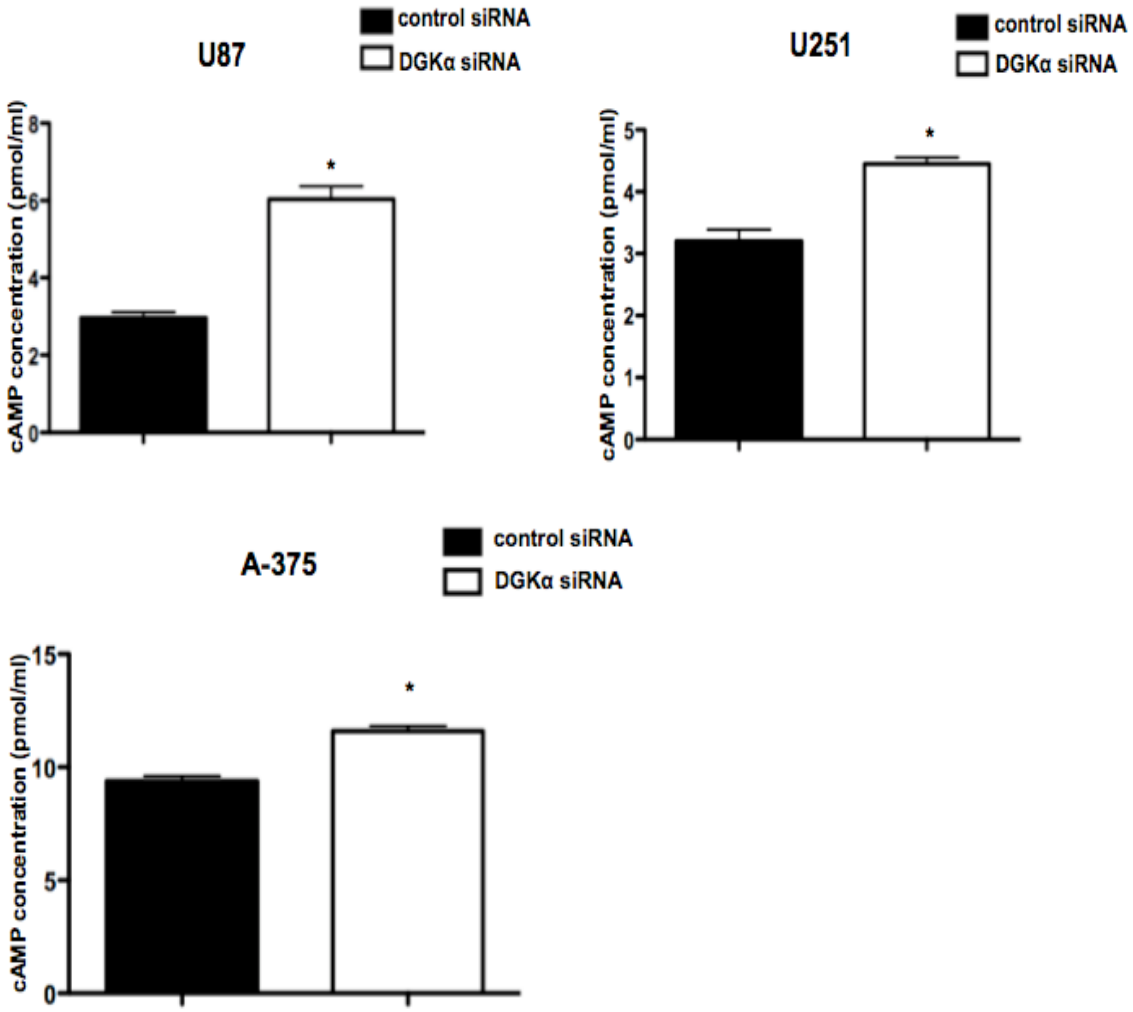

Figure 18. Levels of predicted mediator cAMP were measured by ELISA after attenuation of DGKα by siRNA in U87, U251, and A-375 cells. (*, P<0.05 and **, P<0.01 Student t test).

Figure 19

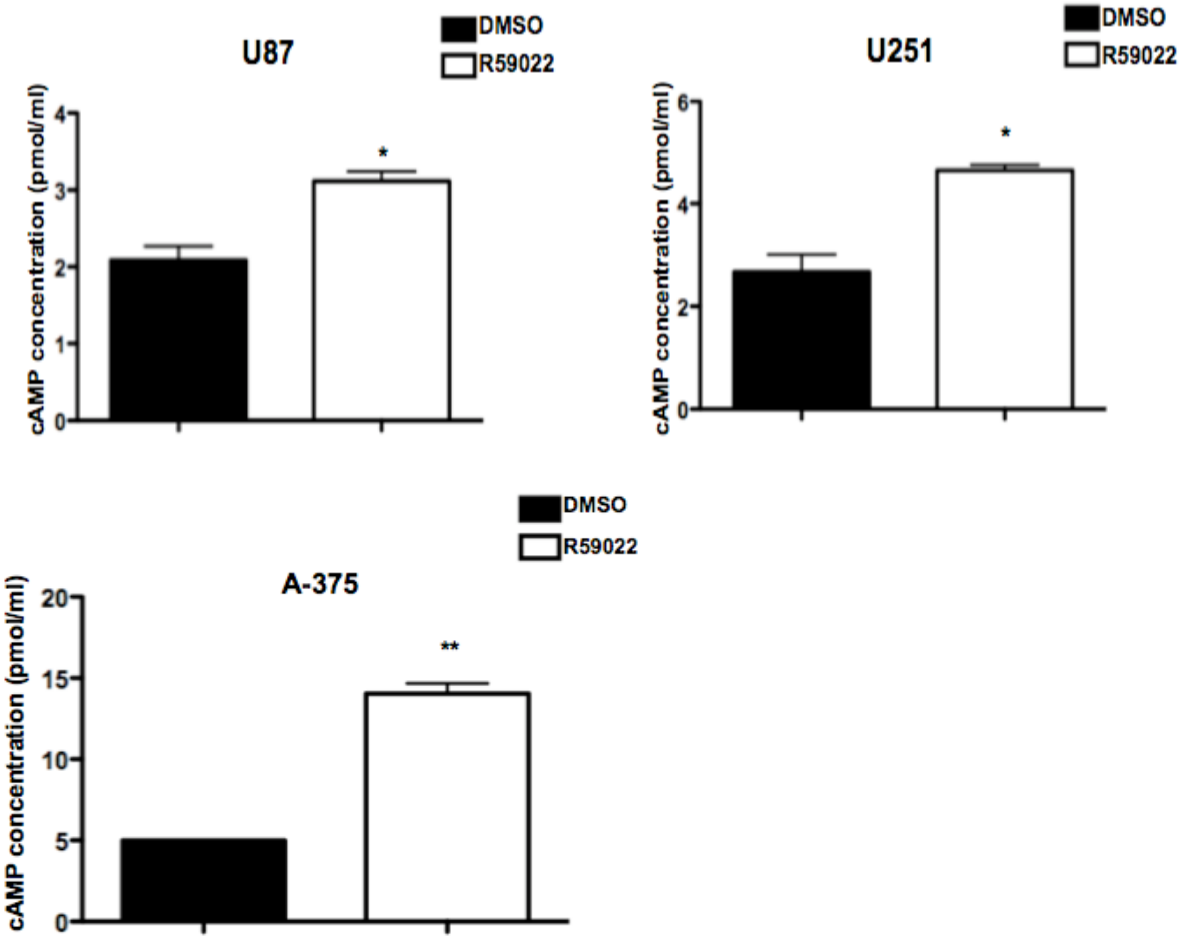

Figure 19. Levels of predicted mediator cAMP were measured by ELISA after attenuation of DGKα by small molecule inhibitor R59022 in U87, U251, and A-375 cells. (*, P<0.05 and **, P<0.01 Student t test).

Figure 20

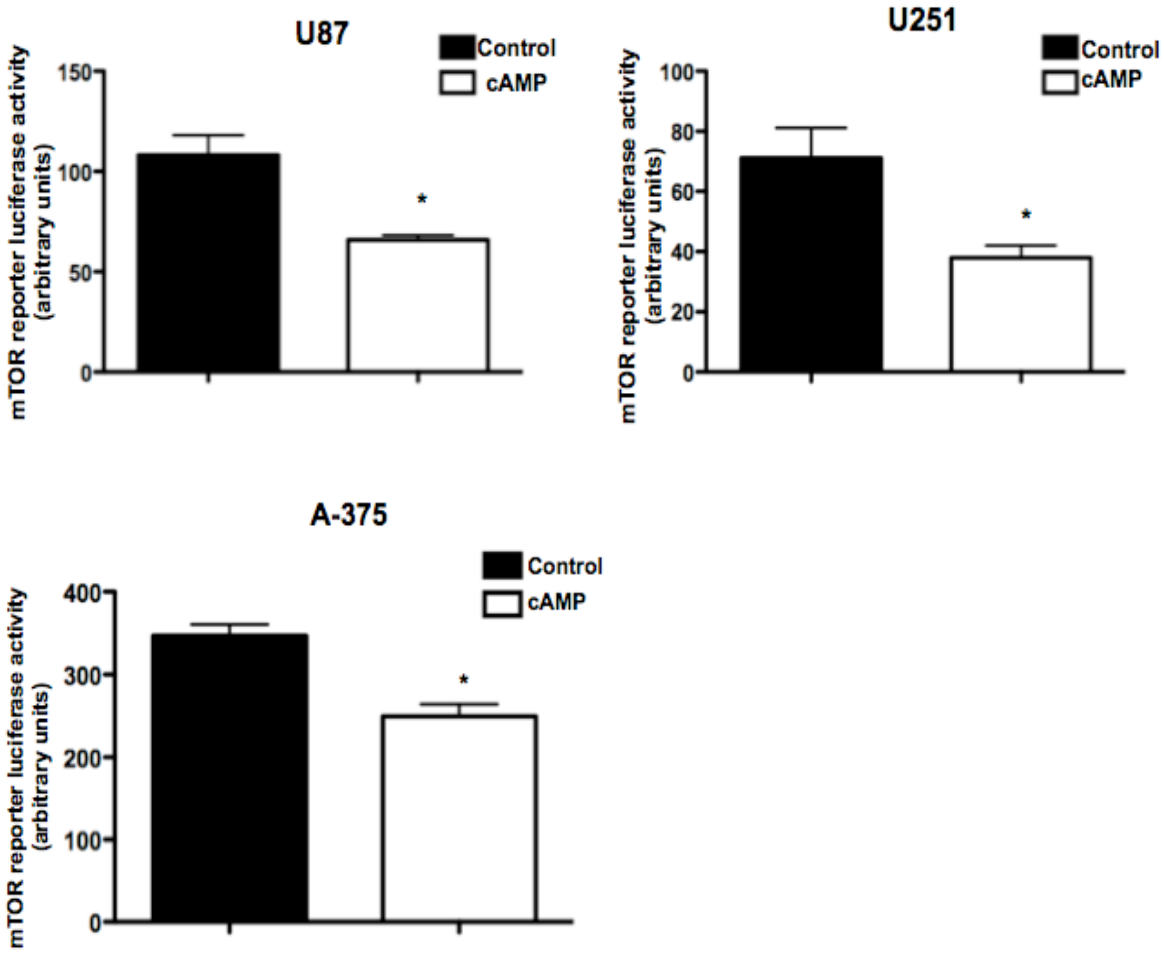

Figure 20. In U87, U251, and A-375 cells the effects of the addition of exogenous cAMP on mTOR transcription were evaluated through mTOR promoter luciferase activity assay. (*, P<0.05 and **, P<0.01 Student t test).

Figure 21

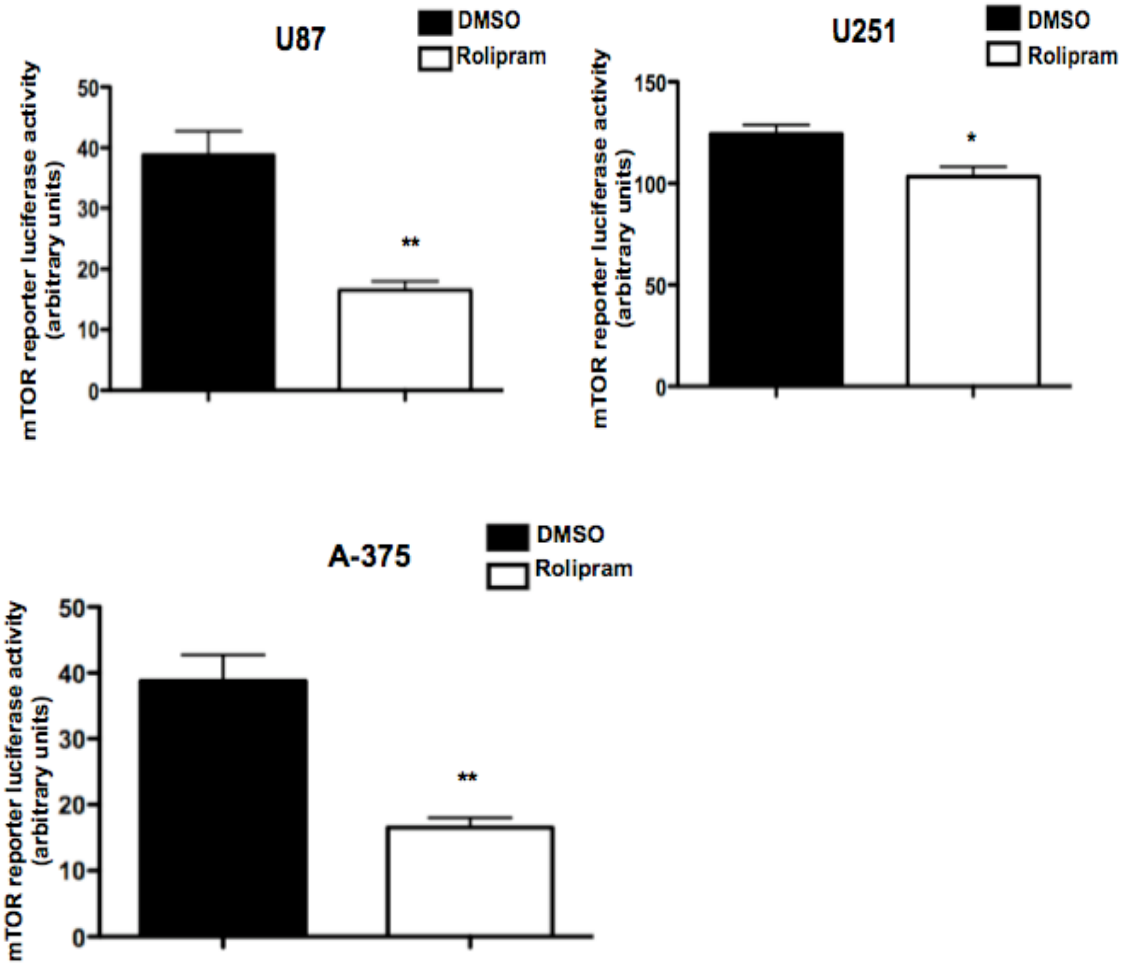

Figure 21. In U87, U251, and A-375 cells the effects of PDE4 inhibitor rolipram at 40 μM were observed to affect mTOR transcription by reporter assay. (*, $P<0.05$ and **, $P<0.01$ Student t test).

Figure 22

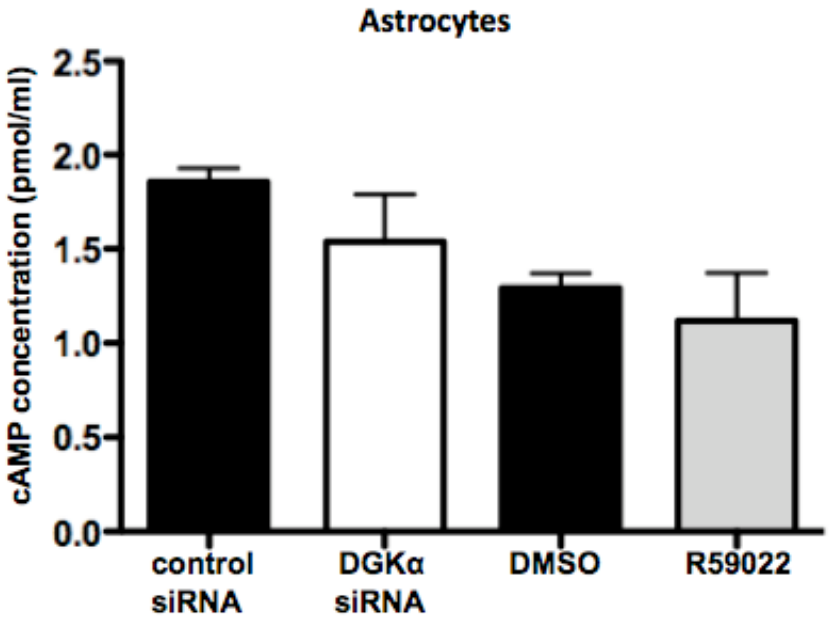

Figures 22. Levels of cAMP were evaluated via ELISA 5 days after knockdown and inhibition of DGKα in astrocytes.

Figure 23

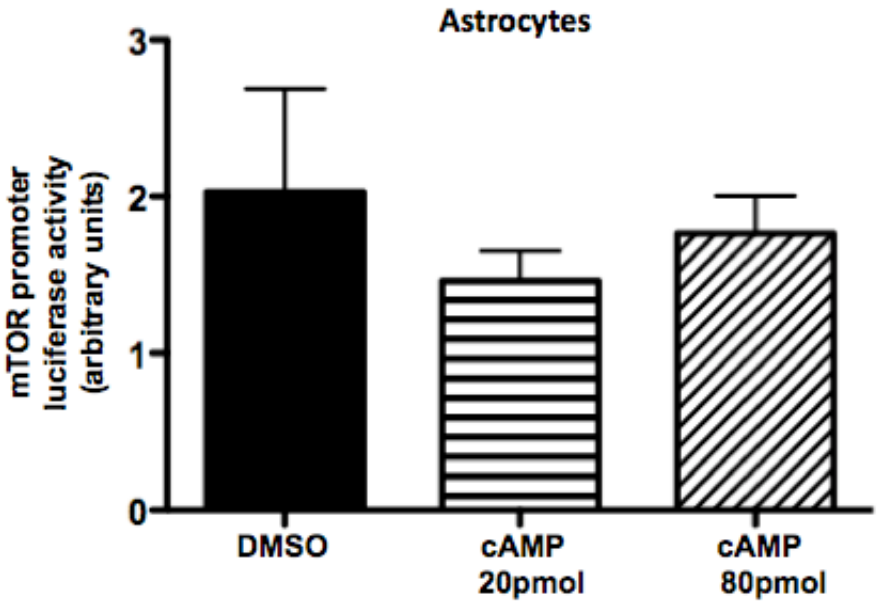

Figure 23. Effects of exogenous cAMP on mTOR transcription in astrocytes were assessed through mTOR promoter luciferase assay 5 days after treatment.

Figure 24

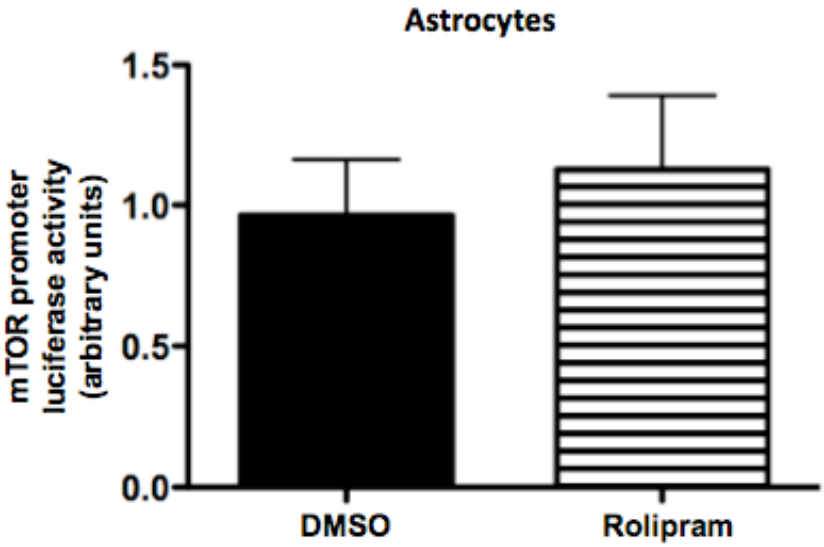

Figure 24. Rolipram was administered at 40 μM to further test the effect of phosphodiesterase inhibition/cAMP levels on mTOR transcription in astrocytes, with promoter activity assayed at 6 days post treatment.

Figure 25

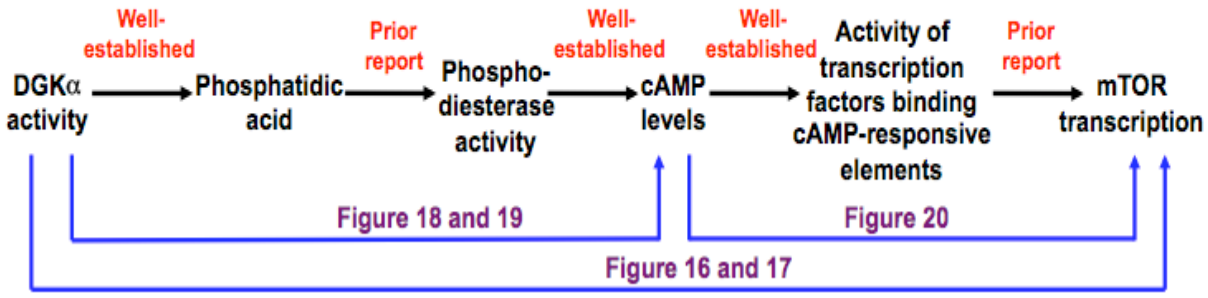

Figure 25. A schematic of the proposed pathway of DGKα regulation of mTOR transcription.

Figure 26

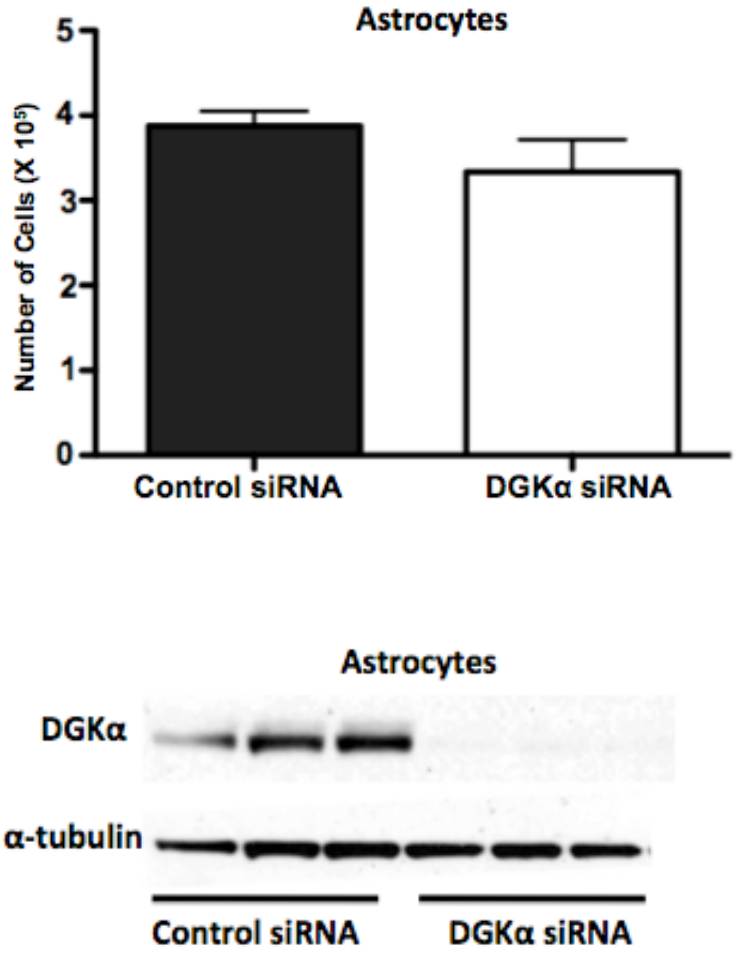

Figure 26. Normal human astrocytes were transfected with either control or DGKα siRNA, and cell number was assessed at 3 days post transfection. An immunoblot was done on cell lysates post-transfection to check for transfection efficiency.

Figure 27

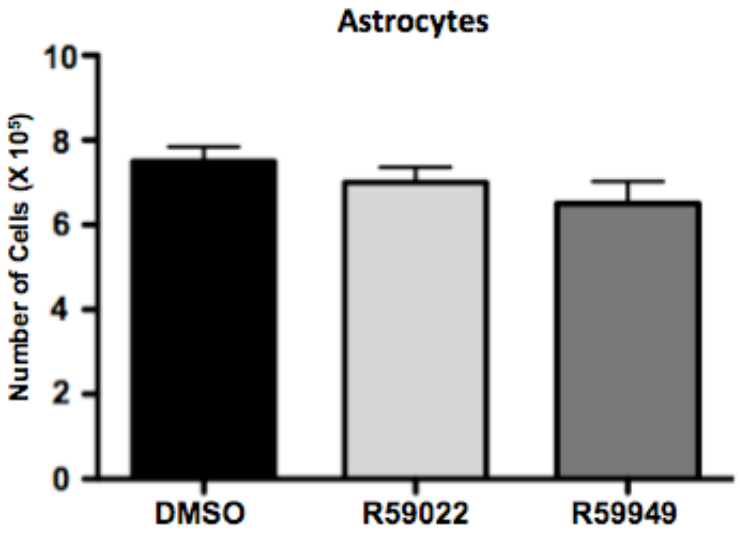

Figure 27. Normal human astrocytes were treated with 10 uM R59022, R59949, or DMSO (v:v) control and cell proliferation was assessed at 3 days post treatment, with no significant decrease observed in cell number.

Figure 28

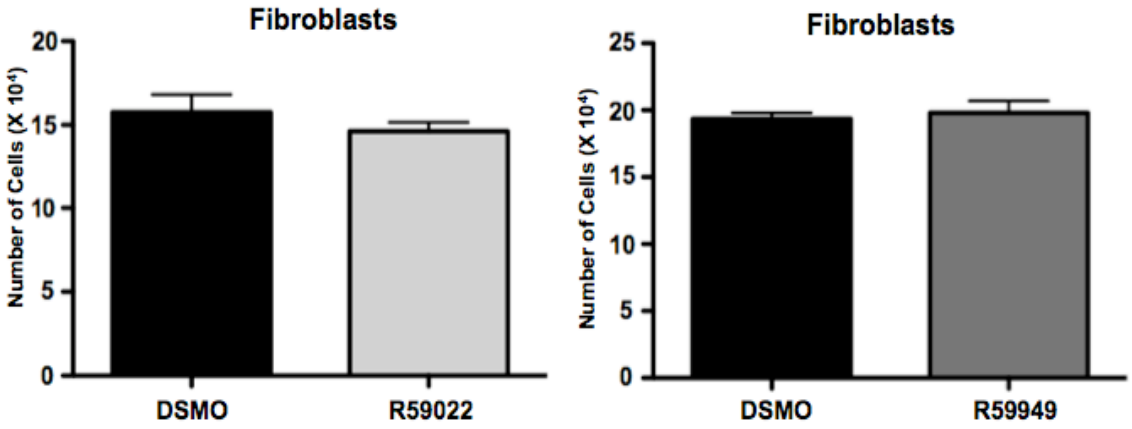

Figure 28. Normal human fibroblasts were treated with 10 uM R59022, R59949, or DMSO (v:v) control and cell proliferation was assessed at 3 days post treatment, with no significant decrease observed in cell number.

Figure 29

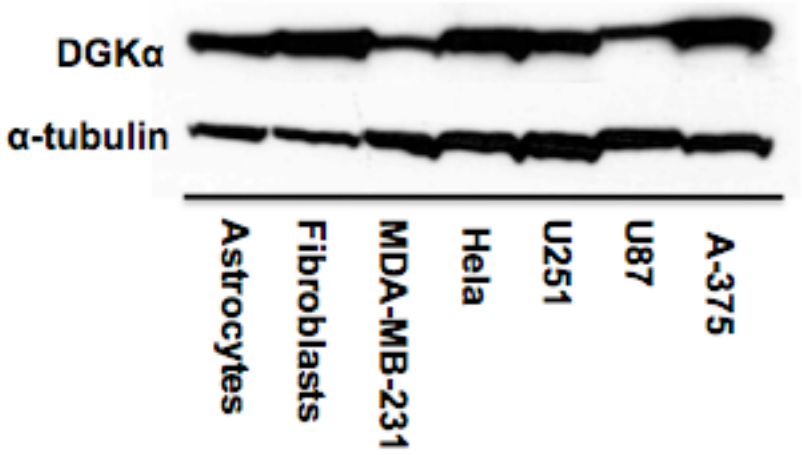

Figure 29. Basal DGKα levels were evaluated by immunoblot in normal human cell lines and various cancer cell lines, with α-tubulin shown as loading control.

Figure 30

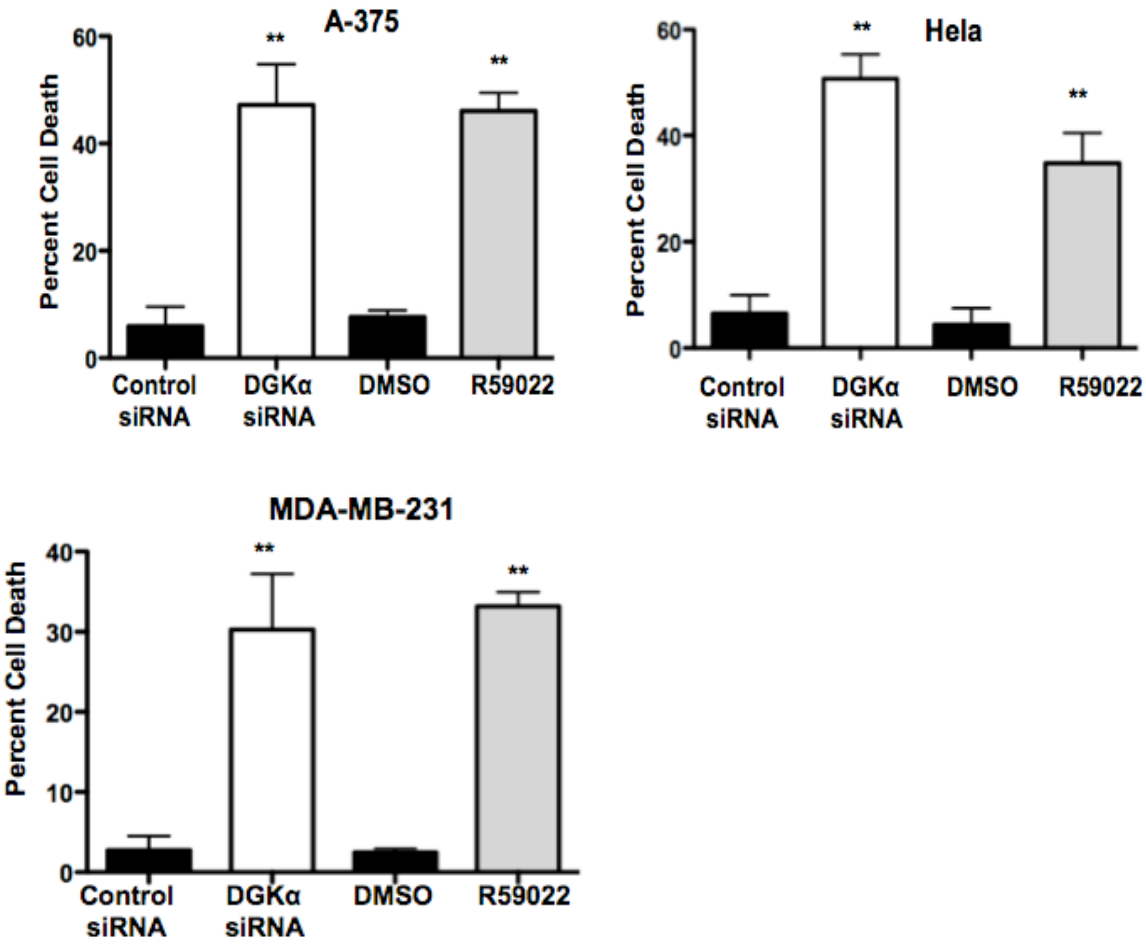

Figure 30. Cell toxicity was assessed by cell counts/trypan blue in A-375 (melanoma), HeLa (cervical cancer), and MDA-MB-231 (breast cancer) lines 4 days after DGKα knockdown or treatment with R59022 at 10 μM or DMSO vehicle. (*, P<0.05 and **, P<0.01 Student t test).

Figure 31

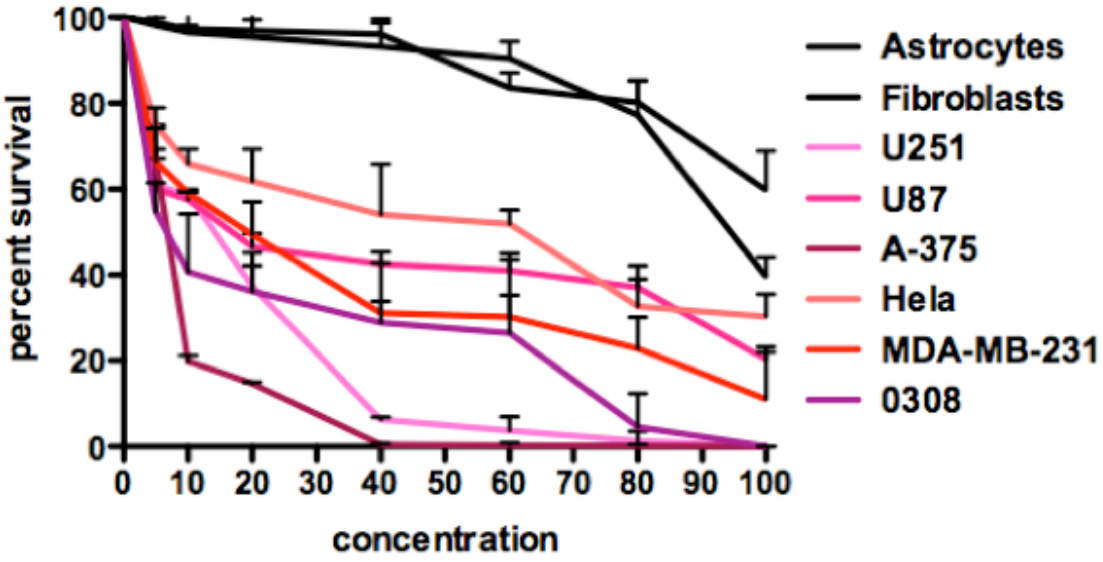

Figure 31. Dose response curves were generated for astrocytes, fibroblasts, U251, U87, A-375, HeLa, MDA-MB-231, and 0308 (GBM stem cell) cells by cell counts and normalized for DMSO (v.v) at 5, 10, 20, 40, 60, 80, and 100 μM R59022 after 4 days of treatment.

Figure 32

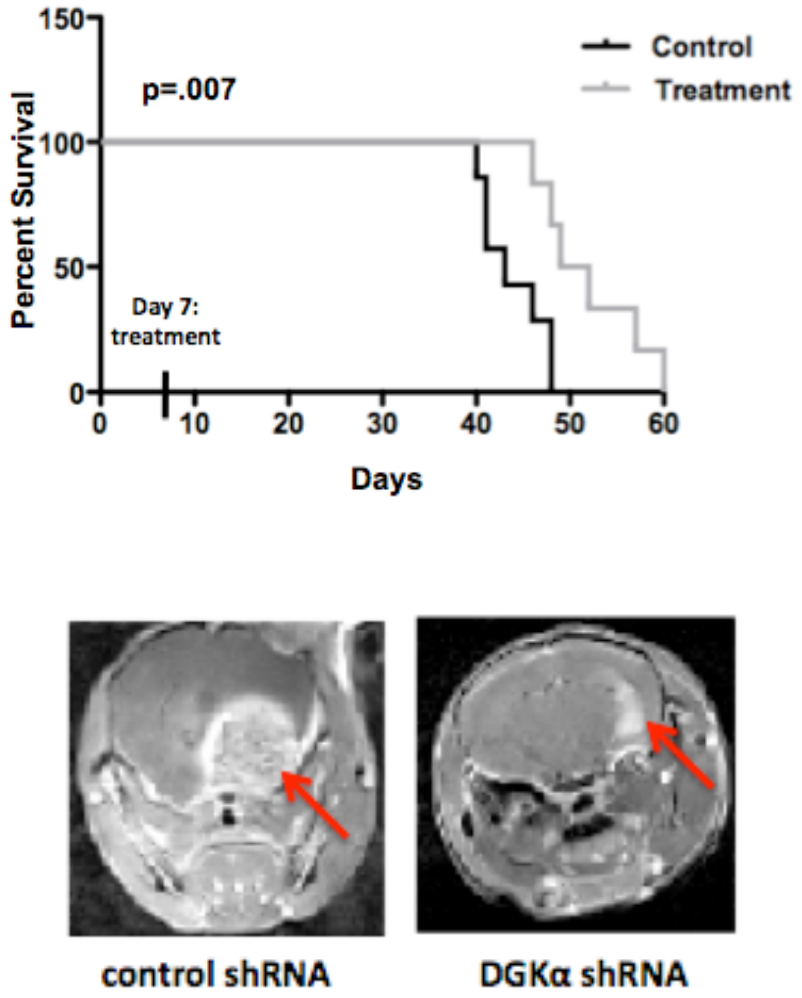

Figure 32. After *in vivo* implantation of 0308 GBM stem cells and CED infusion of lentiviral particles with control or DGKα shRNA one week later, mouse survival was followed. A Kaplan-Meier curve and log-rank analysis exhibits a significant increase in survival of mice in the treatment group when compared to control mice (p=.007). MRIs were also conducted at 40 days post tumor implantation and show characteristically smaller tumors in mice in the treatment group.

(* p<0.01 log-rank analysis).

Figure 33

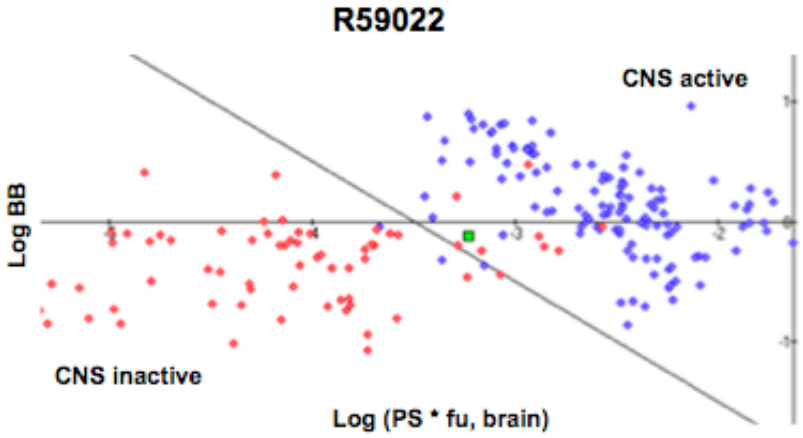

Figure 33. Plot of CNS activity presents several known CNS-penetrating (blue points) and peripherally acting (red points) drugs, with the green point denoting DGKα inhibitor R59022.

Figure 34

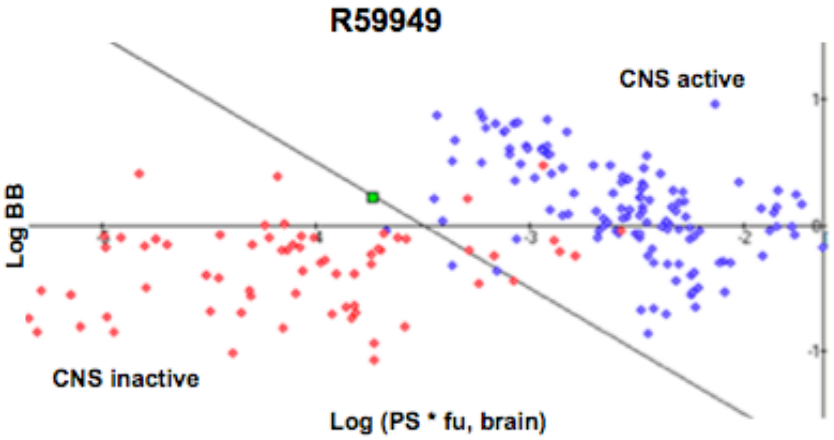

Figure 34. Plot of CNS activity presents several known CNS-penetrating (blue points) and peripherally acting (red points) drugs, with the green point denoting DGKα inhibitor R59949.

Figure 35

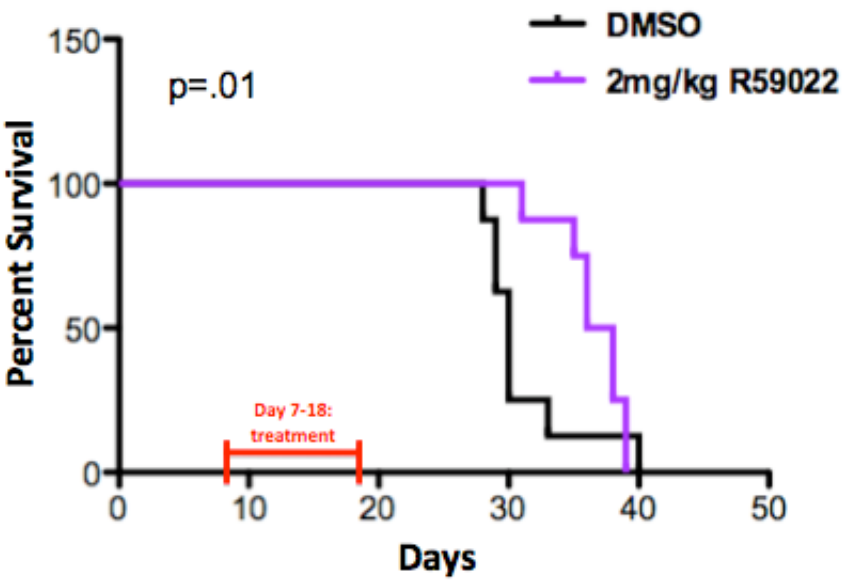

Figure 35. Mice were injected with U87 intracranially and then treated with daily IP injections of R59022 or vehicle on days 8 through 19. IP injections of R59022 at 2 mg/kg significantly increased median survival (p=.01) compared to DMSO (v:v) controls. (* p<0.01 log-rank analysis).

Figure 36

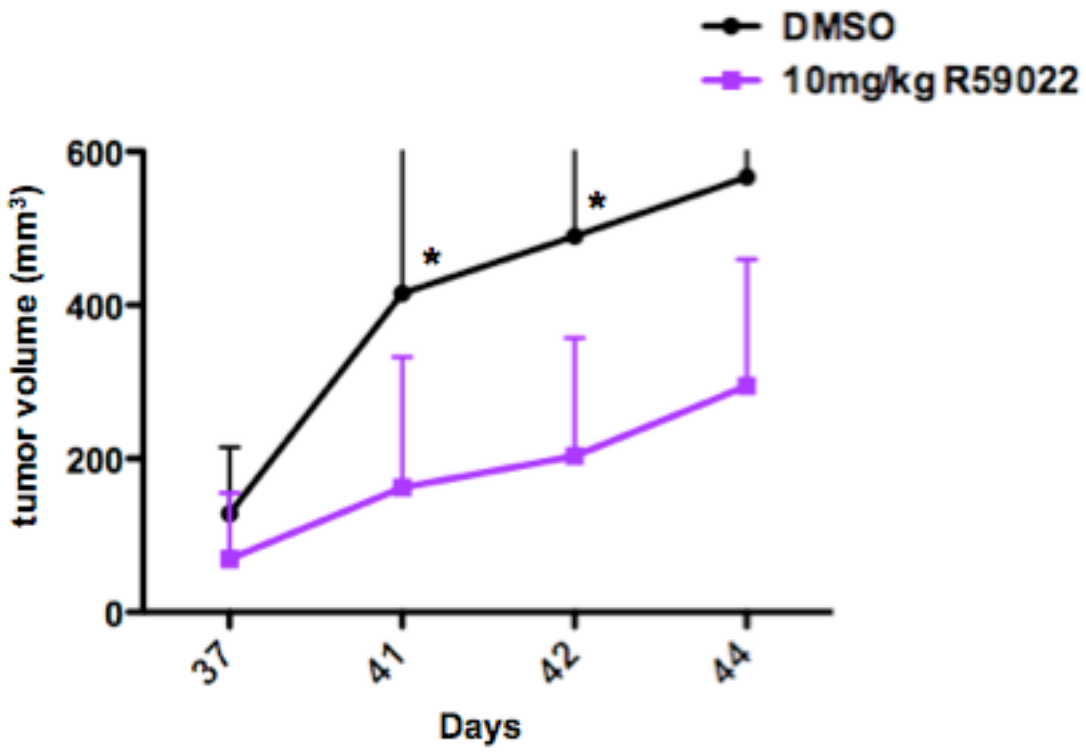

Figure 36: Tumor volume of subcutaneous U87 tumors *in vivo* was assessed after daily treatment with either R59022 10 mg/kg or vehicle, with treatment beginning 37 days after tumor implantation.

Figure 37

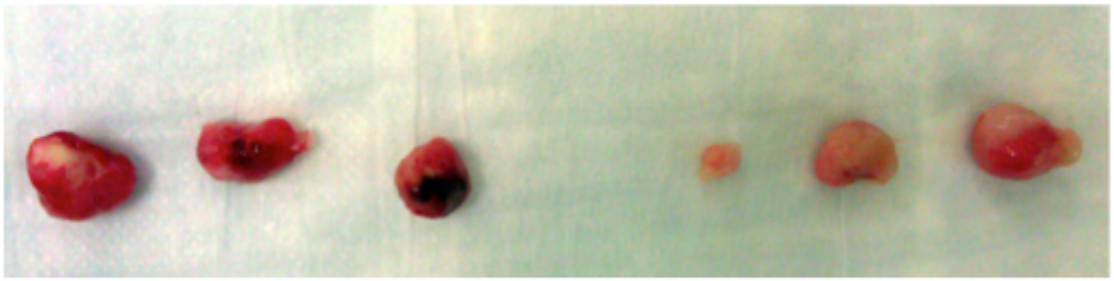

Figure 37: Subcutaneous U87 tumors were resected and exhibited a visible difference in vascularity after treatment with R59022 versus vehicle.

Figure 38

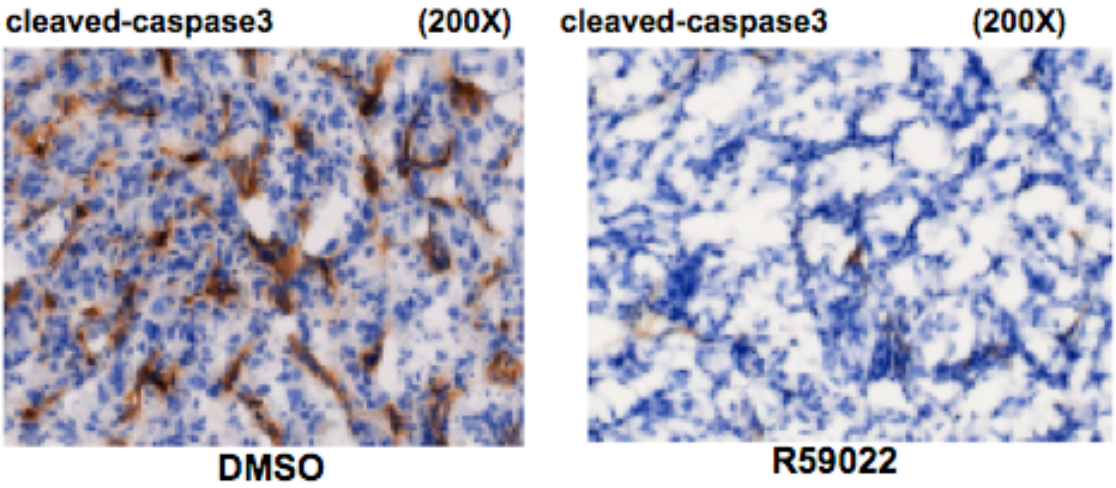

Figure 38. Subcutaneous U87 tumors were resected and frozen sections were stained for CD34 to assess for blood vessels after treatment (magnification of 200X).

Figure 39

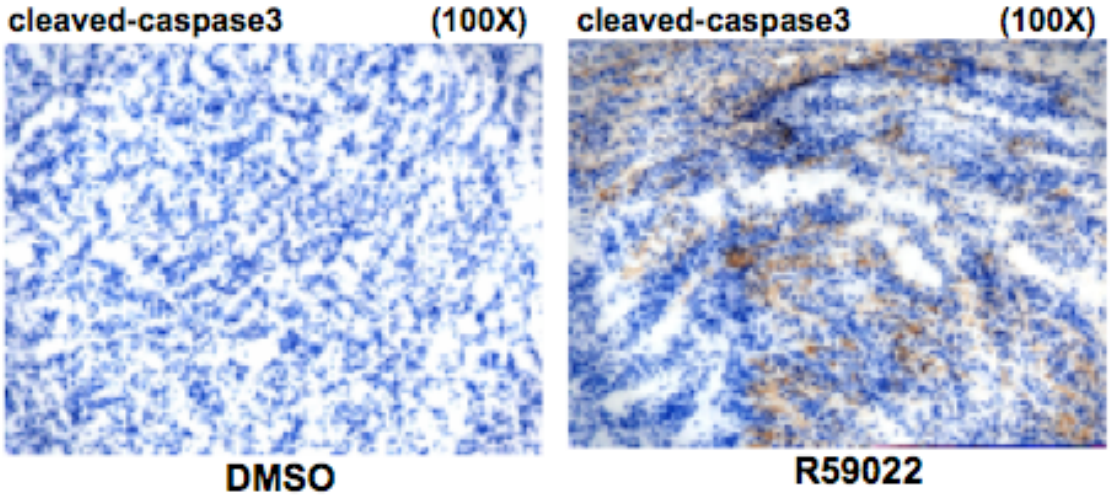

Figure 39. Immunohistochemistry was done for cleaved caspase-3 to assess apoptosis in the resected tumors above (magnification of 100X).

Figure 40

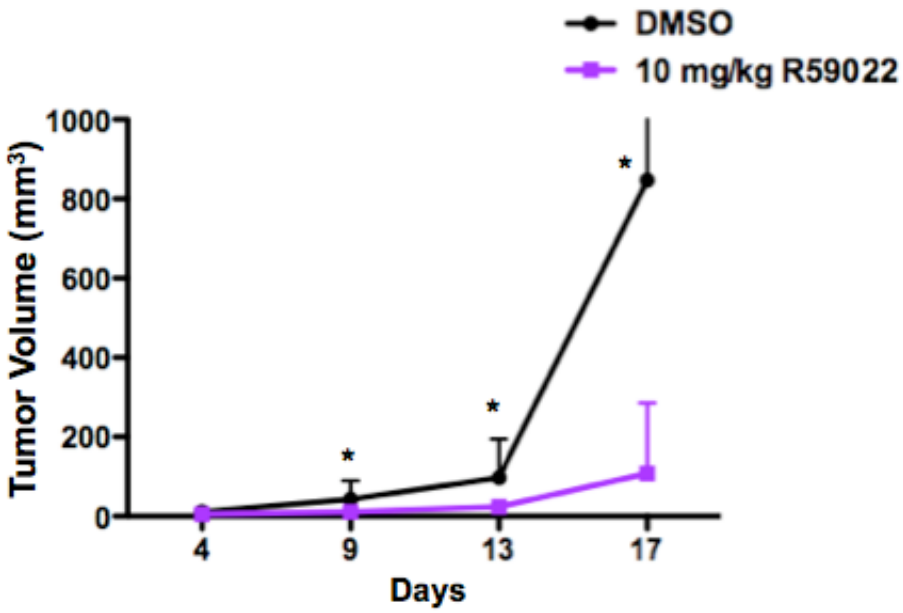

Figure 40: Tumor volume of subcutaneous A-375 tumors *in vivo* was evaluated after daily treatment with DMSO or R59022 at 10 mg/kg starting 4 days after tumor implantation.

Figure 41

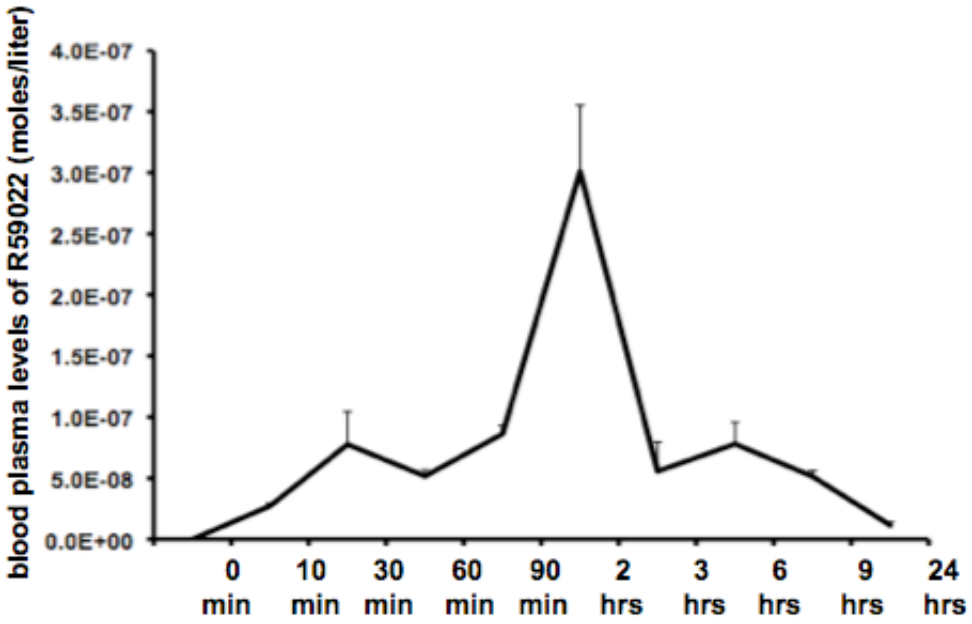

Figure 41. To evaluate the pharmacokinetics of R59022 *in vivo*, after a single IP dose of R59022 blood was collected at various time points via cardiac puncture, with the samples used for mass spectrometry for blood plasma levels of R59022.

III. DISCUSSION

While previous reports have linked DGKα to specific cellular pathways, this research has largely focused on cellular signaling (42, 46, 48, 53, 71, 72) or immunology (73, 74). This kinase has yet to receive significant attention for its impact on cancer cell viability and its potential as a cancer target. Notably, one recent report establishes a key role for DGKα in cancer cell migration (71), and even more recently it was noted that DGKα restrains the anti-tumor immune response (75). Our work establishes DGKα as a promising therapeutic target for the treatment of GBM, with potential for other cancers as well. The attenuation of DGKα through siRNA, shRNA, and small-molecule inhibitors all produce striking cellular toxicity in GBM cells, as well as in other cancers. Conversely, overexpression of this kinase promotes GBM cell proliferation *in vitro*, and expression levels are moderately increased in human GBM tissue samples. DGKα thus exhibits oncogene-like characteristics; however, the increase in DGKα expression is moderate, suggesting the possibility of a cancer-specific non-oncogene addiction and not a classic oncogenic model. The non-oncogene addiction model suggests that certain genes, while not significantly over-expressed in cancer, are nonetheless far more necessary for the survival of cancer cells than normal cells and can represent promising therapeutic targets (8, 9). That being said, profiling studies such as TCGA have indicated amplification of the DGKα locus in 1-4% of several cancers, as noted above. Further studies, with higher sample numbers, need to be done to assess

expression levels of DGKα in patient samples of GBM and other cancers to help clarify its degree of over-expression.

The history of cancer research is rife with examples of promising therapeutic strategies that proved disappointing in patients. This is due in large part to the genetic instability and heterogeneity of cancer cells, which render them able to develop resistance to treatments and adapt cellular networks to maintain a malignant phenotype (76). This seems especially likely for therapies directed toward a single target or pathway, as in therapies specifically targeting angiogenesis (77) or tyrosine kinases (78). Targeting a signaling node such as DGKα, with critical roles in numerous key cancer pathways, represents one answer to these obstacles. We have confirmed and extended the work of others to show that inhibition of DGKα decreases the expression and/or phosphorylation of mTOR (55), HIF-1α (53), Akt (66), and c-Myc (79). We hypothesized that regulation of these key oncogenic pathways underlies the cytotoxicity of DGKα inhibition. To assess their relative importance, we delivered mTOR, HIF-1α, and c-Myc plasmids to GBM cells treated with DGKα inhibition. Both mTOR and HIF-1α plasmids partially rescued cell toxicity, and even more so when combined. While inhibition of mTOR and HIF1-α were critical in mediating DGKα inhibition in GBM cells, it is important to note that other pathways may be more central in other cancers; DGKα has been shown by others to mediate Ras/Raf (80), ALK (81), Met (82), and VEGF (46) signaling. Furthermore, we found a link between DGKα inhibition and the transcriptional regulator SREBP (83), which has recently been found to promote tumor growth in GBM patients through the PI3K/AKT

signaling pathway (68). After DGKα silencing, mRNA expression of several genes induced by SREBP were significantly decreased. It is notable that SREBP has also been linked to mTOR and PA signaling, which suggests that DGKα may regulate SREBP via more than one pathway. While the intricacies of the mechanisms through which DGKα inhibition exerts its toxic effects on different cancers need further investigation, we are optimistic that this approach may damage too many oncogenic pathways for cancer cells to adapt to treatment.

We were initially surprised to see equally strong rescue in cancer cell toxicity from DGKα inhibition with expression vectors for mTOR and constitutively-active mTOR (data not shown). This, along with a strong correlation between DGKα and mTOR expression levels in TCGA GBM samples, suggested that DGKα might be regulating mTOR expression as well as activity. Further experiments supported this, via a unique DGKα—PA—PDE—cAMP—mTOR transcription pathway. This appears to be a significant function for DGKα in cancer cells. These results have importance not only for neuro-oncology, but also for the study and targeting of cAMP and mTOR in cancer. It indicates a new approach to mTOR inhibition, using small-molecule DGKα inhibitors to decrease mTOR expression. Reducing mTOR expression may have advantages over mTOR inhibitors now in use that inhibit mTORC1 and/or mTORC2, given that mTOR has been hypothesized to participate in an mTORC3 complex and may have other pro-cancer functions as well. DGKα inhibition also seems to represent a novel cancer-specific means to elevate cAMP levels selectively in cancer cells, potentially avoiding side effects from non-selective cAMP-elevating agents such

as phosphodiesterase inhibitors. In addition, these findings are likely to have implications for other signaling pathways in cancer that also regulate cAMP levels.

Most successful cancer treatments have a broad therapeutic window, i.e. they affect cancer cells at much lower concentrations than they do normal cells. The ideal treatment would pose little risk to normal cells while efficiently killing cancer cells. It is important to note that DGKα inhibition significantly affects cell viability in normal human cells only at very high concentrations, suggesting there may be a substantial therapeutic window *in vivo*. The minimal effect in non-cancerous cells, combined with the marked toxicity in GBM cells, also points to the possibility of cancer cells having a dependence on DGKα that is not seen in normal cells. Though there have been ten DGK enzymes discovered to date, there does not seem to be functional redundancy and DGKα seems to be particularly relevant for cancer cells. For example, it has been shown that normal melanocytes do not express DGKα, while melanoma cells do express this isoform (48). It is notable that DGKα knockout mice are generally healthy, with a defect in T cell anergy (84). Our *in vivo* experiments supported the potential safety of using DGKα small-molecule inhibitors, as no toxicity was observed and there was no decrease in mouse weights with R59022 treatments at doses of 2 or 10mg/kg (data not shown). While promising in these preliminary studies, the safety profile of DGKα inhibition needs to be evaluated with detailed animal studies.

These results also showed the utility of a single injection of DGKα-targeted therapy in a challenging GBM treatment model, using highly-invasive and resistant GSCs. Convection-enhanced delivery (CED) was utilized for the infusion of lentiviral particles carrying DGKα shRNA, in a manner that could be clinically applicable. The shRNA targeting DGKα was delivered in lentiviral particles to achieve long-term expression (85). The fact that DGKα knockdown through a single infusion had a significant effect on tumor growth *in vivo* is encouraging, and it is likely that repeated treatment with DGKα inhibition would result in improved efficacy.

The therapeutic potential of DGKα inhibition is facilitated by its being druggable, with two compounds already available. While it is always possible with small-molecule agents such as R59022 and R59949 that nonspecific effects contributed to their toxicity in cancer cells, the PA-replacement rescue experiments shown here argue against this. Initial *in vivo* experiments supported the therapeutic potential of these DGKα small-molecule inhibitors. This was true in both orthotopic and subcutaneous GBM models, as well as in a subcutaneous melanoma model. Our experiments also suggested that this *in vivo* efficacy might have been due at least in part to potent antiangiogenic effects. Pharmacokinetic studies indicated that the positive *in vivo* results were obtained despite a short R59022 half-life in the mouse. It is possible that R59022 accumulates in the tumor with repeated dosing, or that tumor cells are sensitive to lower concentrations *in vivo* than they are *in vitro*. We demonstrate that R59022 exhibits a pronounced anti-angiogenic effect *in vivo*, and this may occur

at lower concentrations than what was utilized *in vitro*. Regardless of mechanism, the pharmacokinetic data suggest that better efficacy could be achieved with DGKα inhibitors optimized for *in vivo* usage.

We propose that this work sets the foundation for DGKα as a promising therapeutic target in cancer. These results shed light on the significant effects of DGKα inhibition on cancer cell viability, the possibility it is an oncogene or example of non-oncogene addiction, and its safety for normal cells. Our results establish DGKα as a single therapeutic target linked to multiple oncogenic pathways, with relevance for GBM and other cancers as well. This work also indicates the importance of the DGKα product PA in cancer cell biology, and ongoing studies are evaluating this signaling phospholipid as a therapeutic target in itself.

Inhibition of all three phosphatidic acid synthetic pathways

I. INTRODUCTION

As described in detail above, diacylglycerol kinase alpha is responsible for the phosphorylation of DAG to produce PA. Both DAG and PA are important lipids that act as intermediates in biosynthetic pathways, such as PKC (86) and RasGRPs (87). DGK regulation of intracellular levels of DAG and PA is crucial to maintain the proper balance between these two lipids. While we have shown the potential of DGKα as a therapeutic target alone, some of our data, along with recent publications(69, 70), have made it evident that there is potential in targeting PA itself. Importantly, there are numerous other manners in which PA is produced. There are three major routes of PA synthesis: DGK phosphorylation of DAG, conversion of lysophosphatidic acid (LPA) by lysophosphatidate acyltransferase (LPAAT), and phospholipase D (PLD) hydrolysis of membrane phospholipids.

As shown above, we began working under the hypothesis that DGKα is a promising novel therapeutic target that can act as a crucial regulator of cell signaling in cancer biology. Yet, there are 9 other isoenzymes that we did not explore, all of which produce PA (38). DGKs vary in organ and cellular distribution, which leads to essential differences in functionality. The tissues with the most DGK expression are brain and hematopoietic organs, and DGKs α and ζ are the most common isoenzymes (45). According to the National Center for Biotechnology Information (NCBI) database for expressed sequence tags (ESTs) (http://www.ncbi.nlm.nih.gov/dbEST/), DGKs β, ι, and κ are expressed in fewer

tissues and at lower levels than other DGKs. There are some patterns of distribution that are of note; DGKβ is mainly expressed in neural tissue, while DGK ε and γ are the only isoforms expressed in adipose and pituitary tissue, respectively. DGKα is one of the only DGKs expressed in both lymphocyte-rich tissues and in bone marrow, indicating the important role this isoform plays in the immune system, particularly in T cell function (84). DGKs also differ in cellular distribution, as varying extracellular stimuli can cause the production of nuclear and cell membrane DAG (88). Some, like DGKs α, ι, and ζ (47, 89-91), shuttle to and from the nucleus and plasma membrane. Others remain localized, such as DGKθ in the nucleus (43) and DGKκ (92) at the plasma membrane. The differences in tissue distribution and cellular localization are linked to the diverse interactions each DGK has with different proteins and multiple signal transduction pathways. Modulation of DGK activity is promising as there are no established pathologies and few consequences of knocking out a single isoform (84, 93-95). Given the wide range of functionality of DGKs, the common factor in exploring DGK modulation for developing therapeutic targets is the effect of DGK activity generating PA. This common factor among DGKs, along with the work above that indicates the importance of the DGKα synthesis of PA in cancer cell biology, suggests that this signaling phospholipid needs to be explored as a therapeutic target in itself.

Lysophosphatidate acyltransferase (LPAAT) produces PA from lysophosphatidic acid (LPA). Lisofylline (1-(5-R-hydroxyhexyl)-3,7-dimethylaxanthine), a modified methylxanthine, is a potent inhibitor of this

synthesis. Administration of lisofylline (LSF) has been studied for its potential as a cancer therapy treatment. LSF inhibited the release of hematopoietic inhibitors stimulated by chemotherapeutic agents (96), enhanced response to (cis-diamminedichloroplatinum (II)) cisplatin in ovarian carcinoma cells with p53 deletion (97), and caused a reduction in survival and growth of tumor cells in a mammary carcinoma murine model (98). With evidence of LSF suppression of LPAAT synthesis of PA as a potential therapy for cancers and other medical disorders, the biopharmaceutical company Cell Therapeutics has attempted to advance LSF to clinical use. There are shortcomings to the clinical use of LSF, though; it has low oral bioavailability and a short half-life that might require continual intravenous infusion in humans (99). However, there is evidence that LSF may have lasting effects long after the drug levels are no longer biologically detectable; protection of hematopoiesis from chemotherapeutic agents was still observed 48 hours after pre-treatment with LSF (96). One of the major implications of PA in cancer is its ability to regulate mTOR signaling, and enzymes that generate PA have the potential to regulate mTOR. LPAAT-theta production of PA has been shown to activate mTOR signaling via phosphorylation of p70S6K and 4EBP1 when rapamycin is not present (100). This finding of LPAAT activation of mTOR in the absence of rapamycin adds evidence of mTOR signaling's potential reliance on PA production as a 'backup' or enhancement for optimal signaling in cancer cells. All of this taken together substantiates the production of PA by LPAAT as a potential therapeutic target and an important factor in the extensive effect of PA on cancer cell signaling.

There are two mammalian forms of Phospholipase D, PLD1 and PLD2, which utilize water to hydrolyze phospholipid substrates to generate PA (101). Both isoforms require phosphatidylinositol 4,5-bisphosphate (PIP_2) as an activator, but differ in most other regards. They both have different regulatory functions, localization, and basal activity levels. PLD1 is activated by small G proteins and protein kinase C (PKC), while PLD2 is insensitive to these activators (102). PLD and its production of PA have been linked to many biological processes, such as autophagy, diabetes, inflammation, and cellular pathways in the context of cancer biology. Increased PLD activity has been shown to increase MDA-MB-231 breast cancer cell migration (103), is required for secretion of matrix metalloproteinase-2 in glioma cells (104), is a mediator between Ras/PI3k signaling and downstream effectors MAPK and AKT to promote anchorage independent survival (66), and activates and interacts via a positive feedback loop with the Wnt/β-catenin signaling pathway implicated in tumorigenesis in several cancers (105). Notably, PLD synthesis of PA has been found to be a critical mediator of mTOR signaling. In kidney carcinoma and breast cancer cells, PLD inhibition produced a marked decrease in phosphorylation of S6K and AKT, which are downstream of mTORC1 and mTORC2, respectively [(65), (20)]. In concordance with this observation, the effect of PA absence on phosphorylation of downstream mediators was reversible with the addition of 100μM exogenous PA. Interestingly, mTORC1 and mTORC2 were broken down when PA production was suppressed and were incapable of being restored with the addition of a cross-linking reagent, which contrasts with rapamycin breakdown of

the complexes (20). As PLD has gained more interest as a possible therapeutic target, specific small molecule inhibitors need to be established to replace the classic 1-butanol inhibition of PLD approach, which can have confounding cellular effects. Recently, FIPI (5-fluoro-2-indolyl des-chlorohalopemide) was introduced as a potent PLD inhibitor that selectively inhibits PLD activity without sequestering its activators or altering localization. While FIPI is just beginning to be investigated, it has already been shown to inhibit cell spreading and chemotaxis at low concentrations (106). Taken together, these findings show that PLD production of PA is proving to be a key contributor to this novel target system as well. As evidence mounts for each synthetic pathway of PA as a potential target for cancer therapy, we increasingly believe that PA is a promising single target with high impact on cancer cell biology that can provide a novel therapeutic approach for treatment-resistant cancers, including GBM.

II. RESULTS

Inhibition of PA causes toxicity in multiple cancer cell lines but not in non-cancerous cells

Early experiments utilized the different small molecule inhibitors that target each pathway of PA synthesis. We have employed two established DGKα inhibitors, R59022 and R59949 in our preliminary data as well as above (52). Both of these inhibitors are believed to inhibit the catalytic domain of DGKα. Lisofylline has anti-inflammatory properties and suppresses the function of LPAAT (107). Lastly, there is evidence that 1-butanol (101, 102) selectively inhibits the catalytic activity of PLD1/2. Initially, we sought to explore PA inhibition with the use of R59022, LSF, and 1-butanol with DMSO and tert-butanol as controls (v:v). Each small molecule inhibitor was administered alone, and all three in combination, in U251 glioma, HeLa cervical, and A-375 melanoma cells. Cell proliferation was assessed 5 days post treatment and was significantly decreased with each treatment of single inhibitor, with an even greater decrease in proliferation with combination treatment (Fig. 40). Given the positive data presented above exhibiting the lack of toxicity in non-cancerous human cells with DGKα inhibition with R59022, we sought to assess the effect of combination PA inhibition on non-cancerous cells as well. Normal human fibroblasts were treated with PA inhibition, and similarly we did not observe any significant decrease in cell viability at concentrations toxic to the cancer lines (Fig. 41).

Next, we began to utilize a recently developed small molecule inhibitor specific for PLD1/2, FIPI, to investigate inhibition of PA through all three synthetic

pathways. FIPI was used because of many advantages over 1-butanol. PLD1/2 activity is inhibited by FIPI with greater specificity, as it does not change localization of PLD and it does not sequester PIP2 cofactor (106). R59022, LSF, and FIPI were administered alone and in each combination of double and triple drug combination. Cell viability was assessed 5 days post treatment in U251 glioma and 0308 glioma stem cells (Fig. 42). Similar toxicity was observed in A-375 melanoma cells as well (Fig. 43). According to analysis done by our collaborator Mark Conaway, a 3-way ANOVA statistical test verified that the administration of the triple drug combination proved to have a synergistic effect when compared to either the single or double drug combinations. In addition, upon administration of this treatment in normal human astrocytes and fibroblasts, there was no significant decrease in cell proliferation (Fig. 44). Notably, the phenotype observed through this inhibition can be successfully rescued with administration of exogenous PA (Fig.45). Using these three types of small molecule inhibitors to target the synthesis of this signaling phospholipid should prove to be a highly effective novel therapy for cancer through regulating multiple cancer signaling pathways.

Figure 42

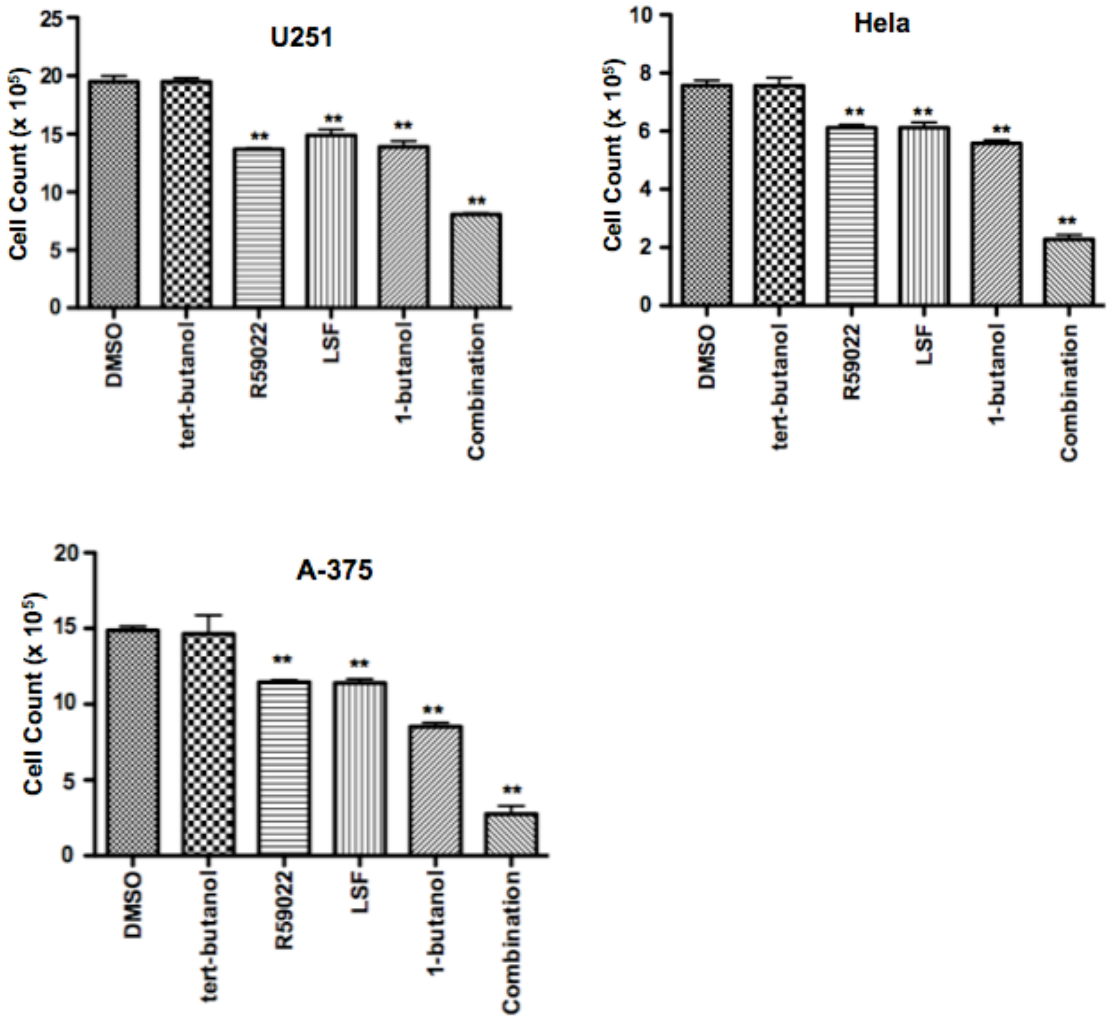

Figure 42: Phosphatidic acid (PA) was inhibited with the use of R59022, Lisofylline (LSF), and 1-butanol. Each of the small molecule inhibitors and 1-butanol were administered alone at 2-5uM and .27%, respectively. Combination of all three inhibitors was administered as well, with tert-butanol and DMSO controls at equal volume to combination treatment in U251, HeLa, and A-375 cells (*, $P<0.05$ and **, $p<0.01$).

Figure 43

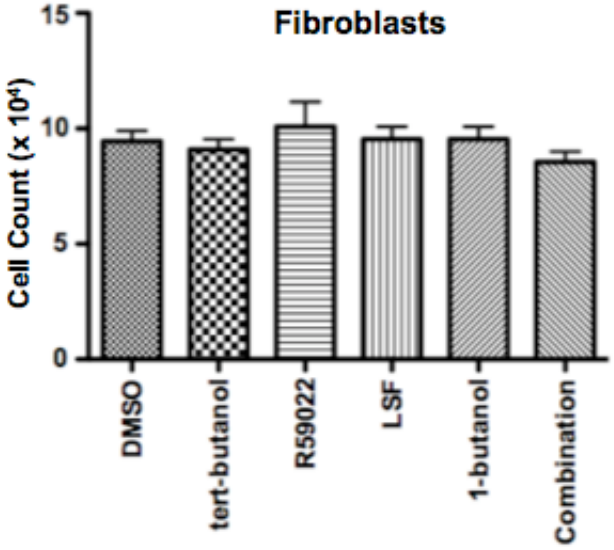

Figure 43: Phosphatidic acid was inhibited in non-cancerous human fibroblasts with and cell proliferation was assessed after 4 days with no significant toxicity observed.

Figure 44

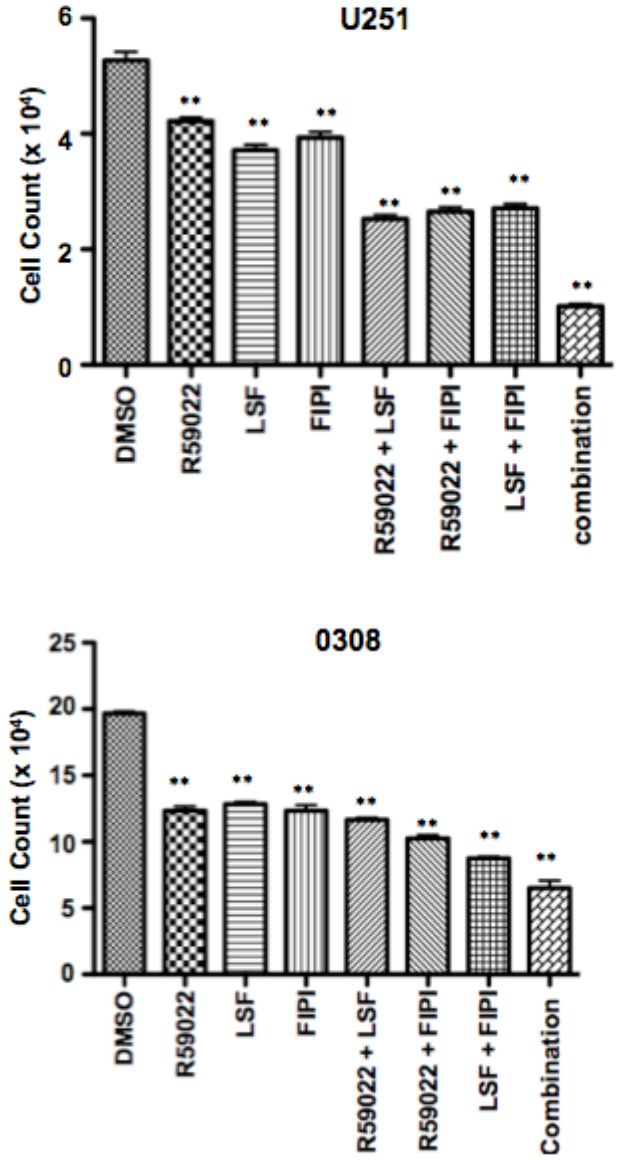

Figure 44. Combination treatment with R59022, LSF, and FIPI for the inhibition of PA synthesis was conducted in U251 glioma and 0308 glioma stem cells. Each small molecule inhibitor was administered at 3uM for each cell line. A 3-Way ANOVA revealed that the combination treatment with triple drug administration has a statistically significant synergistic effect when compared to double drug combination (*, $P<0.05$ and **, $p<0.01$).

Figure 45

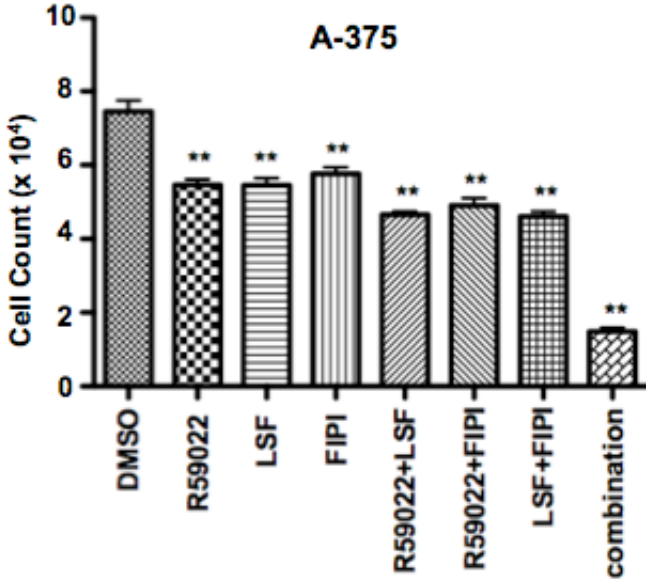

Figure 45. Combination treatment with R59022, LSF, and FIPI for the inhibition of PA synthesis was conducted in A-375 melanoma cells. Each small molecule inhibitor was administered at 3uM for each cell line. A 3-Way ANOVA revealed that the combination treatment with triple drug administration has a statistically significant synergistic effect when compared to double drug combination (*, $P<0.05$ and **, $p<0.01$).

Figure 46

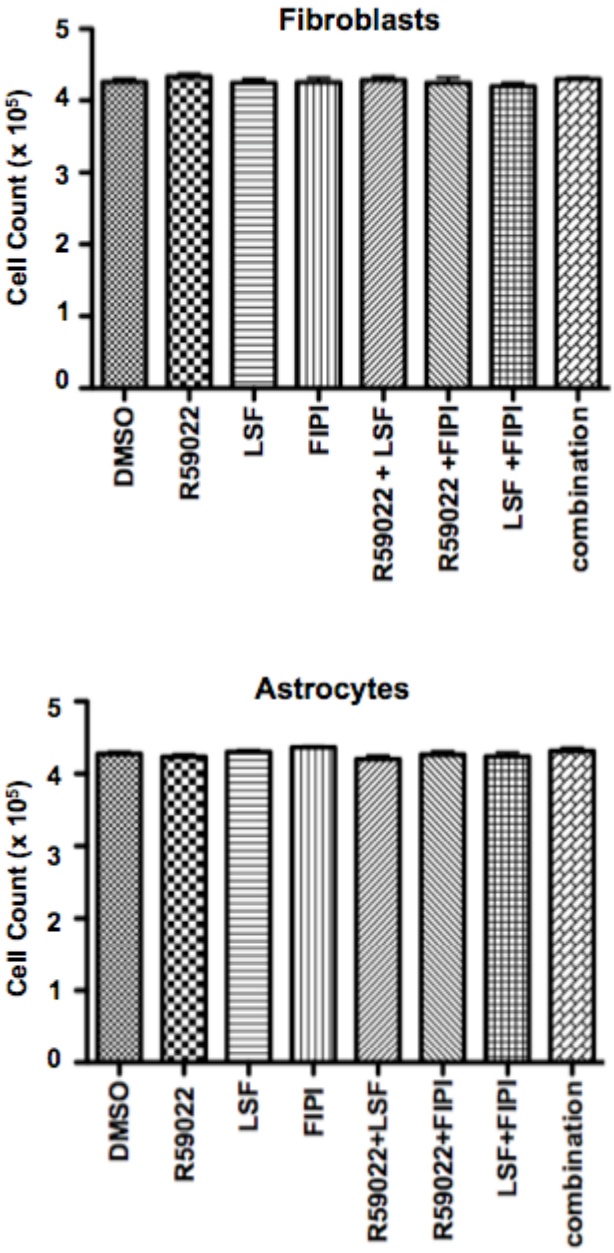

Figure 46: Normal human astrocytes and fibroblasts were treat with each inhibitor at 3uM or DMSO (v:v) control and cell proliferation was assessed at 3 days post treatments, with no significant toxicity observed.

Figure 47

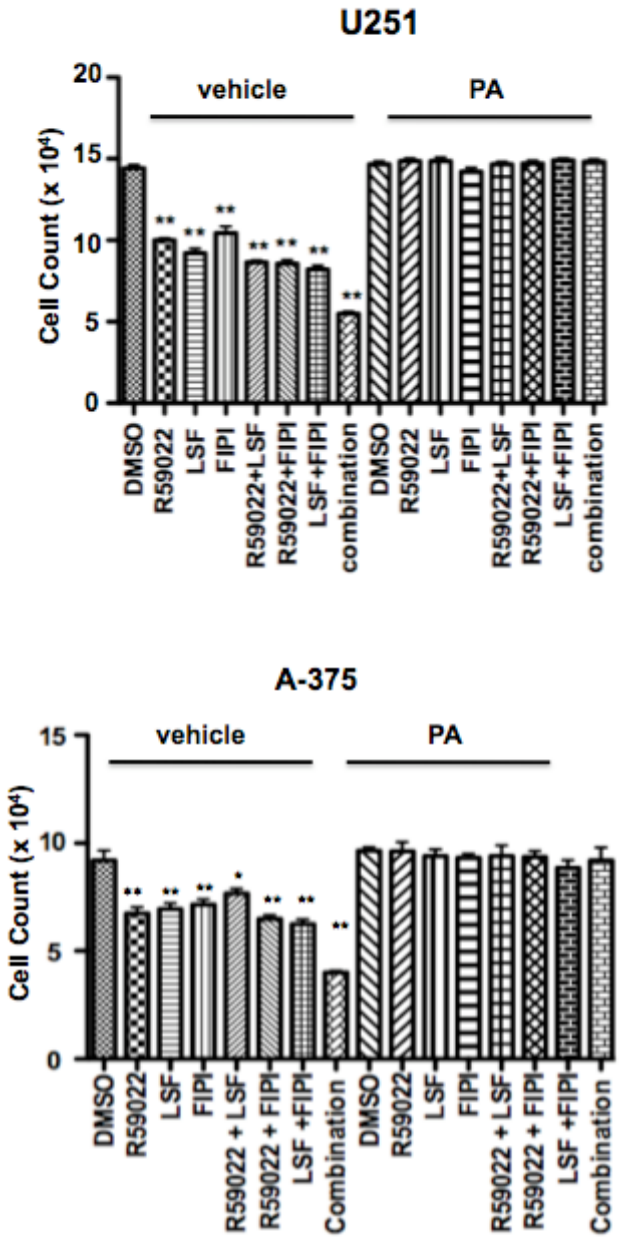

Figure 47: U251 GBM and A-375 melanoma cells were treated with R59022, LSF, and FIPI at 3uM for each treatment with simultaneous administration of exogenous PA at 50uM or vehicle (1methanol : 2 chloroform). Full phenotypic rescue of decreased cell viability was observed upon delivery of PA. (*, $P<0.05$ and **, $p<0.01$).

III. DISCUSSION

Given the work in chapter 1 establishing DGKα as a promising therapeutic target for cancer, as well as previous reports implicating PA in multiple oncogenic pathways, we began to investigate the importance of PA in cancer biology. DGKα synthesis of PA has been shown to be required for mitogenic and angiogenic signaling (46, 55, 82). The inhibition of LPAATs helps to accelerate the recovery of hematopeoisis after exposure to cyotoxic agents (96) and sensitizes cancer cells to chemotherapeutic agents (97). Lastly, PLD1/2 production of PA mediates mTOR signaling (18, 20, 108), Wnt/β-catenin signaling (105), and is needed for the Warburg effect in human cancer cells (109). Individually, each route of PA synthesis has been linked to oncogenic signaling, yet the total inhibition of all three synthetic pathways has not been explored. The attentuation of PA through each small molecule inhibitor causes considerable toxicity in multiple cancer cell lines. This cytotoxic effect increases with the simultaneous administration of all three inhibitors through a synergistic effect, indicating that combined inhibition of PA synthesis may be more crucial for cancer cells than just any one synthetic pathway alone. As mentioned above, cancer treatments that are successful have a broad therapeutic window. Similar to DGKα inhibition alone, LSF and FIPI administered alone and in combination, efficiently killed cancer cells at low concentrations and did not begin to affect normal human cells until much higher concentrations were used. This adds to the therapeutic potential of inhibiting PA, since there seems to be a cancer-specific dependence on PA signaling that is not present in non-cancerous human cells.

Given this, we propose that simultaneous inhibition of all three PA synthetic pathways will effect oncogenic cellular networks more powerfully, leaving cancer cells unable to adapt and survive.

We believe that this work substantiates the need for further examination of the role of PA in cancer biology and as a potential therpeautic target. While our previous work is promising, we cannot ignore the possibilty of resistance to DGKα attenuation treatment. Commonly, resistance to treatment occurs when one synthetic payhway is inhibited and allows for parallel pathways to compensate and promote signaling to ensure tumor cell survival. There is a possibility that tumor cells, when exposed to long term DGKα inihibition, could drive the upregulation of PLD or LPAATs. We believe that simultaneously inhibiting all three modes of PA production can prevent resistance since there will be no redundant signaling to rescue the cells.

While initial studies are promising, there are a number of avenues that still need to be developed. Outside of this work, DGKα small molecule inhibitors have not really been developed for *in vivo* use. LSF has been used clinically, but the bioavailability and half-life are less than optimal. FIPI has not been tested *in vivo*, and little is known about this drug. The pharmacokinetics, dosage, and duration of treatment for each small-molecule inhibitor needs to be studied to optimize treatment conditions. Once more is known about these small molecule inhibitors, we need to test this simultaneous inhibition *in vivo* in a xenograft model of cancer via multiple routes of delivery. We would anticipate a greater increase in survival with PA inhibition treatment, along with a more pronounced decrease in tumor

growth than we observed with DGKα attentuation alone. We have also begun attempts to identify downstream targets via high-throughput proteomic and phospho-proteomic analysis after treatment. Preliminarily, there have been predicted downstream targets that have been identified, yet further experiments need to be conducted to validate their importance in this phenotype. This study provides the rationale for targeting all three synthetic pathways of PA and it will be of interest to determine if this single target can have a widespread effect on cancer biology.

FUTURE DIRECTIONS AND DISCUSSION

The need for the development of a novel therapeutic target is as urgent as ever due to the frequency and lethality of GBM, as well as other cancers discussed in this work. There is a pressing need for a new therapeutic strategy, as the number of promising therapies that target single oncogenes proving disappointing in patients increases. This current standard of care was developed from an oversimplified notion of cancer biology, while there is now a better understanding of the many complex cellular network alterations that contribute to cancer. Although successful inhibition of an oncogene can be achieved, there are still downstream pathways that remain active. Another obstacle to overcome are feedback loops and cross-talk with other oncogenic pathways. The presence of multiple redundant signaling pathways, whose activation can be promoted when another is blocked, needs to be addressed in the search for novel therapeutic strategies (110). There have been exciting new developments in cancer research strategies using viral gene therapy, inhibitory RNA molecules and cancer vaccines [reviewed in (111-113)]. We believe that the focus needs to turn away from single oncogenes that target specific pathways, and should begin to search for therapies that engage multiple signaling pathways in cancer biology.

Throughout this work we have set the foundation for DGKα and its product, PA, as promising therapeutic targets for the treatment of cancer. While there have been minimal prior reports linking DGKα and PA signaling to oncogenic pathways, we are the first to develop the link to direct cancer cell

killing. Before this study, none of the small molecule inhibitors discussed were used to directly kill cancer cells, nor used simultaneously to inhibit PA. Through the *in vitro* work presented, inhibition of both DGKα and PA have proven efficient at killing cancer cells, but not normal cells. In addition, DGKα attenuation has not been studied *in vivo*, nor has the small-molecule inhibitor R59022 been investigated for its pharmacokinetics before the experiments presented here. *In vivo* experiments discussed here have shown that DGKα attentuation can be achieved successfully, with both intracranial and subcutaneous tumors, via lentiviral infection and small-molecule inhibition successfully through single and continuous treatment.

In the search for potential critical signaling nodes that have widespread effects on cell biology, we began to look for small molecules that are structurally similar to DGKα inhibitors R59022 and R59949, identifying candidates such as the compound ritanserin. Ritanserin is a 5-HT_2 receptor antagonist (116) and has been linked to numerous neurochemical systems. This drug has been shown to reduce the negative side effects of schizophrenia in humans (117), block dopamine re-uptake in the rat frontal cortex (118), and improve sleep and anxiety behaviors in recovering alcoholic patients (119). Ritanserin affects the serotonergic, GABAergic, and dopaminergic neurochemical systems, but has not been implicated in cancer cell biology. Importantly, ritanserin has been used safely in clinical trials, has a 40-hour half-life, is orally available, and can penetrate the blood-brain barrier. Due to its similarities to R59022 and R59949 in structure, we tested ritanserin as an inhibitor of DGKα activity with a collaborator,

when compared to R59022, ritanserin had a comparable inhibitory effect. Preliminarily, we have observed significant toxicity in established glioblastoma cells, without a decrease in cell proliferation in normal human astrocytes. The observed toxicity in cancer cells, combined with the safe use of ritanserin in humans and the advantageous effects on mood and sleep, make ritanserin a promising compound with potential to quickly advance to clinical trials for cancer therapy. These initial data have begun to establish the potential of ritanserin as a therapeutic agent, and further development to confirm its mechanism of toxicity in cancer cells and in xenograft cancer models will be conducted in an effort to substantiate this hypothesis.

Figure 48

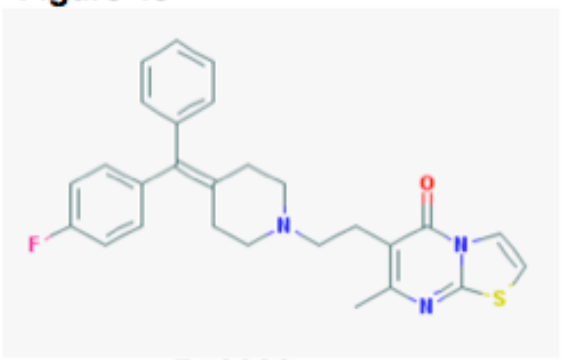

R59022

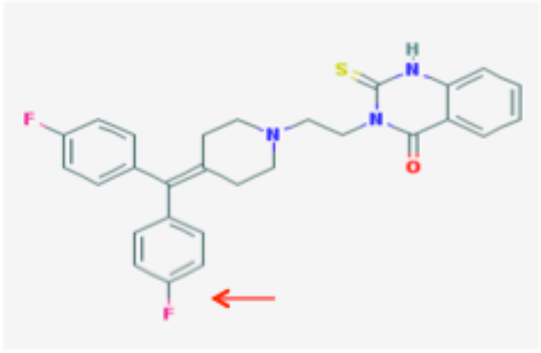

R59949

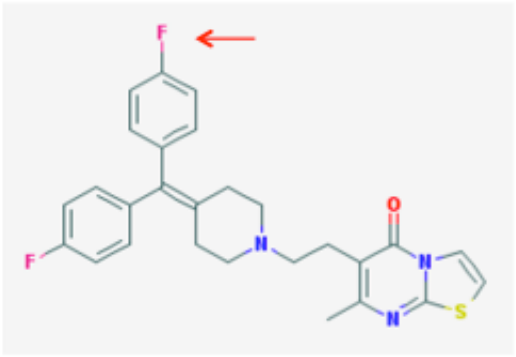

Ritanserin

Figure 48. Ritanserin is structurally similar to known DGKα inhibitors and may have comparable inhibitory activity. Structures of R59022, R59949, and Ritanserin. Arrows indicate the fluorine group present in ritanserin and R59949 (but lacking in R59022).

Figure 49

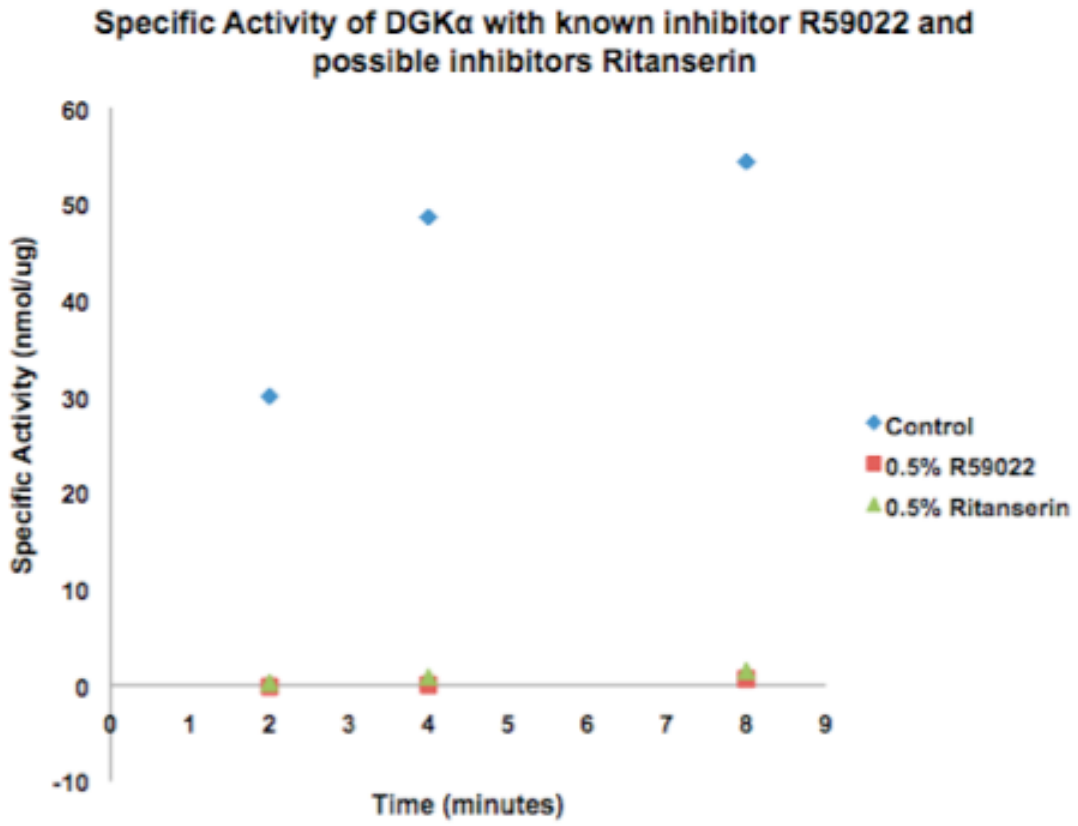

Figure 49. Incorporation of ^{32}P from ^{32}P-ATP into phosphatidic acid by purified DGKα in the presence of equal vol:vol vehicle, 0.5% R59022, or 0.5% ritanserin.

Figure 50

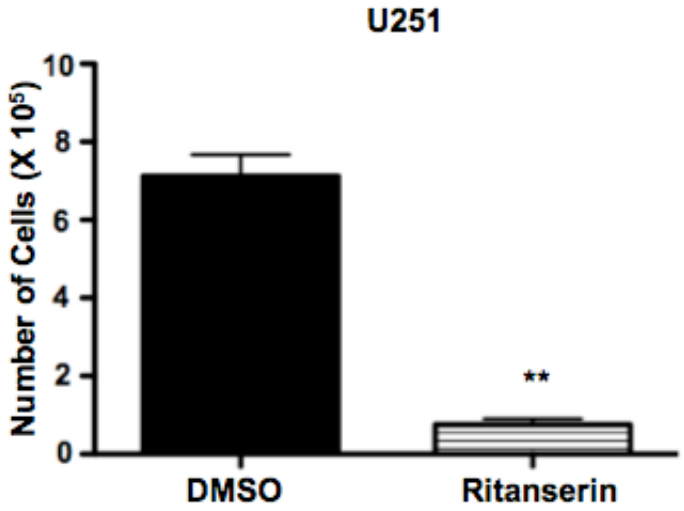

Figure 50. Ritanserin was administered to U251 glioma cells at 10uM and cell proliferation was assessed 4 days post treatment.

Figure 51

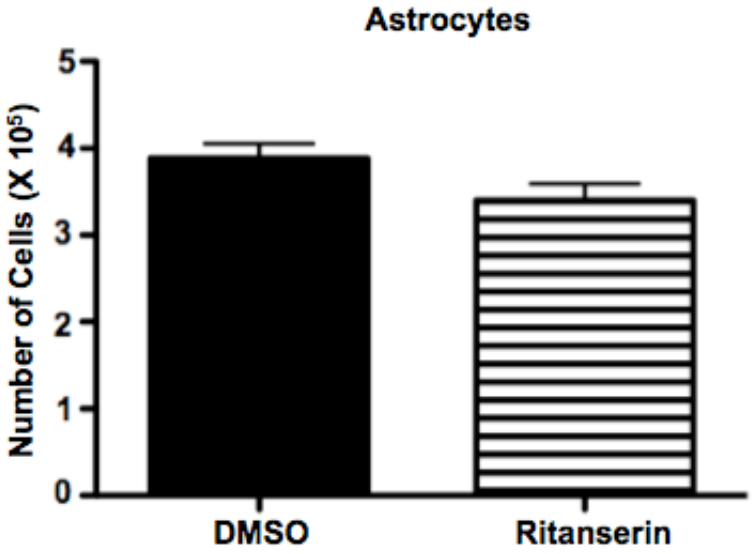

Figure 51. Normal human astrocytes were exposed to 10uM of Ritanserin for 4 days with no significant toxicity observed.

As stated above, DGKα and PA have been linked to multiple pathways, yet we showed for the first time the importance of mTOR and HIF as key mediators of the toxic phenotype observed. Experiments focusing on these key mediators to identify the mechanism responsible for this phenotype led us to construct a new signaling pathway, producing evidence of direct mTOR transcription regulation via DGKα inhibition. We propose DGKα inhibition decreases PA, which should decrease PDE activity. PDEs in turn can not degrade cyclic AMP levels as usual, leading to increased cyclic AMP levels and a reduction in cAMP-modulated transcription factor activation, resulting in a reduction of mTOR transcription. The development of this new pathway also has implications for other pathways such as TGF-β. This cytokine has been shown to play a key role in cancer, and elevated TGF-β activity has been associated with poor patient outcome in GBM (115). TGF-β has been shown to regulate PDE expression (114) and affects mTOR expression (115). This novel signaling pathway needs to be studied further develop its role in TGF-β signaling and to identify other potential targets in cancer biology.

Thoughout this work the data presented have shed light on the significant effects of DGKα and PA inhibition on cancer cell viability, the possibility it represents an example of non-oncogene addiction, and its safety in normal human cells. The results put forth establish DGKα and PA as single therapeutic targets linked to multiple oncogenic pathways, with relevance for multiple types of cancer. This work also indicates the importance of developing the drug ritanserin as a potential cancer treatment due to its potential for rapid clinical

translation. Lastly, ongoing studies are evaluating the potential for combination therapies of DGKα/PA inhibitors with radiation, mTOR inhibitors, and immunotherapy in cancer.

Supplemental Figure 1

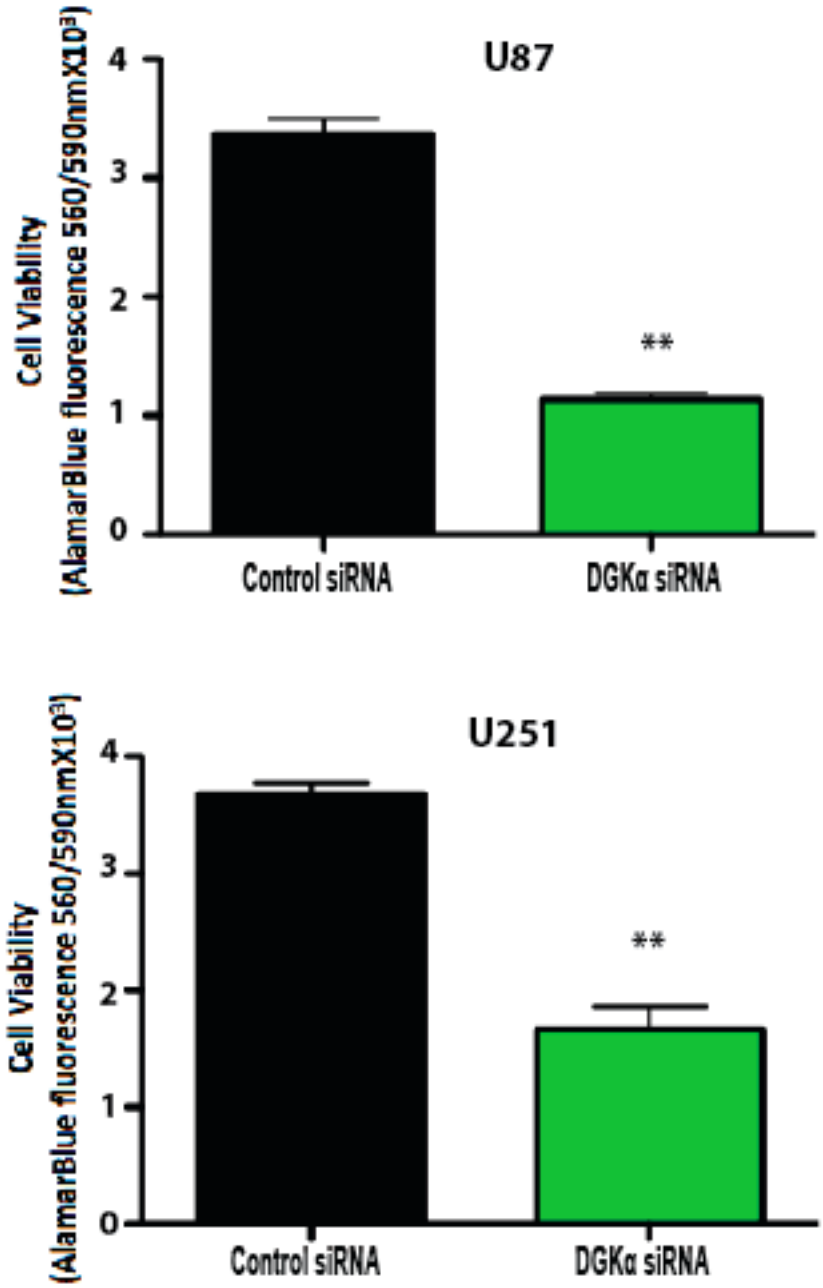

Supplemental Figure 1. Attenuation of DGKα is toxic to glioblastoma cells in vitro. Cell viability by alamarBlue assay was significantly reduced 72 hours after DGKα silencing in both U87 and U251 GBM cell lines. (*, $P<0.05$ and **, $P<0.01$ Student t test).

Supplemental Figure 2.

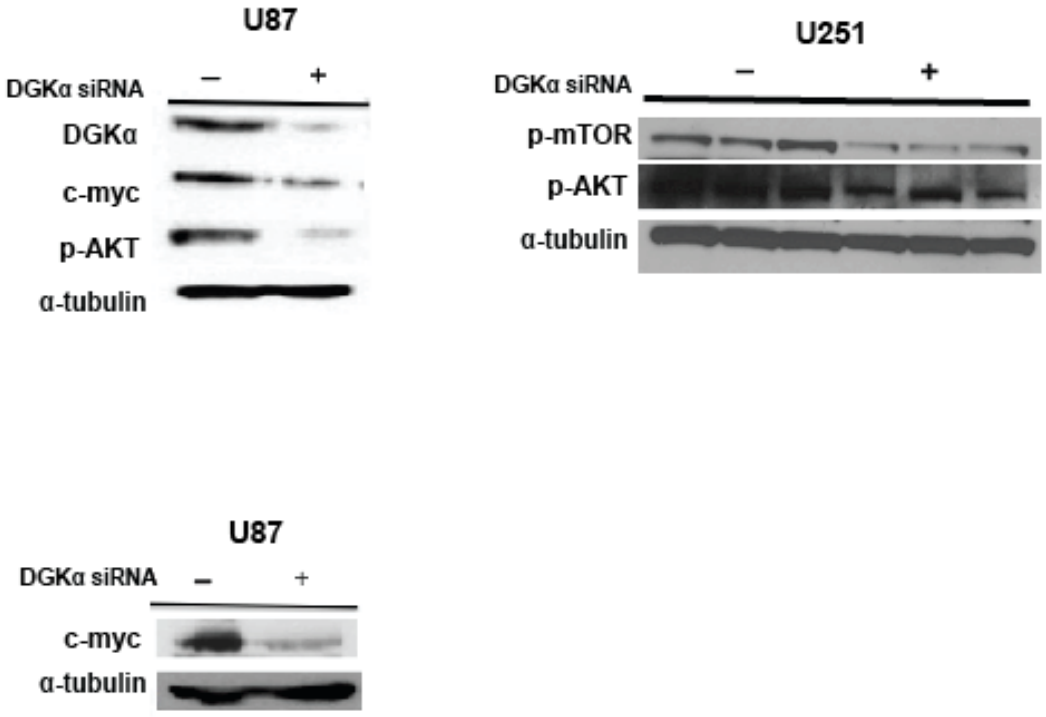

Supplemental Figure 2. DGKa knockdown suppresses several oncogenic pathways. Immunoblot analysis of U87 and U251 cell lysates exhibit a marked reduction in c-Myc and phos-AKTser473 levels with DGKα knockdown.

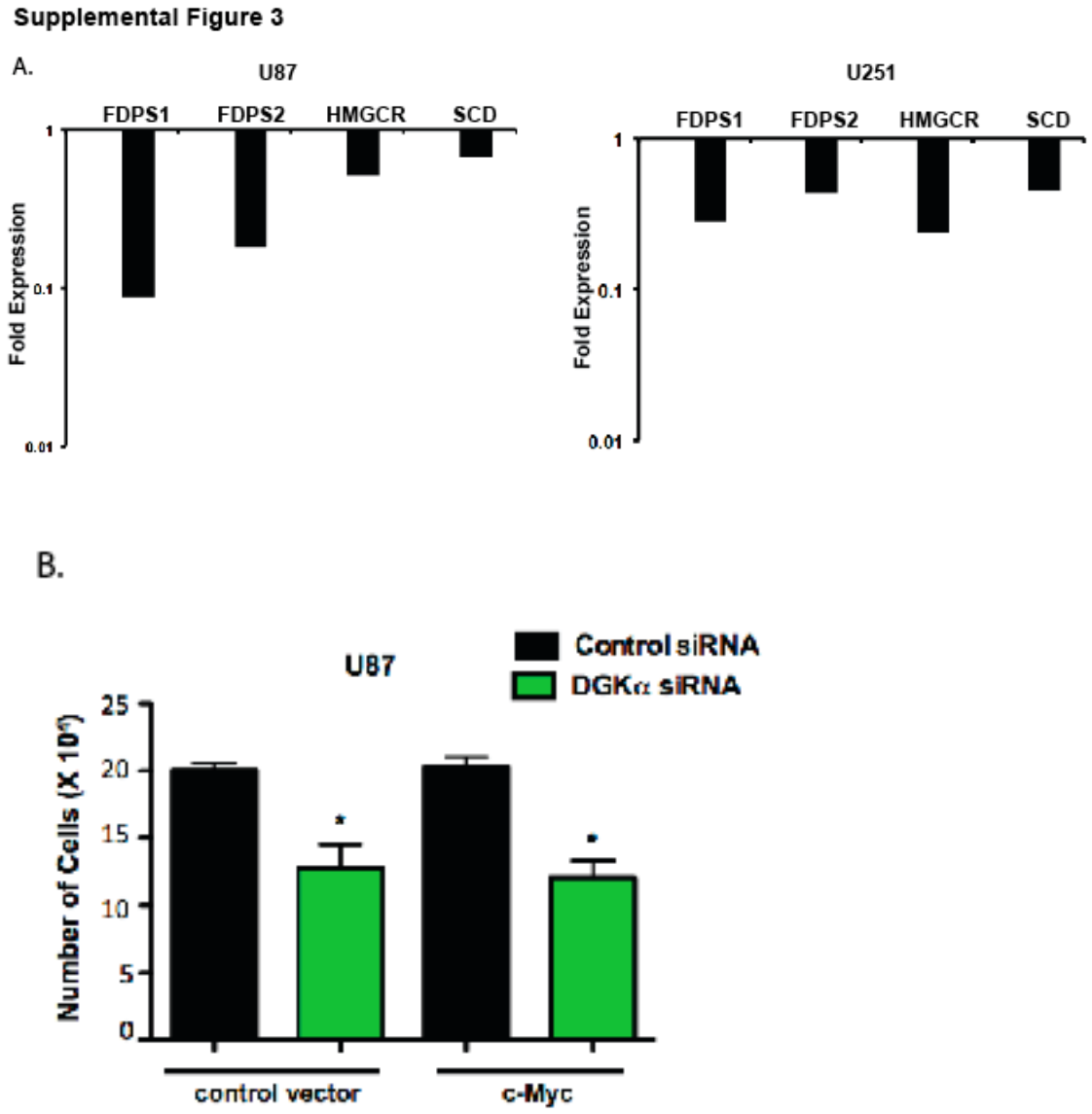

Supplemental Figure 3. DGKα modulates several oncogene-related pathways. A, In both U87 and U251 cells, mRNA levels of FDPS1, FDPS2, HMGCR, and SCD were quantified by qRT-PCR in response to DGKα knockdown via siRNA and log-scale fold expression changes in comparison to control siRNA are shown. B, c-Myc was over-expressed through plasmid transfection after DGKα knockdown via siRNA and cell proliferation was assessed in U87 cells. (*, $P<0.05$ and **, $P<0.01$ Student t test).

Supplemental Figure 4

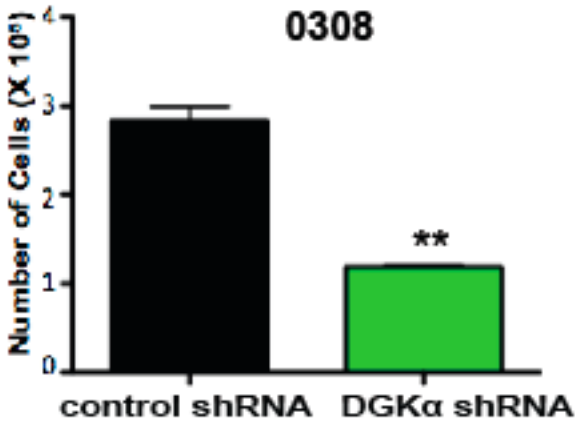

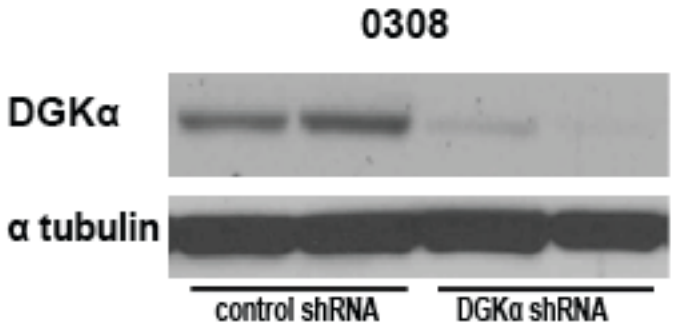

Supplemental Figure 4. Lentivirus infection with DGKα shRNA is efficient in vitro. Lentiviral infection with DGKα shRNA was significantly cytotoxic to 0308 glioblastoma stem cells (GSCs), and immunoblot confirms the shRNA silencing of target. (*, $P<0.05$ and **, $P<0.01$ Student t test).

Supplemental Table 1

Cancer	amplification	mutations
Glioblastoma Multiforme	1.4%	0%
Brain Lower Grade Glioma	0.7%	0%
Breast Invasive Carcinoma	0%	0.4%
Colon and Rectum Adenocarcinoma	0%	0.5%
Lung Squamous Cell Carcinoma	0%	3.4%
Sarcoma	4.3%	0%
Serous Ovarian Cancer	3.16%	0.94%
Bladder Urothelial Carcinoma	1.1%	0%
Lung Adenocarcinoma	1.8%	0%
Skin Cutaneous Melanoma	0.5%	0%
Stomach Adenocarcinoma	3%	0%
Uterine Corpus Endometrial Carcinoma	2.1%	0%
Kidney Renal Clear Cell Carcinoma, Prostate Adenocarcinoma, Cervical Squamous Cell Carcinoma, Head and Neck Squamous Cell Carcinoma, Kidney Renal Papillary Cell Carcinoma, Liver Hepatocellular Carcinoma, Pancreatic Adenocarcinoma, Thyroid Carcinoma	0%	0%

Supplemental Table 1. Data from The Cancer Genome Atlas (15) indicating amplification and mutation rates of DGKα in GBM and several other cancers.

Supplemental Table 2

Cancer Type	Comparison	Pearson's correlation test p-value	Pearson's product moment correlation coefficient	Spearman's correlation test p-value	Spearman's *rho* statistic
GBM	DGKA vs. MTOR	<2.2e-16	0.475	6.159e-16	0.351

Supplemental Table 2. A statistical analysis of 576 human GBM samples from TCGA (15) was conducted to correlate DGKa and mTOR mRNA expression (plot shown in Figure 4).

Supplemental Table 3

Compound	logPS	logBB	Log (PS*fu, brain)	Predicted Brain Penetration
R59022	-1.3	-0.13	-3.2	Sufficient for CNS activity
R59949	-1.6	0.22	-3.7	CNS inactive due to low brain penetration

Supplemental Table 3. Values of quantitative parameters supporting predicted BBB penetration by small molecule inhibitors R59022 and R59949 (47).

Supplemental Table 4

A.

Days	t test p-value	Wilcoxon test p-value
37	.170	.078
41	.042	.031
42	.057	.031
44	.087	.078

B.

Days	t test p-value	Wilcoxon test p-value
4	0.472	0.491
9	0.033	0.028
13	0.018	0.021
17	0.033	0.038

Supplemental Table 4. A statistical analysis was performed at each time point to assess the change in tumor volume of A, U87 and B, A-375 subcutaneous tumors treated with R59022 at 10 mg/kg compared to DMSO treatment.

REFERENCES

1. Adamson C, Kanu OO, Mehta AI, Di C, Lin N, Mattox AK, et al. Glioblastoma multiforme: a review of where we have been and where we are going. *Expert Opin Investig Drugs* 2009; 18:1061-1083.
2. Cerami E, Demir E, Schultz N, Taylor BS, Sander C. Automated network analysis identifies core pathways in glioblastoma. *PLoS One* 2010; 5:e8918.
3. Louis DN, Ohgaki H, Wiestler OD, Cavenee WK, Burger PC, Jouvet A, et al. The 2007 WHO classification of tumours of the central nervous system. *Acta Neuropathol* 2007; 114:97-109.
4. Hadjipanayis CG,Van Meir EG. Brain cancer propagating cells: biology, genetics and targeted therapies. *Trends Mol Med* 2009; 15:519-530.
5. Stommel JM, Kimmelman AC, Ying H, Nabioullin R, Ponugoti AH, Wiedemeyer R, et al. Coactivation of receptor tyrosine kinases affects the response of tumor cells to targeted therapies. *Science* 2007; 318:287-290.
6. Purow BW, Haque RM, Noel MW, Su Q, Burdick MJ, Lee J, et al. Expression of Notch-1 and its ligands, Delta-like-1 and Jagged-1, is critical for glioma cell survival and proliferation. *Cancer Res* 2005; 65:2353-2363.
7. Kefas B, Comeau L, Floyd DH, Seleverstov O, Godlewski J, Schmittgen T, et al. The neuronal microRNA miR-326 acts in a feedback loop with notch and has therapeutic potential against brain tumors. *J Neurosci* 2009; 29:15161-15168.
8. Solimini NL, Luo J, Elledge SJ. Non-oncogene addiction and the stress phenotype of cancer cells. *Cell* 2007; 130:986-988.
9. Luo J, Solimini NL, Elledge SJ. Principles of cancer therapy: oncogene and non-oncogene addiction. *Cell* 2009; 136:823-837.
10. Sharma SV,Settleman J. Exploiting the balance between life and death: targeted cancer therapy and "oncogenic shock". *Biochem Pharmacol* 2010; 80:666-673.
11. Armengol G, Rojo F, Castellvi J, Iglesias C, Cuatrecasas M, Pons B, et al. 4E-binding protein 1: a key molecular "funnel factor" in human cancer with clinical implications. *Cancer Res* 2007; 67:7551-7555.
12. Hasselbalch B, Eriksen JG, Broholm H, Christensen IJ, Grunnet K, Horsman MR, et al. Prospective evaluation of angiogenic, hypoxic and EGFR-related biomarkers in recurrent glioblastoma multiforme treated with cetuximab, bevacizumab and irinotecan. *APMIS* 2010; 118:585-594.
13. Verhoeff JJ, van Tellingen O, Claes A, Stalpers LJ, van Linde ME, Richel DJ, et al. Concerns about anti-angiogenic treatment in patients with glioblastoma multiforme. *BMC Cancer* 2009; 9:444.
14. Quick A, Patel D, Hadziahmetovic M, Chakravarti A, Mehta M. Current therapeutic paradigms in glioblastoma. *Rev Recent Clin Trials* 2010; 5:14-27.
15. Suzuki Y, Shirai K, Oka K, Mobaraki A, Yoshida Y, Noda SE, et al. Higher pAkt expression predicts a significant worse prognosis in glioblastomas. *J Radiat Res (Tokyo)* 2010; 51:343-348.
16. Courtney KD, Corcoran RB, Engelman JA. The PI3K pathway as drug target in human cancer. *J Clin Oncol* 2010; 28:1075-1083.

17. Burris HA, 3rd. Overcoming acquired resistance to anticancer therapy: focus on the PI3K/AKT/mTOR pathway. *Cancer Chemother Pharmacol* 2013; 71:829-842.
18. Winter JN, Fox TE, Kester M, Jefferson LS, Kimball SR. Phosphatidic acid mediates activation of mTORC1 through the ERK signaling pathway. *Am J Physiol Cell Physiol* 2010; 299:C335-344.
19. Liu P, Cheng H, Roberts TM, Zhao JJ. Targeting the phosphoinositide 3-kinase pathway in cancer. *Nat Rev Drug Discov* 2009; 8:627-644.
20. Toschi A, Lee E, Xu L, Garcia A, Gadir N, Foster DA. Regulation of mTORC1 and mTORC2 complex assembly by phosphatidic acid: competition with rapamycin. *Mol Cell Biol* 2009; 29:1411-1420.
21. Masri J, Bernath A, Martin J, Jo OD, Vartanian R, Funk A, et al. mTORC2 activity is elevated in gliomas and promotes growth and cell motility via overexpression of rictor. *Cancer Res* 2007; 67:11712-11720.
22. Grzmil M,Hemmings BA. Overcoming resistance to rapalogs in gliomas by combinatory therapies. *Biochim Biophys Acta* 2013.
23. Semenza GL. HIF-1: mediator of physiological and pathophysiological responses to hypoxia. *J Appl Physiol* 2000; 88:1474-1480.
24. Wang GL, Jiang BH, Rue EA, Semenza GL. Hypoxia-inducible factor 1 is a basic-helix-loop-helix-PAS heterodimer regulated by cellular O2 tension. *Proc Natl Acad Sci U S A* 1995; 92:5510-5514.
25. Chau NM, Rogers P, Aherne W, Carroll V, Collins I, McDonald E, et al. Identification of novel small molecule inhibitors of hypoxia-inducible factor-1 that differentially block hypoxia-inducible factor-1 activity and hypoxia-inducible factor-1alpha induction in response to hypoxic stress and growth factors. *Cancer Res* 2005; 65:4918-4928.
26. Ebert BL,Bunn HF. Regulation of transcription by hypoxia requires a multiprotein complex that includes hypoxia-inducible factor 1, an adjacent transcription factor, and p300/CREB binding protein. *Mol Cell Biol* 1998; 18:4089-4096.
27. Giaccia A, Siim BG, Johnson RS. HIF-1 as a target for drug development. *Nat Rev Drug Discov* 2003; 2:803-811.
28. Moeller BJ, Cao Y, Li CY, Dewhirst MW. Radiation activates HIF-1 to regulate vascular radiosensitivity in tumors: role of reoxygenation, free radicals, and stress granules. *Cancer Cell* 2004; 5:429-441.
29. Tang WJ,Gilman AG. Adenylyl cyclases. *Cell* 1992; 70:869-872.
30. Houslay MD. Underpinning compartmentalised cAMP signalling through targeted cAMP breakdown. *Trends Biochem Sci* 2010; 35:91-100.
31. Rocha AS, Paternot S, Coulonval K, Dumont JE, Soares P, Roger PP. Cyclic AMP inhibits the proliferation of thyroid carcinoma cell lines through regulation of CDK4 phosphorylation. *Mol Biol Cell* 2008; 19:4814-4825.
32. Follin-Arbelet V, Hofgaard PO, Hauglin H, Naderi S, Sundan A, Blomhoff R, et al. Cyclic AMP induces apoptosis in multiple myeloma cells and inhibits tumor development in a mouse myeloma model. *BMC Cancer* 2011; 11:301.
33. Xie J, Ponuwei GA, Moore CE, Willars GB, Tee AR, Herbert TP. cAMP inhibits mammalian target of rapamycin complex-1 and -2 (mTORC1 and 2) by

promoting complex dissociation and inhibiting mTOR kinase activity. *Cell Signal* 2011; 23:1927-1935.
34. Dery MA, Michaud MD, Richard DE. Hypoxia-inducible factor 1: regulation by hypoxic and non-hypoxic activators. *Int J Biochem Cell Biol* 2005; 37:535-540.
35. Derrick M, Krakauer D, Magill S, Mikunas D, Musgrave B, Jr O, et al. The ZEUS Leading Proton Spectrometer and its use in the measurement of elastic rho(0) photoproduction at HERA. *Z Phys C Part Fields* 1997; 73:253-268.
36. Topham MK. Signaling roles of diacylglycerol kinases. *J Cell Biochem* 2006; 97:474-484.
37. Merida I, Avila-Flores A, Merino E. Diacylglycerol kinases: at the hub of cell signalling. *Biochem J* 2008; 409:1-18.
38. Sakane F, Imai S, Kai M, Yasuda S, Kanoh H. Diacylglycerol kinases: why so many of them? *Biochim Biophys Acta* 2007; 1771:793-806.
39. Kanoh H, Yamada K, Sakane F. Diacylglycerol kinases: emerging downstream regulators in cell signaling systems. *J Biochem* 2002; 131:629-633.
40. Hokin LE,Hokin MR. Diglyceride kinase and phosphatidic acid phosphatase in erythrocyte membranes. *Nature* 1961; 189:836-837.
41. Kanoh H, Kondoh H, Ono T. Diacylglycerol kinase from pig brain. Purification and phospholipid dependencies. *J Biol Chem* 1983; 258:1767-1774.
42. Kanoh H, Yamada K, Sakane F, Imaizumi T. Phosphorylation of diacylglycerol kinase in vitro by protein kinase C. *Biochem J* 1989; 258:455-462.
43. van Blitterswijk WJ,Houssa B. Properties and functions of diacylglycerol kinases. *Cell Signal* 2000; 12:595-605.
44. Wang X, Devaiah SP, Zhang W, Welti R. Signaling functions of phosphatidic acid. *Prog Lipid Res* 2006; 45:250-278.
45. Shulga YV, Topham MK, Epand RM. Regulation and functions of diacylglycerol kinases. *Chem Rev* 2011; 111:6186-6208.
46. Baldanzi G, Mitola S, Cutrupi S, Filigheddu N, van Blitterswijk WJ, Sinigaglia F, et al. Activation of diacylglycerol kinase alpha is required for VEGF-induced angiogenic signaling in vitro. *Oncogene* 2004; 23:4828-4838.
47. Flores I, Casaseca T, Martinez AC, Kanoh H, Merida I. Phosphatidic acid generation through interleukin 2 (IL-2)-induced alpha-diacylglycerol kinase activation is an essential step in IL-2-mediated lymphocyte proliferation. *J Biol Chem* 1996; 271:10334-10340.
48. Yanagisawa K, Yasuda S, Kai M, Imai S, Yamada K, Yamashita T, et al. Diacylglycerol kinase alpha suppresses tumor necrosis factor-alpha-induced apoptosis of human melanoma cells through NF-kappaB activation. *Biochim Biophys Acta* 2007; 1771:462-474.
49. de Chaffoy de Courcelles DC, Roevens P, Van Belle H. R 59 022, a diacylglycerol kinase inhibitor. Its effect on diacylglycerol and thrombin-induced C kinase activation in the intact platelet. *J Biol Chem* 1985; 260:15762-15770.
50. de Chaffoy de Courcelles D, Roevens P, Van Belle H, Kennis L, Somers Y, De Clerck F. The role of endogenously formed diacylglycerol in the propagation and termination of platelet activation. A biochemical and functional analysis

using the novel diacylglycerol kinase inhibitor, R 59 949. *J Biol Chem* 1989; 264:3274-3285.
51. Bishop WR, Ganong BR, Bell RM. Attenuation of sn-1,2-diacylglycerol second messengers by diacylglycerol kinase. Inhibition by diacylglycerol analogs in vitro and in human platelets. *J Biol Chem* 1986; 261:6993-7000.
52. Jiang Y, Sakane F, Kanoh H, Walsh JP. Selectivity of the diacylglycerol kinase inhibitor 3-[2-(4-[bis-(4-fluorophenyl)methylene]-1-piperidinyl)ethyl]-2, 3-dihydro-2-thioxo-4(1H)quinazolinone (R59949) among diacylglycerol kinase subtypes. *Biochem Pharmacol* 2000; 59:763-772.
53. Temes E, Martin-Puig S, Acosta-Iborra B, Castellanos MC, Feijoo-Cuaresma M, Olmos G, et al. Activation of HIF-prolyl hydroxylases by R59949, an inhibitor of the diacylglycerol kinase. *J Biol Chem* 2005; 280:24238-24244.
54. Matsumoto T,Claesson-Welsh L. VEGF receptor signal transduction. *Sci STKE* 2001; 2001:re21.
55. Avila-Flores A, Santos T, Rincon E, Merida I. Modulation of the mammalian target of rapamycin pathway by diacylglycerol kinase-produced phosphatidic acid. *J Biol Chem* 2005; 280:10091-10099.
56. Lee J, Kotliarova S, Kotliarov Y, Li AG, Su Q, Donin NM, et al. Tumor stem cells derived from glioblastomas cultured in bFGF and EGF more closely mirror the phenotype and genotype of primary tumors than do serum-cultured cell lines. *Cancer Cell* 2006; 9:391-403.
57. Folch J, Lees M, Sloane Stanley GH. A simple method for the isolation and purification of total lipides from animal tissues. *J Biol Chem* 1957; 226:497-509.
58. Neschen S, Morino K, Hammond LE, Zhang D, Liu ZX, Romanelli AJ, et al. Prevention of hepatic steatosis and hepatic insulin resistance in mitochondrial acyl-CoA:glycerol-sn-3-phosphate acyltransferase 1 knockout mice. *Cell Metab* 2005; 2:55-65.
59. Nagle CA, An J, Shiota M, Torres TP, Cline GW, Liu ZX, et al. Hepatic overexpression of glycerol-sn-3-phosphate acyltransferase 1 in rats causes insulin resistance. *J Biol Chem* 2007; 282:14807-14815.
60. Folch J, Lees M, Sloane Stanley GH. A simple method for the isolation and purification of total lipids from animal tissues. *J Biol Chem* 1957; 226:497-509.
61. Murphy RC, James PF, McAnoy AM, Krank J, Duchoslav E, Barkley RM. Detection of the abundance of diacylglycerol and triacylglycerol molecular species in cells using neutral loss mass spectrometry. *Anal Biochem* 2007; 366:59-70.
62. Anonymous (ACD/ADME Suite from ACD Labs
63. Japertas P, Didziapetris R, Petrauskas A. Fragmental methods in the analysis of biological activities of diverse compound sets. *Mini Rev Med Chem* 2003; 3:797-808.
64. Cerami E, Gao J, Dogrusoz U, Gross BE, Sumer SO, Aksoy BA, et al. The cBio cancer genomics portal: an open platform for exploring multidimensional cancer genomics data. *Cancer Discov* 2012; 2:401-404.

65. Foster DA. Phosphatidic acid signaling to mTOR: signals for the survival of human cancer cells. *Biochim Biophys Acta* 2009; 1791:949-955.
66. Yalcin A, Clem B, Makoni S, Clem A, Nelson K, Thornburg J, et al. Selective inhibition of choline kinase simultaneously attenuates MAPK and PI3K/AKT signaling. *Oncogene* 2010; 29:139-149.
67. Peterson TR, Sengupta SS, Harris TE, Carmack AE, Kang SA, Balderas E, et al. mTOR complex 1 regulates lipin 1 localization to control the SREBP pathway. *Cell* 2011; 146:408-420.
68. Guo D, Reinitz F, Youssef M, Hong C, Nathanson D, Akhavan D, et al. An LXR agonist promotes GBM cell death through inhibition of an EGFR/AKT/SREBP-1/LDLR-dependent pathway. *Cancer Discov* 2011; 1:442-456.
69. Nemoz G, Sette C, Conti M. Selective activation of rolipram-sensitive, cAMP-specific phosphodiesterase isoforms by phosphatidic acid. *Molecular Pharmacology* 1997; 51:242-249.
70. Sheng Z, Ma LY, Sun JYE, Zhu LHJ, Green MR. BCR-ABL suppresses autophagy through ATF5-mediated regulation of mTOR transcription. *Blood* 2011; 118:2840-2848.
71. Rainero E, Caswell PT, Muller PA, Grindlay J, McCaffrey MW, Zhang Q, et al. Diacylglycerol kinase alpha controls RCP-dependent integrin trafficking to promote invasive migration. *J Cell Biol* 2012; 196:277-295.
72. Tyagi MG, Shanthi M, Keshavan V, Vikram GS. Phospholipid mediators and MgATPase modulation causes changes in the cardiovascular effects of vasopressin in lithium carbonate-induced polyuric rats. *Methods Find Exp Clin Pharmacol* 2004; 26:257-262.
73. Olenchock BA, Guo R, Carpenter JH, Jordan M, Topham MK, Koretzky GA, et al. Disruption of diacylglycerol metabolism impairs the induction of T cell anergy. *Nat Immunol* 2006; 7:1174-1181.
74. Zha Y, Marks R, Ho AW, Peterson AC, Janardhan S, Brown I, et al. T cell anergy is reversed by active Ras and is regulated by diacylglycerol kinase-alpha. *Nat Immunol* 2006; 7:1166-1173.
75. Prinz PU, Mendler AN, Masouris I, Durner L, Oberneder R, Noessner E. High DGK-alpha and disabled MAPK pathways cause dysfunction of human tumor-infiltrating CD8+ T cells that is reversible by pharmacologic intervention. *J Immunol* 2012; 188:5990-6000.
76. Weinstein IB,Joe A. Oncogene addiction. *Cancer Res* 2008; 68:3077-3080; discussion 3080.
77. Young R,Reed M. Anti-angiogenic Therapy: Concept to Clinic. *Microcirculation* 2011.
78. Rich JN, Reardon DA, Peery T, Dowell JM, Quinn JA, Penne KL, et al. Phase II trial of gefitinib in recurrent glioblastoma. *J Clin Oncol* 2004; 22:133-142.
79. Flores I, Jones DR, Cipres A, Diaz-Flores E, Sanjuan MA, Merida I. Diacylglycerol kinase inhibition prevents IL-2-induced G1 to S transition through a phosphatidylinositol-3 kinase-independent mechanism. *J Immunol* 1999; 163:708-714.

80. Rizzo MA, Shome K, Watkins SC, Romero G. The recruitment of Raf-1 to membranes is mediated by direct interaction with phosphatidic acid and is independent of association with Ras. *J Biol Chem* 2000; 275:23911-23918.
81. Bacchiocchi R, Baldanzi G, Carbonari D, Capomagi C, Colombo E, van Blitterswijk WJ, et al. Activation of alpha-diacylglycerol kinase is critical for the mitogenic properties of anaplastic lymphoma kinase. *Blood* 2005; 106:2175-2182.
82. Cutrupi S, Baldanzi G, Gramaglia D, Maffe A, Schaap D, Giraudo E, et al. Src-mediated activation of alpha-diacylglycerol kinase is required for hepatocyte growth factor-induced cell motility. *EMBO J* 2000; 19:4614-4622.
83. Bengoechea-Alonso MT,Ericsson J. SREBP in signal transduction: cholesterol metabolism and beyond. *Curr Opin Cell Biol* 2007; 19:215-222.
84. Guo R, Wan CK, Carpenter JH, Mousallem T, Boustany RM, Kuan CT, et al. Synergistic control of T cell development and tumor suppression by diacylglycerol kinase alpha and zeta. *Proc Natl Acad Sci U S A* 2008; 105:11909-11914.
85. Kay MA, Glorioso JC, Naldini L. Viral vectors for gene therapy: the art of turning infectious agents into vehicles of therapeutics. *Nat Med* 2001; 7:33-40.
86. Newton AC. Regulation of protein kinase C. *Curr Opin Cell Biol* 1997; 9:161-167.
87. Regier DS, Higbee J, Lund KM, Sakane F, Prescott SM, Topham MK. Diacylglycerol kinase iota regulates Ras guanyl-releasing protein 3 and inhibits Rap1 signaling. *Proc Natl Acad Sci U S A* 2005; 102:7595-7600.
88. Divecha N, Lander DJ, Scott TW, Irvine RF. Molecular species analysis of 1,2-diacylglycerols and phosphatidic acid formed during bombesin stimulation of Swiss 3T3 cells. *Biochim Biophys Acta* 1991; 1093:184-188.
89. Topham MK, Bunting M, Zimmerman GA, McIntyre TM, Blackshear PJ, Prescott SM. Protein kinase C regulates the nuclear localization of diacylglycerol kinase-zeta. *Nature* 1998; 394:697-700.
90. Ding L, Traer E, McIntyre TM, Zimmerman GA, Prescott SM. The cloning and characterization of a novel human diacylglycerol kinase, DGKiota. *J Biol Chem* 1998; 273:32746-32752.
91. Wada I, Kai M, Imai S, Sakane F, Kanoh H. Translocation of diacylglycerol kinase alpha to the nuclear matrix of rat thymocytes and peripheral T-lymphocytes. *FEBS Lett* 1996; 393:48-52.
92. Imai S, Kai M, Yasuda S, Kanoh H, Sakane F. Identification and characterization of a novel human type II diacylglycerol kinase, DGK kappa. *J Biol Chem* 2005; 280:39870-39881.
93. Ishisaka M, Kakefuda K, Oyagi A, Ono Y, Tsuruma K, Shimazawa M, et al. Diacylglycerol kinase beta knockout mice exhibit attention-deficit behavior and an abnormal response on methylphenidate-induced hyperactivity. *PLoS One* 2012; 7:e37058.
94. Seo J, Kim K, Jang S, Han S, Choi SY, Kim E. Regulation of hippocampal long-term potentiation and long-term depression by diacylglycerol kinase zeta. *Hippocampus* 2012; 22:1018-1026.

95. Rodriguez de Turco EB, Tang W, Topham MK, Sakane F, Marcheselli VL, Chen C, et al. Diacylglycerol kinase epsilon regulates seizure susceptibility and long-term potentiation through arachidonoyl- inositol lipid signaling. *Proc Natl Acad Sci U S A* 2001; 98:4740-4745.
96. de Vries P,Singer JW. Lisofylline suppresses ex vivo release by murine spleen cells of hematopoietic inhibitors induced by cancer chemotherapeutic agents. *Exp Hematol* 2000; 28:916-923.
97. Husain A, Rosales N, Schwartz GK, Spriggs DR. Lisofylline sensitizes p53 mutant human ovarian carcinoma cells to the cytotoxic effects of cis-diamminedichloroplatinum (II). *Gynecol Oncol* 1998; 70:17-22.
98. Wong JS, Ara G, Keyes SR, Herbst R, Coleman CN, Teicher BA. Lisofylline as a modifier of radiation therapy. *Oncol Res* 1996; 8:513-518.
99. Cui P, Macdonald TL, Chen M, Nadler JL. Synthesis and biological evaluation of lisofylline (LSF) analogs as a potential treatment for Type 1 diabetes. *Bioorg Med Chem Lett* 2006; 16:3401-3405.
100. Tang W, Yuan J, Chen X, Gu X, Luo K, Li J, et al. Identification of a novel human lysophosphatidic acid acyltransferase, LPAAT-theta, which activates mTOR pathway. *J Biochem Mol Biol* 2006; 39:626-635.
101. Shukla SD,Halenda SP. Phospholipase D in cell signalling and its relationship to phospholipase C. *Life Sci* 1991; 48:851-866.
102. Peng X,Frohman MA. Mammalian Phospholipase D Physiological and Pathological Roles. *Acta Physiol (Oxf)* 2011.
103. Zheng Y, Rodrik V, Toschi A, Shi M, Hui L, Shen Y, et al. Phospholipase D couples survival and migration signals in stress response of human cancer cells. *J Biol Chem* 2006; 281:15862-15868.
104. Park MH, Ahn BH, Hong YK, Min do S. Overexpression of phospholipase D enhances matrix metalloproteinase-2 expression and glioma cell invasion via protein kinase C and protein kinase A/NF-kappaB/Sp1-mediated signaling pathways. *Carcinogenesis* 2009; 30:356-365.
105. Kang DW, Choi KY, Min do S. Phospholipase D meets Wnt signaling: a new target for cancer therapy. *Cancer Res* 2011; 71:293-297.
106. Su W, Yeku O, Olepu S, Genna A, Park JS, Ren H, et al. 5-Fluoro-2-indolyl des-chlorohalopemide (FIPI), a phospholipase D pharmacological inhibitor that alters cell spreading and inhibits chemotaxis. *Mol Pharmacol* 2009; 75:437-446.
107. Yang Z, Chen M, Nadler JL. Lisofylline: a potential lead for the treatment of diabetes. *Biochem Pharmacol* 2005; 69:1-5.
108. Fang Y, Vilella-Bach M, Bachmann R, Flanigan A, Chen J. Phosphatidic acid-mediated mitogenic activation of mTOR signaling. *Science* 2001; 294:1942-1945.
109. Toschi A, Lee E, Thompson S, Gadir N, Yellen P, Drain CM, et al. Phospholipase D-mTOR requirement for the Warburg effect in human cancer cells. *Cancer Lett* 2010; 299:72-79.
110. Markman B, Dienstmann R, Tabernero J. Targeting the PI3K/Akt/mTOR pathway--beyond rapalogs. *Oncotarget* 2010; 1:530-543.

111. Aalbers CJ, Tak PP, Vervoordeldonk MJ. Advancements in adeno-associated viral gene therapy approaches: exploring a new horizon. *F1000 Med Rep* 2011; 3:17.
112. Mao CP,Wu TC. Inhibitory RNA molecules in immunotherapy for cancer. *Methods Mol Biol* 2010; 623:325-339.
113. Larocca C,Schlom J. Viral vector-based therapeutic cancer vaccines. *Cancer J* 2011; 17:359-371.
114. Dunkern TR, Feurstein D, Rossi GA, Sabatini F, Hatzelmann A. Inhibition of TGF-beta induced lung fibroblast to myofibroblast conversion by phosphodiesterase inhibiting drugs and activators of soluble guanylyl cyclase. *Eur J Pharmacol* 2007; 572:12-22.
115. Lamouille S, Connolly E, Smyth JW, Akhurst RJ, Derynck R. TGF-beta-induced activation of mTOR complex 2 drives epithelial-mesenchymal transition and cell invasion. *J Cell Sci* 2012; 125:1259-1273.
116. Leysen JE, Gommeren W, Van Gompel P, Wynants J, Janssen PF, Laduron PM. Receptor-binding properties in vitro and in vivo of ritanserin: A very potent and long acting serotonin-S2 antagonist. *Mol Pharmacol* 1985; 27:600-611.
117. Duinkerke SJ, Botter PA, Jansen AA, van Dongen PA, van Haaften AJ, Boom AJ, et al. Ritanserin, a selective 5-HT2/1C antagonist, and negative symptoms in schizophrenia. A placebo-controlled double-blind trial. *Br J Psychiatry* 1993; 163:451-455.
118. Ruiu S, Marchese G, Saba PL, Gessa GL, Pani L. The 5-HT2 antagonist ritanserin blocks dopamine re-uptake in the rat frontal cortex. *Mol Psychiatry* 2000; 5:673-677.
119. Monti JM, Alterwain P, Estevez F, Alvarino F, Giusti M, Olivera S, et al. The effects of ritanserin on mood and sleep in abstinent alcoholic patients. *Sleep* 1993; 16:647-654.